MEMBRANE ACTION IN THE PROFILED STEEL SHEETING DRY BOARD (PSSDB) FLOOR SYSTEM

MAHMOOD SERAJI

THESIS SUBMITTED IN FULFILMENT OF THE DEGREE OF
DOCTOR OF PHILOSOPHY

FACULTY OF ENGINEERING AND BUILT ENVIRONMENT
UNIVERSITI KEBANGSAAN MALAYSIA
BANGI

2013

TINDAKAN MEMBRAN DALAM SISTEM LANTAI KEPINGAN KELULI BERPROFIL KERING PAPAN KERING (PSSDB)

MAHMOOD SERAJI

TESIS YANG DIKEMUKAKAN UNTUK MEMPEROLEH IJAZAH
DOKTOR FALSAFAH

FAKULTI KEJURUTERAAN DAN ALAM BINA
UNIVERSITI KEBANGSAAN MALAYSIA
BANGI

2013

DECLARATION

I hereby declare that the work in this thesis is my own except for quotations and summaries which have been duly acknowledged.

12 July 2013

MAHMOOD SERAJI
P49948

ACKNOWLEDGMENTS

First and foremost praise to Almighty Allah for all his blessings for giving me patience and good health throughout the duration of this PhD research.

This research project would not have been possible without the support of many people. I wish to express my deepest gratitude to my supervisor, Prof. Ir. Dr. Wan Hamidon Wan Badaruzzaman who was abundantly helpful and offered invaluable assistance, support and guidance. Many thanks is also due to my co-supervisor, Assoc. Prof. Dr. Siti Aminah Osman, for her help and co-operation throughout the study.

Special thanks also to all my graduate friends, especially group members for sharing the literature and invaluable assistance. Not forgetting to my best friends who always been there.

I would also like to convey appreciation to the Mechanical Engineering and Civil & Structural Engineering departments for co-operation to perform the tests and using the laboratory facilities. I am also thankful to the technicians of these departments specially Mr. Ferdous, Mr. Raizal, and Mr. Fairul for their help in the experimental tests of this study.

I wishes to express my love and gratitude to my beloved parents for their understanding and endless love, through the duration of my studies. And special thanks to my wife who stayed with me in Malaysia throughout the entire study for her sacrifices, patience, and understanding which were inevitable to make this study possible.

Last but not least, I gratefully acknowledge financial support provided by UKM.

ABSTRACT

The Profiled Steel Sheeting Dry Board (PSSDB) system consists of profiled steel sheeting and dry board attached together by self-drilling and self-tapping screws as the basic structural components. Various materials may be used as an infill in the troughs of the deck to enhance stiffness and strength of the system and to act as insulation materials against sound and heat. Review of the literatures found vast earlier analytical and experimental studies on the behaviour of the PSSDB system including studying the interaction between components, the behaviour of a simple and continuous PSSDB floor, the effect of various infill materials on the stiffness, strength, heat/fire and sound resistance, comfortableness of the floor system, and etc. However, the potential of the PSSDB floor to develop 'membrane action' in order to improve the flexural capacity of the system has not been considered so far. This research is with the objective to assess the membrane action effect in order to develop a better performance PSSDB floor. Normally, mid-span deflection of simply supported floors subjected to bending load is correlated with the horizontal movements of the floor at the supports. In other words, as the mid-span deflection increases, the slab ends tend to move outward and inward in the first and last steps of loading respectively. Restricting the horizontal movements and/or rotation of the slab ends causes the formation of the compressive membrane action (arching action) in the slab in the first steps of loading. The flexural capacity of the slab also enhances after the deformation of the arch due to the development of tensile membrane action in the slab in last steps of loading. To achieve the defined objective, experimental and non-linear finite element approaches were employed in this study. An experimental test on simply supported PSSDB floor with concrete infill verified the proposed finite element model within 91% accuracy. In addition, two (2) experimental tests on concrete-filled PSSDB floor with restrained ends (‘pinned-pinned’ and ‘fixed-fixed’ supports) confirmed the existence of the membrane action, with results showing enhancement in flexural rigidity of more than 70% in the ‘fixed-fixed’ situation. Parametric studies were then conducted to further investigate (for the three said boundary conditions) the effect of various parameters on the development of membrane action in the PSSDB floor, namely (i) concrete infill, (ii) concrete topping, (iii) thickness of components, and (iv) continuous configuration of the PSSDB floor system. For cases (ii), (iii) and (iv), the models involved concrete-filled PSSDB floors. The parametric studies revealed, at best, i.e. in the fixed-fixed support condition, the concrete infill enhanced the flexural capacity by up to 294%, while the improvement was found to be 161% in the case when topping was introduced to the concrete-filled floor. Furthermore, varying the dry board thickness did not have any notable effect on the flexural strength, while the effect was found considerable with change in the profiled steel sheeting’s thickness. In the case of continuous configuration of the floor, the membrane effect was significant (87% increase) when the end supports were fixed.

ABSTRAK

Sistem lantai kepingan keluli berprofil papan kering terdiri daripada kepingan keluli yang disambung kepada papan kering dengan menggunakan skru menggerudi dan mengulir sendiri bagi membentuk komponen asas struktur lantai. Pelbagai bahan isian boleh digunakan untuk meningkatkan kekukuhan dan kekuatan struktur lantai, di samping dapat menjadi bahan penebat terhadap bunyi dan haba. Kajian literatur mendapati pelbagai kajian terdahulu yang dilakukan secara analitikal dan ujikaji tentang kelakuan sistem PSSDB yang merangkumi kajian interaksi di antara komponen, kelakuan lantai PSSDB tersokong mudah dan selanjar, kesan pelbagai bahan isian terhadap kekukuhan, kekuatan, rintangan haba/api dan bunyi, dan keselesaan lantai, dan sebagainya. Walaubagaimanapun, kajian mengenai kemungkinan terjadinya tindakan membran dalam sistem PSSDB belum dipertimbangkan selama ini bagi meningkatkan kapasiti lenturannya. Objektif kajian ini adalah untuk menilai kesan tindakan membran dalam sistem lantai PSSDB untuk membangunkan sistem lantai PSSDB yang berprestasi lebih baik. Biasanya pesongan yang berlaku di tengah rentang lantai tersokong mudah yang dikenakan beban lenturan berhubung rapat dengan pergerakan mendatar pada penyokong lantai. Dalam erti kata lain, dengan peningkatan pesongan di tengah rentang, kedua-dua hujung papak, cenderung untuk bergerak keluar dan masuk pada tahap pembebanan awal dan terakhir masing-masing. Kekangan terhadap pergerakan mendatar dan/atau putaran di hujung papak menghasilkan tindakan membran mampatan (tindakan 'gerbang') pada papak di tahap pembebanan awal. Kapasiti lenturan pada papak juga meningkat selepas 'gerbang' berubah bentuk akibat tindakan membran tegangan pada papak di tahap pembebanan terakhir. Untuk mencapai objektif yang ditetapkan, pendekatan secara eksperimen dan analisis unsur terhingga tak lelurus telah digunakan dalam kajian ini. Satu ujikaji dijalankan ke atas lantai PSSDB dengan isian, dalam keadaan hujung tersokong mudah mengesahkan model unsur terhingga yang dicadangkan dengan ketepatan 91%. Sebagai tambahan, dua (2) ujikaji ke atas lantai PSSDB dengan isian dalam keadaan hujung terkekang ('pin-pin' dan 'tegar-tegar) mengesahkan berlakunya tidakan membran, dengan keputusan menunjukkan peningkatan dalam kekukuhan lebih daripada 70% dalam kes 'penyokong 'tegar-tegar'. Kajian parametrik kemudiannya dijalankan untuk menyiasat lebih lanjut (bagi ketiga-tiga keadaan sempadan yang dinyatakan) kesan terhadap pembangunan tindakan membran pada lantai PSSDB. Parameter yang dikaji merangkumi, (i) isian konkrit, (ii) penutup konkrit, (iii) ketebalan komponen, dan (iv) konfigurasi keselanjaran sistem lantai PSSDB. Kes (ii), (iii) dan (iii) melibatkan lantai-lantai PSSDB dengan isian konkrit. Keputusan yang terbaik kajian parametrik (kes penyokong 'tegar-tegar') menunjukkan isian konkrit dapat meningkatkan kapasiti lenturan sehingga 294%, manakala peningkatan sebanyak 161% didapati bagi kes lantai dengan penutup konkrit. Sebagai tambahan, perubahan ketebalan papan kering tidak memberi sebarang kesan yang nyata dalam kekuatan lenturan, tetapi agak jelas kesannya apabila ketebalan keluli berprofil diubah. Dalam kes konfigurasi selanjar, kesan membran amat jelas (peningkatan 87%) apabila sempadan hujung dikekang.

TABLE OF CONTENTS

LIST OF TABLES

LIST OF FIGURES

LIST OF ABBREVIATIONS

ACI	American Concrete Institute
AISI	American Iron and Steel Institute
ASCE	American Society of Civil Engineers
ASTM	American Society for Testing and Materials
BC	Boundary Conditions
BCCFP	BondekII/Cemboard Composite Flooring Panel
BS	British Standard
FEM	Finite Element Method
PSSDB	Profiled Steel Sheeting Dry Board
PSS	Profiled Steel Sheeting
UKM	Universiti Kebangsaan Malaysia

LIST OF SYMBOLS

µm	Micrometer
ds/dx	Slip strain
E	Young's modulus
E_c	Young's modulus of concrete
F, G	Load
$f_c^{'}$	Ultimate compressive strength of concrete
f_s	Stress in steel
f_{sy}	Minimum specified yield strength
ft	Foot
f_t	Applied tensile stress in concrete
f_t^u	Ultimate tensile strength of concrete
GPa	Giga Pascal
I	External forces
kg	Kilogram
kN	Kilonewton
L, *l*	Span length
L/h	Span to depth ratio (slenderness ratio) of the slab
h	Thickness of slab
M	Moment
m	Meter
mm	Millimetre
MPa	Mega Pascal
N	Newton
P	External forces

R	Reaction force
R(u)	Residuals
S	Stiffness
ST	Strain gauge
T	Axial force
u, v	displacement
Width, W	Width of specimen
w	Distributed load
δ/h	Deflection to thickness ratio
$(\varepsilon_c)_{bot}$	Strain at bottom of concrete
$(\varepsilon_s)_{top}$	Strain at top of steel
ε_t'	Strain corresponding to ultimate tensile strength of concrete
ε_y	Yield strain

CHAPTER I

INTRODUCTION

1.1 RESEARCH BACKGROUND

Recently, the development of construction technology and the demand for lightweight structures have resulted in the increasing application of composite structures. Given their incredible advantages, composite structures have attracted the attention of researchers and designers all over the world.

The popularity of composite structures is due mainly to their valuable characteristics, such as economy, flexible design, and the combined benefits of concrete and structural steel. The proper application of concrete and steel in the form of composite structures increases the strength and stiffness compared with that of conventional structures, such as reinforced concrete elements and bare steel. In this regard, appropriate interaction between the layers of a composite section is essential to achieve composite action (Nethercot 2003).

The speed of construction with composite floors makes such material a cost-effective alternative to traditional reinforced concrete slabs or precast units. Moreover, the application of composite sections decreases the weight of structural elements. Aside from these major advantages, profiled steel sheeting is manufactured under controlled conditions in the factory, resulting in remarkable accuracy in construction.

Normally, a new construction system has to satisfy some requirements to be accepted as a better alternative. Less construction time, less dependency on heavy equipment, fewer specialised treat, better structural integrity, better thermal and sound barriers, better quality, less cost, less material wastage, durability, and no formwork are some of the goals of the new proposed new systems.

Intensive research on composite structures has led to the introduction of various lightweight composite systems, such as the Profiled Steel Sheet Dry Board (PSSDB) system proposed by Wright et al. (1989). The PSSDB flooring system is the focus of the present study. The primary intention of the PSSDB system is to be used as an alternative to the traditional timber joist system, because the latter system is associated with many problems, such as worm attacks, rot, and the misuse of occupants, which considerably shorten the life of most floors.

Historically, the solution for the drawbacks of the timber joist system was in-situ concrete. However, although this alternative increases the span-to-depth ratio to 20, it has inherent disadvantages, such as heavy self-weight, difficult placement of wet concrete at top levels, and temporary formwork and propping. Although these problems are resolved, to some extent, by precast concrete because of its light self-weight, the applications of precast concrete are limited to new structures. Considering the need for the congestion of formwork and the difficulty in the casting of concrete, in-situ slab and precast concrete are unsuitable solutions.

The introduction of the PSSDB system overcame these drawbacks to some degree. The PSSDB system is composed of profiled steel sheeting and dry board, the basic structural components, connected by mechanical fasteners, such as self-drilling and self-tapping screws. The empty space between profiled steel sheeting and dry board can be filled by lightweight material to increase the sound insulation and fire/heat resistance of the system. Although infill generally does not have a structural contribution to the system, concrete infill has structural and non-structural functions.

The PSSDB system has various applications, such as composite slabs and walls. PSSDB panel is used as a floor in the simple form and in the form of folded plate, is used as roofs. Figure 1.1 illustrates the typical PSSDB system and its basic components.

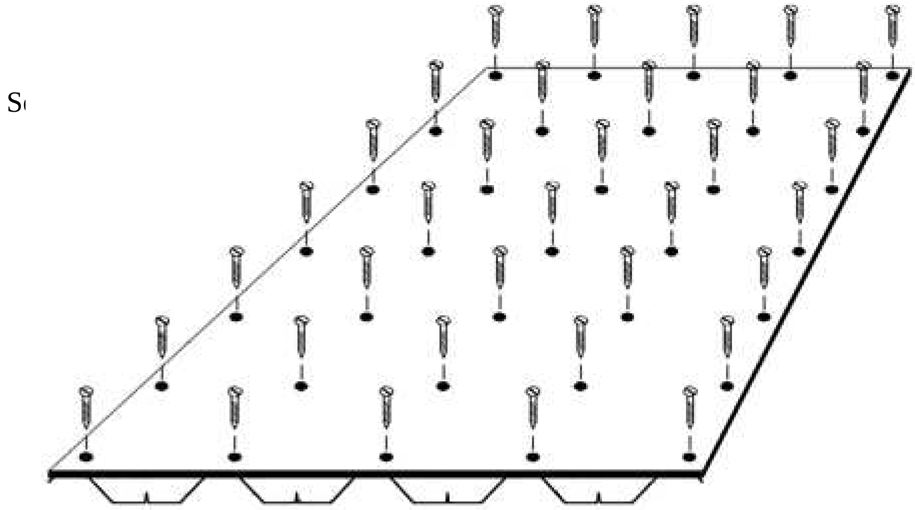

Figure 1.1 Typical PSSDB system

The profiled steel sheeting and dry board in the PSSDB system bear the tensile and compressive stresses, respectively, in the simply supported floor. The self-drilling and self-tapping screws transmit the horizontal shear forces between the main components when the floor is subjected to the bending load. When concrete is used in the troughs of the steel sheeting, the dry board and concrete jointly resist the compressive stresses above the neutral axis of the section.

1.2 MEMBRANE ACTION IN THE FLOOR

The ultimate load of the simply supported floor subjected to the vertical loading according to yield line theory is based solely on the moment and shear forces at yield lines in the slab. The predicted ultimate load according to the yield line theory could be reliable if the formation of yield lines in the slab does not generate in-plane (membrane) forces. Ignoring the effect of membrane forces in the slab may lead to the conservative results of the load-carrying capacity of the slab (Park & Gamble 2000).

When the simply supported slab deflects under vertical loading, the boundaries of the slab tend to move laterally outward in the first steps of loading and inward in the last steps. Limiting the horizontal movements of the slab ends causes compressive membrane action (i.e., arch action) from boundary to boundary. As the load increases, arch deformation in the slab causes tensile membrane action in the last steps of loading (Abdullah 2010; Bailey 2001; Bailey 2004; Bailey & Moore 2000; Zhang & Yi 2009).

Increasing the load in the first steps of loading causes compressive membrane action in the slab, thereby improving the ultimate load of the slab. Predicted ultimate load from the yield line theory is considered as bending action and the enhancement of the ultimate capacity and stiffness is attributed to the effect of compressive membrane action in the slab. As the slab deflection exceeds the displacement corresponding to the enhanced ultimate capacity, the compressive membrane forces in the slab are reduced. The reduction in the compressive forces is the reason for decreasing the load capacity of the slab to reach the predicted load according to yield line theory.

Once the mid-span deflection exceeds certain value, the compressive membrane forces decrease to approach zero. Further mid-span deflection leads to tensile membrane forces in the slab, thereby enhancing the load-carrying capacity of the slab.

As the slab goes into tensile membrane action, the steel resists the tensile membrane forces. The load-carrying capacity and mid-span deflection of the slab increase correspondingly until the rupture point of the steel. Compressive and tensile membrane actions normally develop with low and high mid-span deflections, respectively. The current research mostly focuses on the enhancement of the flexural capacity of the PSSDB system due to the development of compressive membrane action.

1.3 PROBLEM STATEMENTS

Since the introduction of the PSSDB system, research on the system has been intensely conducted to investigate its behaviour in various applications of floor, roof, and wall applications. The PSSDB floor behaviour has been considered in both linear and nonlinear approaches (Ahmed et al. 1996; Akhand et al. 2004; Akhand et al. 2004). Although numerous attractive advantages of the PSSDB floor have been reported in past research (Wan Badaruzzaman 1994; Ahmed 1996; Ahmed et al. 2000; Akhand 2001; Ahmed et al. 2002; Wan Badaruzzaman et al. 2003; Wan Badaruzzaman et al. 2003; Wan Badaruzzaman et al. 2007; Awang 2008; Wan Badaruzzaman 2009; Gandomkar 2012), some drawbacks of the system have not been investigated, thus leaving a research gap in this area.

In the PSSDB system, the top flanges of profiled steel sheeting, along with the dry board, resist the compressive stresses above the neutral axis of the section. The dry board increases moment capacity and reduces the probability of local buckling in bare steel sheeting. Nevertheless, the compressive stresses in the PSSDB floor makes the top flanges and webs of the steel sheeting vulnerable to local buckling, which marks the failure of the system.

The use of concrete as infill in the troughs of the steel sheeting strengthens the structural stiffness of the PSSDB system in two ways. First, a part of concrete above the neutral axis carries some portion of the compressive stresses in the section. Second, concrete infill partly limits the lateral deformation of the steel sheeting, thereby delaying the occurrence of local buckling in the thin plates of the steel sheeting. Local buckling at the webs and top flanges of the steel sheeting in PSSDB floors leads to the early failure of the system. In other words, although the top flanges of the steel sheeting reach plastic instability, the stress at the lower flanges of the sheeting is still below the tensile strength of steel. Accordingly, the full tensile potential of the steel has no effect on the ultimate load of the PSSDB system.

The local buckling of the PSSDB floor is closely associated with the mid-span deflection of the floor. As the mid-span deflection increases, local buckling is more likely to develop in the compression part of the section. Decreasing the mid-span deflection of the floor delays the formation of the local buckling. On the other hand, compressive membrane action in the floor reduces mid-span deflection.

Normally, PSSDB floors are considered in analyses with simply supported boundary conditions for single- or multi-span continuous configuration. The flexural strength of the floor is due only to its bending strength, and the in-plane force in the slab does not contribute to floor strength. However, restricting the horizontal movement of slab boundaries subjected to vertical loading causes arching action in the slab from boundary to boundary, and thus, the flexural strength due to the arch is added to the bending strength of the floor.

Obviously, taking the effect of in-plane forces into account improves the rigidities and flexural capacity of the slab in the first and last steps of loading. Although the effect of membrane action has not been commonly considered in the codes of practice, many researchers take this effect as a silent safety factor (Woodson & Krauthammer 1999). Considering the potential of the PSSDB system for developing the compressive membrane action in the evaluation of the load-carrying capacity of the floor leads to the use of the reserve capacity of the system and optimises the system for practical applications. Furthermore, limiting the inward horizontal movement of the slab in the last steps of loading puts the slab in the tensile membrane region in which flexural capacity improves according to the tensile strength of the steel.

The basic components of the PSSDB system, with various types of material, are available in the local market. In the experimental program of this study, 1 mm thick Peva 45 and 12 mm thick PRIMA*flex* were considered as PSS and dry board, respectively. The overall thickness of the PSSDB floor with these materials (57 mm) is lower than the code requirement for fire emergencies. The application of topping concrete over the dry board improves the performance of the PSSDB system in fire insulation. The topping concrete can also improve the flexural capacity of the system by increasing the thickness of the compression part in the cross-section and facilitate compressive membrane action in the slab.

1.4 RESEARCH OBJECTIVES AND SCOPE OF WORKS

The analysis of the PSSDB system is based on the simply supported boundary conditions in past studies; therefore, the reserve strength of the flooring system is not considered. Limiting the horizontal movements and/or rotations of the floor at the boundaries enables the two phases of compressive and tensile membrane action. The first phase (i.e., compressive membrane action) increases the rigidities and flexural capacity of the floor. Accordingly, the capability of the PSSDB floor system is optimised for practical applications.

Given these observations, the following objectives are to be achieved in this research:

i. To determine the shear connection behaviour between the PSS and dry board, the main components of the PSSDB floor, through an experimental test;

ii. To develop a nonlinear finite element model with simple span considering the probable source of nonlinearity, and to verify the developed model through experimental results;

iii. To explore the effect of compressive membrane action on the PSSDB floor on single-span samples with different boundary conditions through experimental test; and

iv. To explore the behaviour of the PSSBD floor with different boundary conditions through experimental tests on single-span samples

v. To study the effect of membrane action on PSSDB floors with practical applications and continuous configuration using the verified nonlinear finite element model.

1.5 RESEARCH PROGRAMME

Experimental and numerical studies have been conducted to achieve the defined objectives. The research outline could be developed according to the following groups:

i. Determination of the shear connection characteristics through experimental work for the basic components of the PSSDB system

ii. Development of the nonlinear finite element model and theoretical study of the behaviour of the system

iii. Experimental work on the PSSDB samples for simply supported, pinned-pinned, and fixed-fixed boundary conditions to investigate the formation of the membrane action in the sample in the first and last steps of loading

iv. Theoretical study on the PSSDB flooring system, with and without concrete as infill, to examine the effect of concrete on the flexural capacity of the system

v. Theoretical study on the verified finite element model to identify the enhancement of the performance of PSSDB floors for practical applications and continuous configuration due to membrane action in the floor

The adopted methodology in this thesis is illustrated in Figure 1.2.

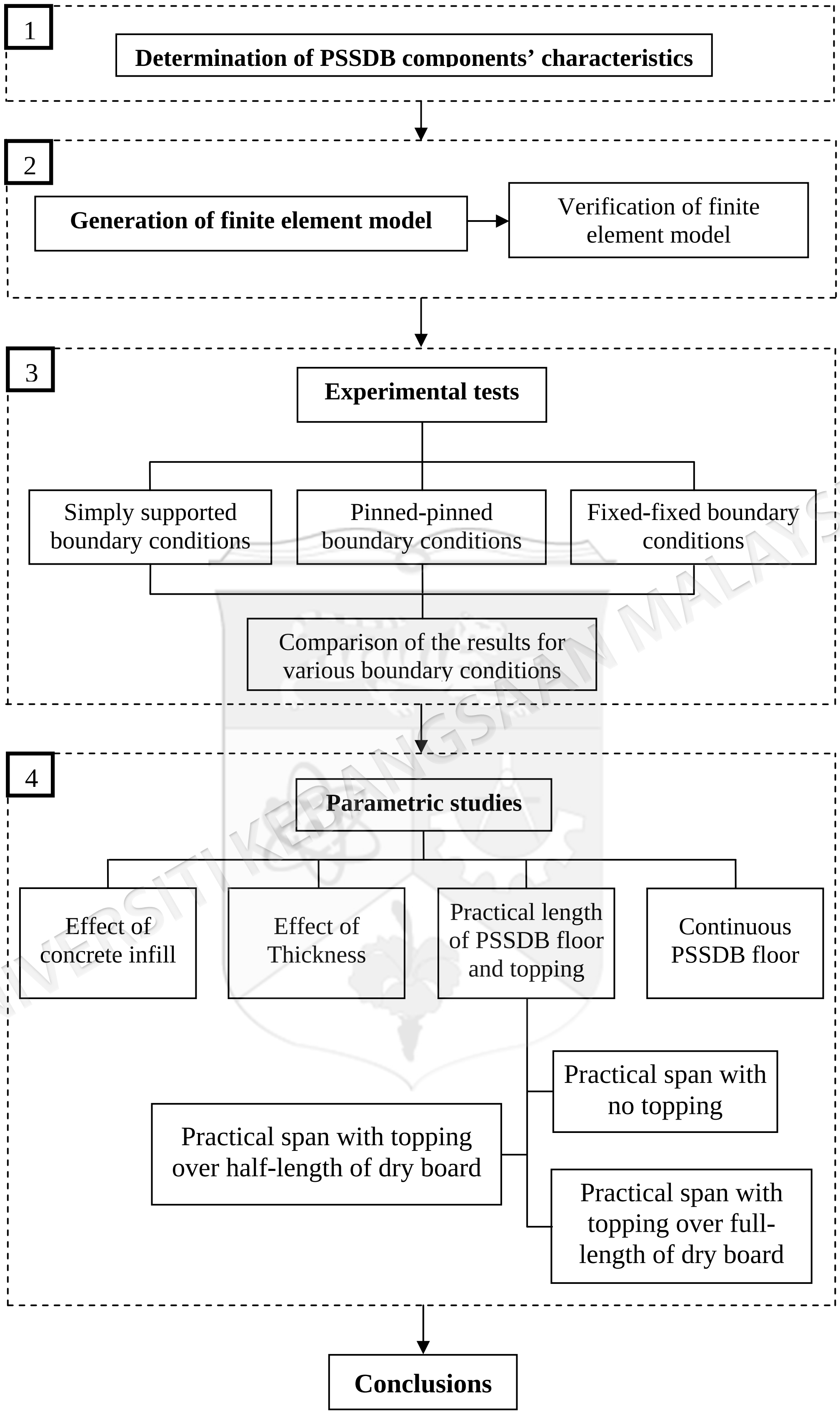

Figure 1.2 Methodology of the research

1.6 RESEARCH SIGNIFICANCE

As mentioned earlier, the prediction of the flexural strength of the system is due only to the bending strength of the sample because past research on the PSSDB floor has focused only on slabs with simply supported single- or multi-span boundary conditions. However, restricting the rotation and/or horizontal movements of the slab at the boundaries develops the membrane action (i.e., a reserve capacity) as two phases, namely, compressive and tensile membrane action. That is, restricting the outward movements of slab ends at the first steps of loading leads to arching action from boundary to boundary (i.e., the first phase). The developed arch enables the slab to increase its load-carrying capacity. Conversely, the second phase of membrane action enhances the flexural capacity of the slab in the last steps of loading. Thus, using the reserve capacity of the PSSDB floor optimises the system for practical applications.

Aside from improving the fire insulation of the system, the concrete, as a topping on the dry board, enhances the flexural capacity of the slab even with simply supported boundary conditions. Clearly, in PSSDB floors with topping, compressive membrane action is more likely to develop.

Therefore, by modifying the supports conditions, that induces the compressive membrane action in the PSSDB floor, the spanning capability of the structure would be significantly enhanced. This will have a great impact on the development of PSSDB system that will help open it up for wider applications as floor in building.

1.7 OUTLINE OF THE THESIS

The main scope of this thesis is the reserve strength of the PSSDB floor derived from compressive membrane action in the slab. Brief explanations about the membrane action theory are included in the thesis. The method of investigation using experimental programme and finite element approach is also reported in this thesis. The reported experimental programme and the numerical model for the various boundary conditions are delineated. This thesis covers the entire conduct of the research in eight chapters, as explained below.

Chapter 1 describes the research background, that is, on membrane action in the floor, and explains the problem statements and thesis objectives. The research programme, significance, and scope are briefly discussed.

Chapter 2 reviews the literature on membrane action and its fundamentals in floors. Moreover, previous research on the behaviour of the PSSDB system, especially of the floor, is considered, along with explanation about the various applications of the system.

Chapter 3 describes the experimental programme on the connection characteristics of the basic components of the system, namely, PSS and dry board.

Chapter 4 focuses on the procedures for developing the nonlinear finite element model, and discusses the behaviour of the structural components of the PSSDB system. This chapter also considers the probable nonlinearity in the system and the methods for the loading and boundary conditions in the developed model, and explains the interactions between the components of the system. Finally, the simulation results are verified through the experimental results for further parametric study.

Chapter 5 briefly explains the experimental programme on the effect of membrane action in the system, and describes the specimens and equipment employed in this experimental programme. The test procedures and results are then presented.

Chapter 6 discusses the effect of concrete infill and the various thicknesses of the PSSDB main components on load-carrying capacity, considering the different types of boundary conditions.

Chapter 7 describes the development of the practical applications of PSSDB floors for the single span without topping and of floors with topping over the full- or half-length of the dry board, and examines the effect of compressive membrane action in the slab with continuous configuration and various boundary conditions.

Chapter 8 summarises the significant findings of the current research and some proposals for future study.

CHAPTER II

LITERATURE REVIEW

2.1 INTRODUCTION

Many earlier publications have provided valuable insight into the effect of membrane action in reinforced concrete slab. This chapter summarises the most important contributions about the membrane action effect in slabs and the fundamentals for the development of membrane action. Moreover, two types of membrane action are delineated to describe the enhancement of the flexural capacity of the slab when the membrane action develops. The basic components and various applications of the PSSDB system are also discussed.

2.2 MEMBRANE ACTION THEORY

Membrane action has significantly improved the flexural capacity of reinforced concrete floors. Membrane action consists of two stages, namely, compressive and tensile membrane action, which occurs at small and large deflections, respectively. Restraining the outward movement at the initial stages of loading develops the compressive membrane action in the slab as an arch from boundary to boundary, and enhances the flexural capacity of the PSSDB floor (Taylor et al. 2001; Huang et al. 2003; Muthu et al. 2007; Zheng et al. 2007; Zheng et al. 2009; Li & Zhang 2010). Increasing the mid-span displacement of the slab, from compressive membrane action, beyond the displacement associated with peak capacity, develops the tensile membrane action in the slab. Park (1964b), Hayes and Taylor (1969), and Eyre and Kemp (1983) have investigated the effect of membrane action on the flexural capacity of the slab.

Horizontal movement must be sufficiently prevented to utilise the potential of membrane action in a one-way slab. In this regard, this research explores and develops beneficial membrane action to improve the load-bearing characteristics of PSSDB panels subjected to the distributed vertical loadings.

2.2.1 Fundamentals of Membrane Action Theory

General discussion of membrane action should consider the fundamentals of the theory; review the elastic theories, plastic theories (such as yield line theory), and the moment axial load interaction diagram.

a) Yield Line Theory

Yield line theory, an applied method for reinforced concrete slab, was introduced by Ingerslev in 1923 and significantly advanced by Johansen. This analytical method is an upper-bound approach, and the estimation of the ultimate load of the slab is premised on the collapse mechanism with boundary conditions. The moments on the plastic hinge lines in the slab are the ultimate moments of resistance in the section. The principle of virtual work or the equations of equilibrium are used to evaluate the ultimate load. All possible collapse mechanisms must be considered to avoid the overestimation of the load-carrying capacity of the slab. Furthermore, yield line theory considers a flexural collapse mode assuming that shear failure is avoided by the sufficient shear strength of the slab (Park & Gamble 2000).

According to yield line theory, slab segments between plastic hinge lines show elastic behaviour and have no effect on ultimate capacity. However, yield line theory of Johansen ignores the effect of compressive membrane forces in the slab with restrained lateral movement at the supports ((Bazan 2008).

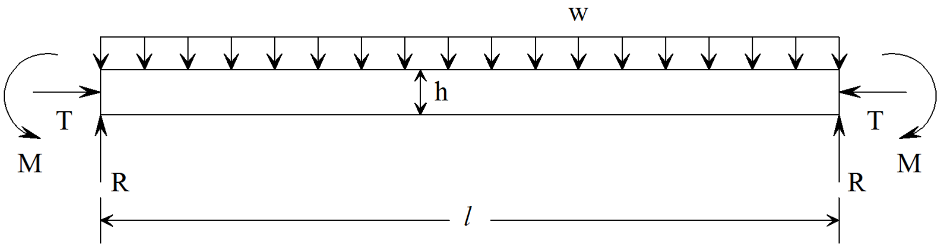

Figure 2.1 Free body diagram of slab

A slab test by Ockleston on the interior panel of the under-reinforced concrete slab of a dental hospital building showed that the slab experienced greater load than anticipated by yield line theory, which was caused not by the strain hardening of the reinforcement or the tensile strength of the concrete, but by membrane compressive forces acting in such an arch or dome in the restrained slab. Thereafter, Ockleston conducted further research on slabs with restrained ends to explore the effect of compressive membrane thrusts, (see Figure 2.1) and revealed that the enhancement of moment capacity on hinge lines is attributed to the thrust caused by axial force-moment interaction (Woodson 1994).

b) Axial Force-Moment Interaction

Hognestad (1951) presented an axial force–moment interaction diagram to illustrate the effect of membrane forces on the moment capacity of the reinforced concrete section (Figure 2.2) as well as the combinations of membrane thrust and moments based on material failure (i.e., the crushing of concrete and yielding of steel). The tensile strength of concrete and the strain hardening of steel are ignored in this diagram. According to the figure, ultimate moment capacity is achieved when the crushing failure of the extreme fibre of concrete happens at the same time as the yielding of tensile reinforcement.

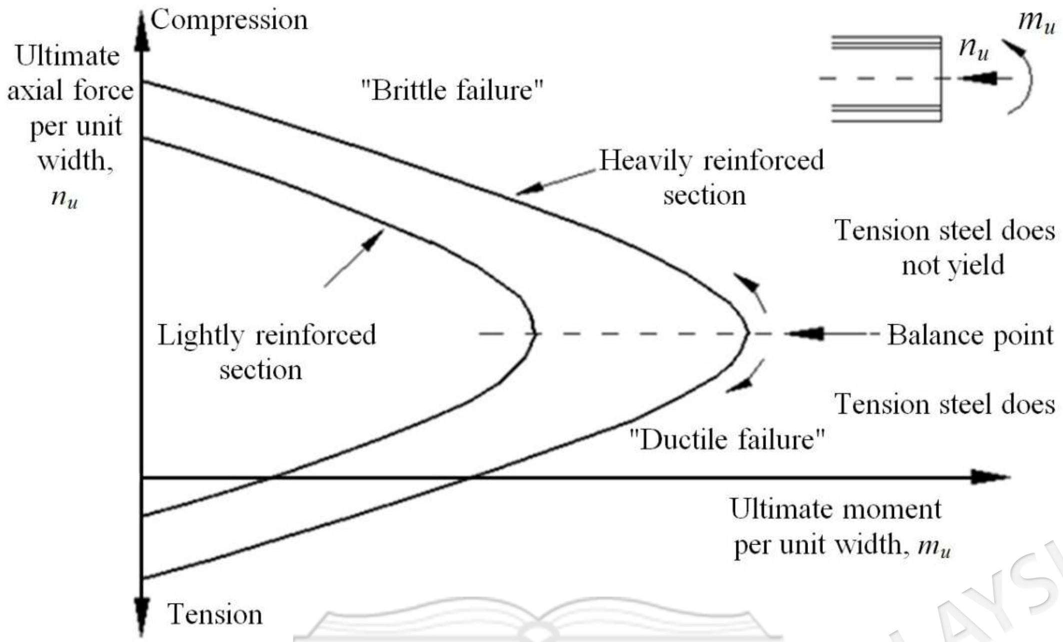

Figure 2.2 Ultimate moment-axial force interaction of symmetrically reinforced concrete section

Source: Park and Gamble 2000

When the combination of the thrust-moment is above the balance point (dashed line in Figure 2.2), brittle failure is expected from the section; when the combination is below the balance point, the reinforced concrete section tends to carry the constant load with continually increasing deflection. Therefore, the diagram shows the ultimate strength and ductility of the concrete cross-section under membrane forces (Welch et al. 1999).

c) Compressive Membrane Force and Flexural Capacity of the Beam

Cracks appear under normal reinforced concrete beams subjected to vertical loading. The growth of cracks in the beam is accompanied by the elongation of the lower surface of the beam, known as beam growth. Meanwhile, the neutral axis of the section moves higher than its original position. The outward elongation of beam ends causes horizontal displacement at the roller support of the beam. Restricting horizontal displacement causes horizontal reaction at the supports, thereby generating compressive membrane forces in the beam (Bazan 2008).

2.2.2 Membrane Action

In the early 1920s, Westergaard and Slater conducted the first research into the effect of membrane action on the flexural capacity of slabs by performing some full-scale floor panel tests, which revealed the presence of membrane forces in floors. However, intensive research on the behaviour of membrane action was initiated in the 1960s, following the research of Ockleston on compressive axial forces (Bailey et al. 2008).

The membrane action mechanism in beams and floors should be studied to understand that load redistribution and progressive collapse resistance in load-bearing elements are subject to failure. The general mechanism of membrane action in reinforced concrete slab shows nonlinear behaviour (see Figure 2.3). Figure 2.3 presents the load-deflection relationship for a one-way slab with restrained ends against the applied pressure load.

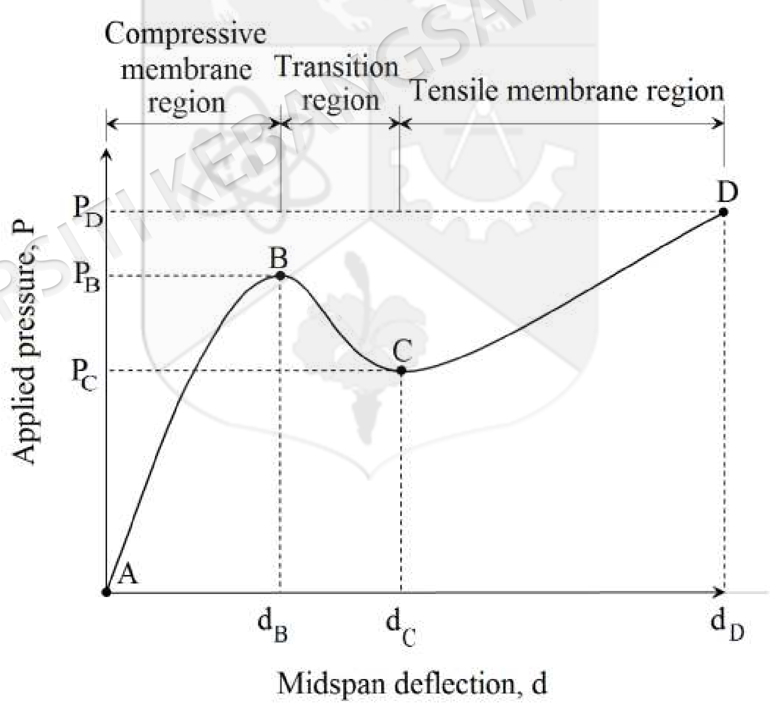

Figure 2.3 Load-deflection relationship for a one-way slab with restrained ends
Source: Woodson 1994

In the first steps of loading, the load-deflection curve represents almost linear behaviour until the crack point of concrete and nonlinear behaviour thereafter (see Figure 2.4). As loading increases up to point B (in Figure 2.3), the ultimate load also increases due to the effect of compressive membrane action in the slab. The compressive axial forces cause the slab strips to arch from boundary to boundary at small deflections, thereby improving the flexural capacity of the slab. Figure 2.4 illustrates the level of ultimate capacity improvement due to compressive membrane action.

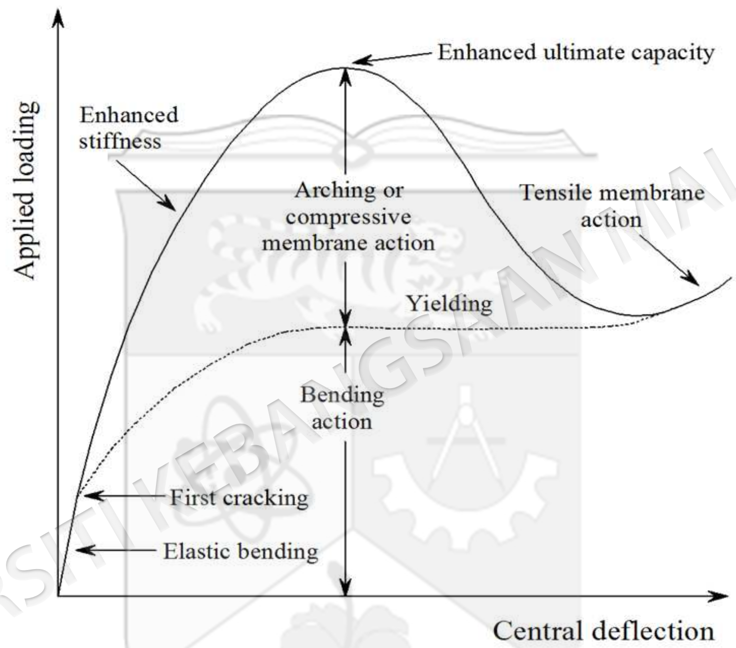

Figure 2.4 The effect of compressive membrane action
Source: Rankin et al. 1991

The elastic behaviour of the slab during the initial stages shifts to inelastic behaviour as the load exceeds point B, and the load decreases rapidly in the transition region because of reduction in compressive membrane forces (Figure 2.3). In a one-way slab, the disappearance of compressive membrane forces allows the slab to act in the catenary mode with the generation of tensile membrane forces. The supports take the tensile axial forces; otherwise, the slab collapses. By carrying the tensile forces, the supports cause the slab to follow point C to point D (Figure 2.3). The load in the load-deflection curve continually increases until the rupture point of steel. Therefore, the two phases of compressive and tensile membrane action can be distinguished in the slab when the horizontal movements of the slab ends are restricted.

a) Compressive Membrane Action

Conventional civil engineering design has ignored the findings of the three-decade study of compressive membrane action (Park & Gamble 2000). Accordingly, conventional elastic and plastic flexural methods, which produce over-conservative designs, are used. Although the potential of compressive membrane forces is not considered in the design, existing flooring system designs provide a silent safety factor (Woodson & Krauthammer 1999).

Compressive membrane action develops in slab at the first steps of loading because of compressive membrane forces at the centre of the slab above the mid-depth. The formation of pressure line in a shallow arch from boundary to boundary generates dramatically higher load-carrying capacity compared with the value predicted by yield line theory.

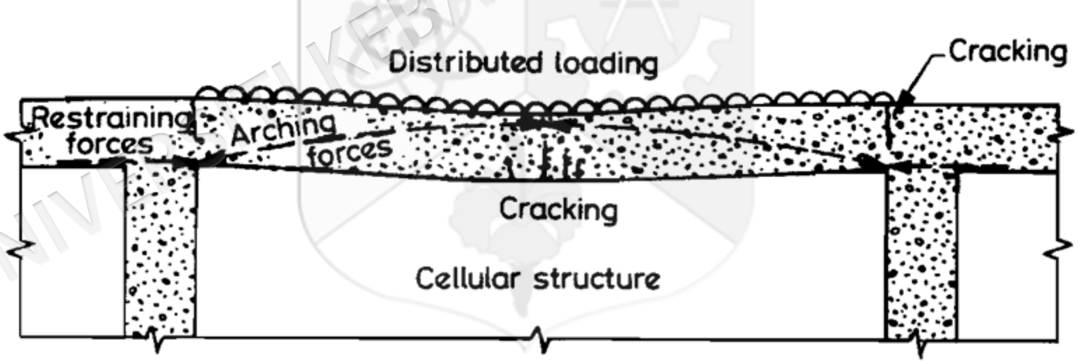

Figure 2.5 Compressive membrane action in a laterally restrained slab
Source: Rankin et al. 1991

Compressive membrane forces were applied by the Ministry of Transportation and Communications of Ontario to the design of the beams and slabs of bridge decks in the 1970s following intensive research on existing structures. An empirical method with certain requirements, the Ontario Highway Bridge Design Code, was developed in the research (Rankin et al. 1991).

Guice et al. (1986) proposed an analytical procedure for evaluating the ultimate flexural capacity of the one-way slab considering the effect of generated compressive membrane forces in the slab. Assuming the formation of three hinges in the one-way slab, Guice et al. proved that the estimated value of yield line theory is far lower than the real flexural capacity. The interaction between the bending moment and the compressive forces in the slab increases the ultimate moment capacity along the yield lines, thereby enhancing the flexural capacity of the slab. The procedure of Guice et al. was examined by Woodson (1985) through tests on 25 one-way fully restrained slabs.

The flexural capacity of the slab is dependent on the ratio of mid-span deflection to slab thickness. For instance, the ultimate flexural capacity of a slab with a span-to-depth ratio of 20 is obtained when the ratio of mid-span deflection to depth is 0.5. This ratio may be lower for slabs with a lower ratio of span to thickness. The restriction of outward horizontal movements and/or rotations at slab ends must be guaranteed by providing sufficient flexural rigidities for the supporting beams ((Park & Gamble 2000; Hon et al. 2005; Eyre 2007; Zheng et al. 2010). Similarly, the inward movement at slab ends must be prevented to develop tensile membrane action in the slab. Park and Gamble (2000) argued that the minimum stiffness of supports is at least $2E_c/(L/h)$, where E_c is the Young's modulus of concrete, and (L/h) is the span-to-depth or slenderness ratio of the slab.

b) Tensile Membrane Action

The second form of membrane forces is tensile membrane forces, which develop with large deflection and in slabs with anchored boundary movements. In one-way slabs, tensile membrane action, similar to the compressive membrane action, is highly associated with the restriction of the in-plane movements of slab ends. However, tensile membrane action may even be developed in two-way slabs with simply supported boundary conditions because of the formation of a compressive ring beam around the edge of the slab.

In conventional reinforced concrete, the tensile membrane domain develops in the slab when central deflection is $1 \leq \delta/h \leq 2$, which is associated with the yield line capacity of the slab (see point C in Figure 2.3). Further loading on the slab is carried by the tensile strength of the steel (Krauthammer 2008). In the transition region (Figure 2.3), outward membrane forces decrease and are nullified (point C); therefore, the load capacity of the slab decreases. Although no membrane forces exist in point C, the slab capacity is greater than that of yield line theory because of the strain hardening of the bonded reinforcement (Miltenburg 1998). The load-carrying capacity of the slab in the tensile membrane action stage is dependent on the ultimate strength of the reinforcement. According to Bazan (2008), the increase in resisting force in this stage is initiated by the continuous bottom reinforcement rupture point and developed when top reinforcements continuously bear the tensile stress. The failure of the slab happens in large displacements, and depends on the fracture point and the quantity of reinforcements acting as a tensile net as well as on the level of the restriction of slabs in boundaries to resist inward movement.

The improvement in the flexural strength of the slab caused by the development of compressive membrane action may not be as huge as the improvement caused by the development of tensile membrane action in the slab. Accordingly, tensile membrane behaviour reduces disastrous failure in the slab. As discussed earlier, the tensile net formed by reinforcements bears the progressive load up to the rupture point. An increase in the carried load is accompanied by an increase in central deflection, a result known as the *reserve capacity* of the slab (Krauthammer 2008).

The enhanced ultimate capacity of the slab due to compressive membrane action is normally considered the ultimate load of the slab, because compressive membrane action happens with small deflections when cracks in the concrete have not spread through the slab depth. Moreover, tensile membrane action highly depends on the quantity of reinforcements and their sufficient anchorage at the supports (Miltenburg 1998).

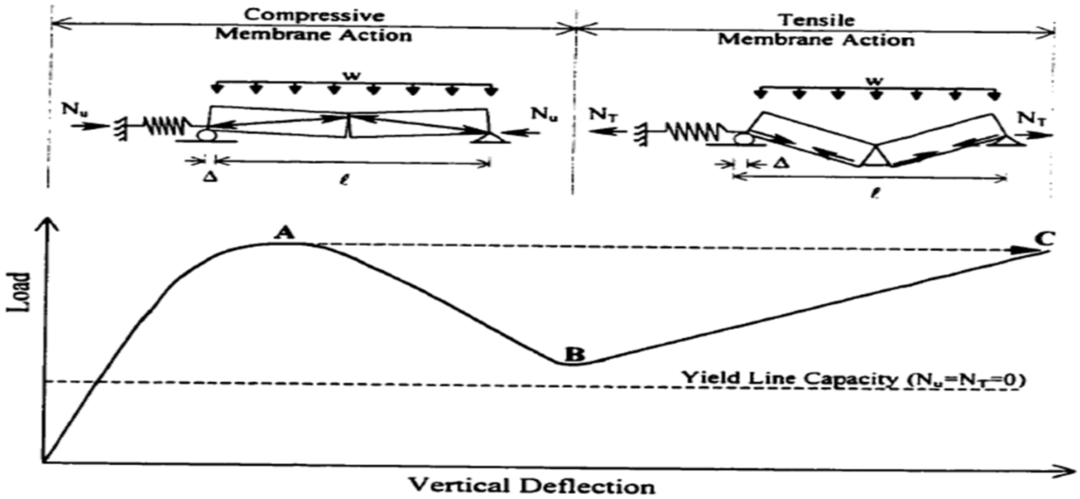

Figure 2.6 Typical load-deflection curve for restrained slab

Source: Park and Gamble 1980

According to Park and Gamble, tensile membrane action is initiated in the slab when the central deflection of the slab subjected to vertical loading reaches one-time slab thickness. During this deflection, lateral forces at the supports are zero, and this deflection point is considered as the starting point of tensile membrane action (Wang et al. 2010).

2.2.3 Membrane Action in One-Way Slab

Research on the effect of membrane action on one-way slabs and on that of two-way slabs has always been conducted separately. The latter was started in the 1960s and 1970s, whereas the former was initiated in the 1980s. The first research on the membrane behaviour of the one-way slab was done within the defence community for protective construction (Welch et al. 1999).

Park (1964b) proposed an approach to describe the effect of compressive membrane action in one-way slab subjected to the distributed load. Meamarian et al. (1994) later improved the model, taking the effect of pre-stressing force and creep into account. Miltenburg (1998) further enhanced the model to consider the strain hardening of the steel, shrinkage, temperature changes, and post-tensioning steel profiles.

The model was developed according to the following steps premised on the plastic failure mechanism: The derived expression for the slab elongation is based on failure mechanism geometry. The restraint of slab ends at the supports were idealised and measured. Similarly, forces in the concrete and reinforcement in the assumed plastic hinges were explained by the derived expressions. Next, the neutral axis in the plastic hinges was determined through equilibrium and geometric compatibility. Then, sectional analysis was applied to calculate the membrane force and moment in the plastic hinges. The ultimate capacity of the slab could then be evaluated through equilibrium (Miltenburg 1998).

Figure 2.7 illustrates the formation of yield lines in continuous one-way slabs. Based on the plastic failure mechanism in the model, three plastic hinges need to be generated in the continuous one-way slab subjected to vertical distributed loading so that slab segments between the hinges can be assumed to be unreformed.

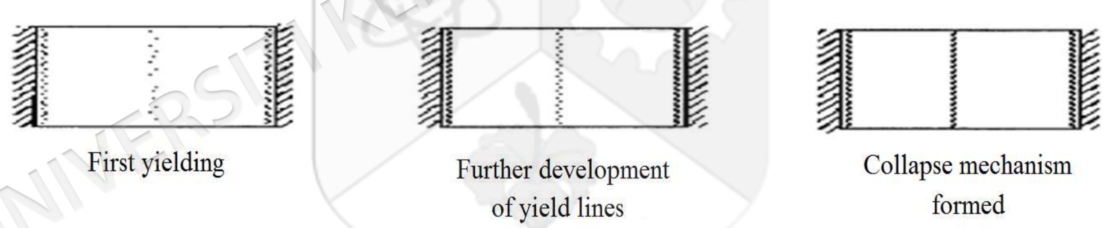

Figure 2.7 Yield lines in one-way slabs

The behaviour of slab with pinned boundary conditions is associated with the thrust force line at the supports and the provided restraint against the horizontal movement of the slab ends. Conversely, the behaviour of the slab with ends restrained against rotation is better in fire resistance compared with the slab with pinned boundary conditions owing to the moment redistribution. Moreover, with regard to fire conditions, resistance against compressive membrane forces in pinned supported slabs is convenient provided that the neutral axis of the slab is located higher than the line of thrust at the supports (Lim et al. 2004).

The experimental work conducted on the one-way slab has proved the effect of compressive membrane action in the enhancement of the flexural capacity of the slab. In this regard, the results obtained from 16 one-way slab tests conducted by Woodson (1994) showed the approximate improvement of 1.2 to 4.0 times the predicted value by the Johansen yield-line resistance.

The contribution of the compressive membrane action in a one-way slab can be clearly defined compared with that of a two-way slab, with an additional complication of twisting moments (Welch et al. 1999).

a) Compressive Membrane Analysis of One-Way Slab

Guice (1986) conducted a test on slab with restrained boundary conditions against the translation and partly against rotation to investigate the effect of rotational restraint. Although the allowed small support rotation increased the inward membrane translation of the ends, it did not decrease the enhanced load capacity by the compressive membrane action. According to Guice, if the support rotational freedom was greater than 2.0/2.5 degrees in slab with a slenderness ratio of 14.8/10.4, respectively, the compressive membrane action does not develop in the slab, and the tensile membrane forces are induced in the slab with no snap through. Therefore, rotational restraint is essential.

Welch et al. (1999) used the point of peak thrust to evaluate the peak load capacity of the slab rather than utilising the mid-span deflection due to the large variability of mid-span deflection. The peak thrust was employed in conjunction with a modification to the proposed compressive membrane action theory by Park and Gamble (1980) and the overall agreement with the experimental results for the wide range of span-to-thickness ratios ($2.7 < L/h < 28.3$).

Vecchio and Tang (1990) conducted two large scale tests for the slab specimens subjected to the concentrated mid-span load in which one specimen was prevented from lateral movement at the supports and the other was free to move at the end. The induced compressive axial forces in the slab with restrained boundaries enhance the flexural stiffness and load-carrying capacity of the slab. Figure 2.8

illustrates the mid-span load against the lateral displacement of the slab ends in the specimen with free lateral movement at the supports.

The application of peak thrust instead of mid-span deflection in the developed compressive membrane action (Park and Gamble) by Welch et al. (2008) led to an approach for the thick slab (L/h <18) to predict the compressive membrane resistance of the restrained edges in the one-way slabs. The results obtained as a predicted were as good as the predicted results by the mid-span deflection proposed by Park and Gamble using mid-span deflection. As a reason to change from mid-span deflection to the peak thrust, the difficult step of measuring the mid-span deflection in the proposed method is eliminated.

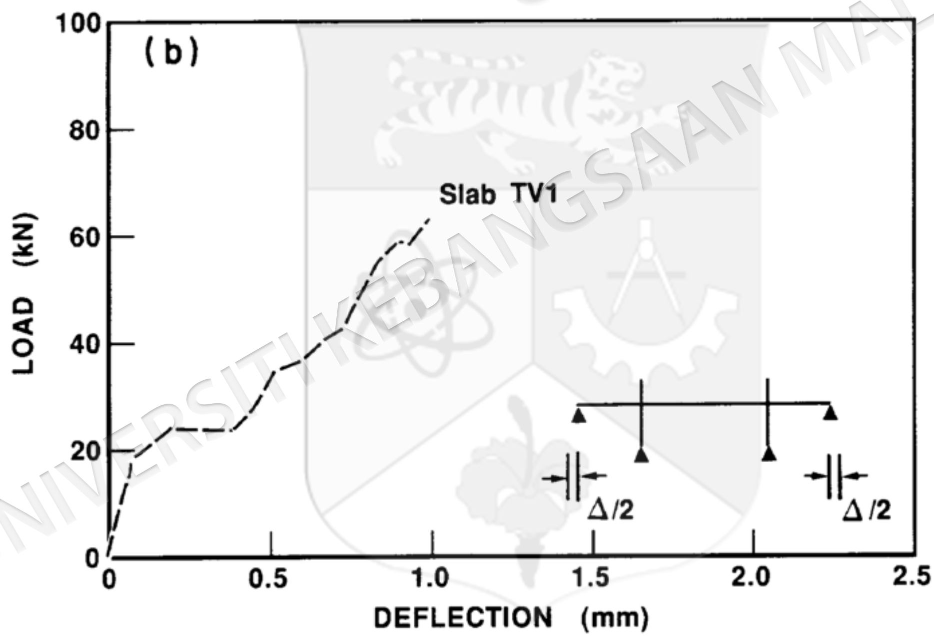

Figure 2.8 Relative lateral displacement of the slab
Source: Vecchio and Tang 1990

2.2.4 Membrane Action in Two-Way Slab

Restraining the boundaries in two-way slab to benefit the reserve strength of the slab, for the sake of the development of the compressive membrane action, is inevitable. Gvozdev (1939) conducted research on the effect of membrane action in two-way slabs, and came up with a comment on Russian code for the 20% reduction of the reinforcement for interior panels (Welch et al. 1999). Ockleston (1955) continued the research on membrane action, and confirmed that the improvement of load capacity of the slab with restrained ends is due to either arching action or moment-axial load interaction.

The first experimental test was conducted by Powell (1956), who proposed the general rigid-plastic approach with empirical deflection. Analytical approach was then proposed by Wood (1961) for the circular slab, clarifying the basic mechanics for the yield criterion changing when the axial compression is considered. The approach introduced by Powel and Wood was expanded by Park (P1964a; 1964b; 1964c; 1965) using a rigid-plastic strip method (as a landmark analysis). The hinge points were assumed to be in the long-established yield lines. The added contribution of the strips in orthogonal direction was used to make the approach applicable for the two-way slabs.

Park considered the partial lateral restraint to study the axial shortening and support movements of the slab. As his approach requires the estimation of the peak compressive membrane deflection, he recommended 0.5 h. Brochie et al. (1965) claimed that the flexural capacity improvement in the slab with a low rate of reinforcement is higher. According to them, the load-carrying capacity of the slab increases when the reinforcement rate is increased, but the enhancement is higher due to the higher thickness of the slab. Furthermore, they argued that the thrust developed in the restrained lateral edge slab is associated with the slab thickness, and restraining the end movements is the principal parameter to develop the compressive membrane action in the slab.

Gamble et al. (1961; 1969) conducted experimental tests and found that the support beams do not need to be taken rigidly, and that the enhancement is twice the yield line capacity. The decrease in the post-peak capacity to the yield line capacity was demonstrated by Keenan (1969). Gamble et al. (1970) used the known thrust value to precisely calculate the slab capacity through a reinforcement concrete thrust-moment interaction diagram. The approach of Park was then improved to take into account the elastic edge beam bowing (Ramesh & Datta 1973; Datta & Ramesh 1975).

2.3 PROFILED STEEL SHEET DRY BOARD SYSTEM

The profiled steel sheeting dry board (PSSDB) system is a thin-walled, lightweight composite structural system composed of steel sheeting and dry board connected by mechanical fasteners. Figure 2.9 demonstrates the basic structural components of the PSSDB system. The inception of the PSSDB system can be traced back to Wright and Evans (1986) in the United Kingdom. The PSSDB system was invented to serve as an alternate to the traditional timber joist floor in domestic buildings (Wright & Evans 1986). Timber joists were used as a traditional form of construction for many centuries. The problems associated with timber joists, such as structural performance, durability, and installation, were unpleasant background that paved the road for the conception of the PSSDB system (Wan Badaruzzaman 1994). The structural and non-structural behaviour of the PSSDB system has been conceptually investigated by many researchers in Universiti Kebangsaan Malaysia (UKM) since 1994.

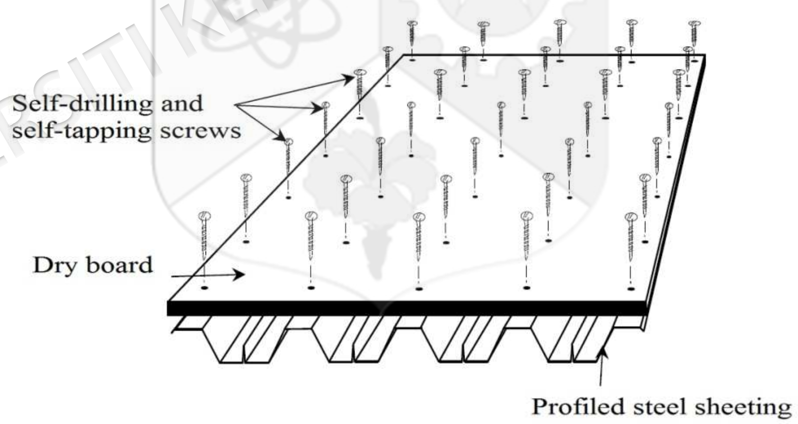

Figure 2.9 Basic structural components of PSSDB system

2.3.1 Component Material Research

As mentioned earlier, the PSSDB system is mainly constructed from steel sheeting, dry board, and connectors. Different types of these components are available in the construction market for a variety of applications. Better understanding of component behaviour and material is essential to explore the structural behaviour of the system.

a) Profiled Steel Sheeting

The presence of profiled steel sheeting in the PSSDB system is considered as a major load-bearing component (Akhand 2001). Wright et al. (1989) studied the structural behaviour of many types of steel sheeting for the PSSDB at the inception of the system, and found that available steel sheeting in the market adopted as composite metal decking could be mostly used for the PSDDB system. The stiffness of PSSDB floors is highly dependent on the adopted type of the profiled steel sheeting, dry board, and the extent of the interaction between the main components. Therefore, the purposely designed steel sheeting for the PSSDB system should be used to optimise its structural role in the system.

The profiled steel sheeting plays a dual role in composite systems, which makes it popular in high-rise buildings. First, the steel sheeting acts as permanent formwork in slab. Second, it is used as a tensile reinforcement (see Figure 2.10). However, the only application of steel sheeting since 1940 has been as permanent formwork (Wright et al. 1987; Wright & Hossain 1997). The profiled steel sheeting is generally used for speedier and simpler unpropped construction. Steel sheeting thickness, applied for structural purposes, is normally between 0.86 mm and 1.16 mm. Many types of profiled steel sheeting are used in composite slabs, the variety of which is based on span length and required resistance and stiffness in the construction stage. These types can be broadly classified into two: open-trough and re-entrant profiles (EN 1994 - Eurocode 4 1994).

The possible reasons for employing the profiled steel sheeting in a structural system are as follows:

- It serves as a safe working platform at the construction site.
- It can carry the load during the construction period, and propping is no longer required.

- It is used as a permanent formwork and as a tensile-bearing component in the concrete slab if adequate interaction with concrete is provided.

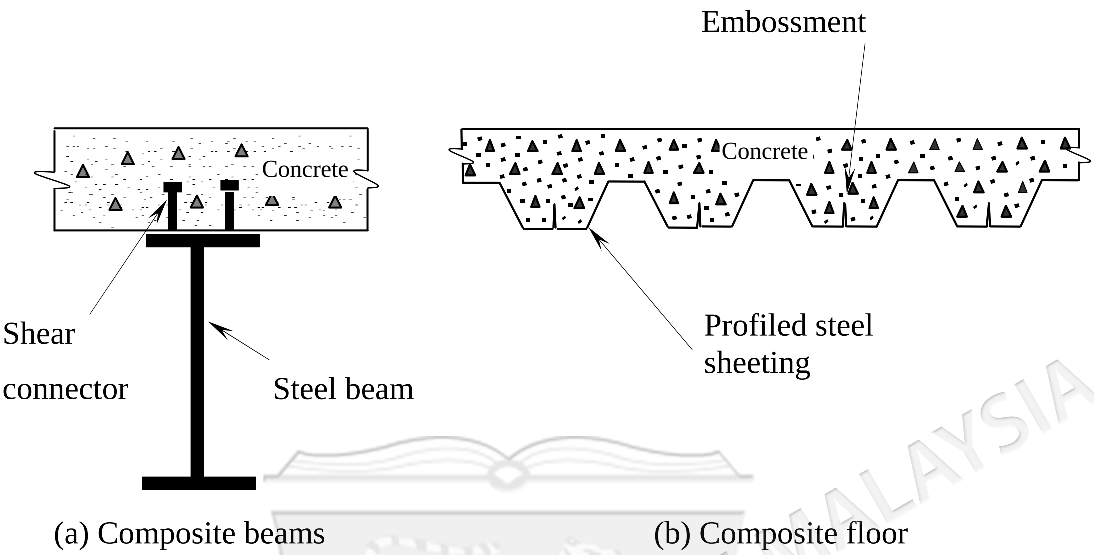

Figure 2.10 Typical composite structures

The profiled steel sheeting is produced from coil or strip folded into a continuous ridge profiled by cold forming in a rolling mill. Aside from the non-structural utilisation of profiled steel sheeting in Malaysia, it is also utilised for the conventional cast in-situ concrete. The locally available Bondek II exists in two types, such as dovetail and re-entrant, and is produced from high-strength steel strip. Re-entrant can be filled with infill material to enhance the fire resistance and sound proofing properties (Wan Badaruzzaman et al. 2008). Considering the yield strength per unit cost, high-strength steel is cheaper than other types. Moreover, it firmly maintains the form and resists accidental buckling and other damages. Therefore, soft infill material can be used, unlike composite concrete floors (Wan Badaruzzaman et al. 2003).

The profiled steel sheeting fails mostly because of the early appearance of local buckling in the top flanges of the sheeting when subjected to in-plane compressive stress (Hiriyur & Schafer 2005). However, the introduction of dry board to the steel sheeting could postpone the mentioned weakness of the steel deck. The stiffness of the steel sheeting with dry board improved from 14% to 70% compared with that of sheeting alone. Figure 2.11 demonstrates different types of profiled steel sheeting common to be used in PSSDB system.

Peva 45 was used as profiled steel sheeting in this study. The detailed characteristics of Peva 45 are illustrated in Figure 2.12. The reasons that could be mentioned in this regard are the wide applicability of Peva 45 and ready availability in the local market. This product is manufactured by Asia Roofing in Malaysia. Peva 45 is made of sheet Z36-275N by rolling, with two thicknesses of 0.8 and 1.0 mm, and the zinc coating used in this product for both sides is 275 g/m^2. Peva 45 has potential to be used for wide applications, such as residential buildings, business premises, industrial buildings, schools and hospitals, public buildings in general, agricultural buildings, and bridges and other constructions for traffic. In accordance with Asia Roofing Industries Sdn. Bhd., Peva 45 can be used for construction with different frames, including the following (Asia Roofing Industries Sdn. Bhd 1996):

- Steel structures
- In-situ cast reinforced concrete structures
- Pre-cast structures
- Wooden structures

(a) PMFL D35

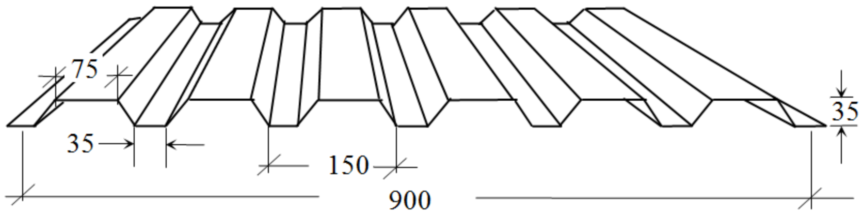

(b) PMFL CF60

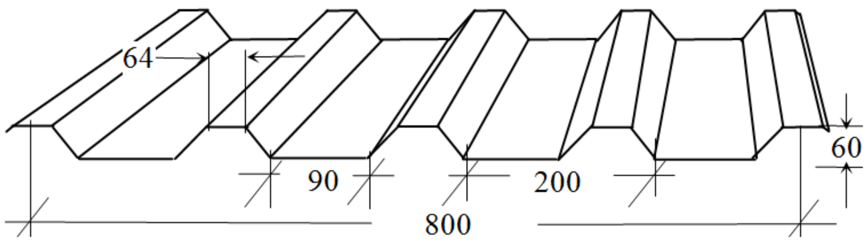

(c) Peva 45

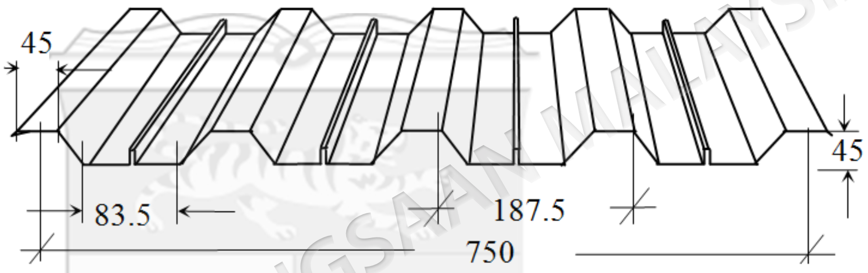

(d) Bondek II

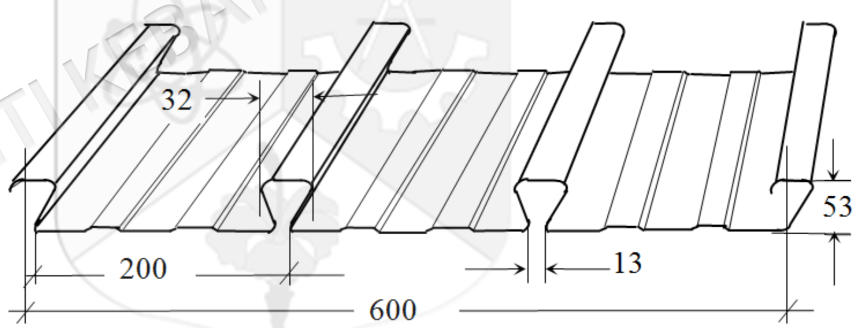

(e) BUILDECK

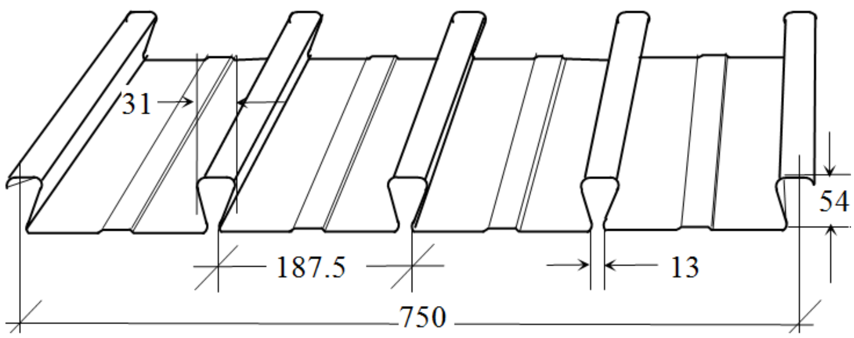

(All dimensions in mm)

Figure 2.11 Different types of profiled steel sheeting common to be used in PSSDB system

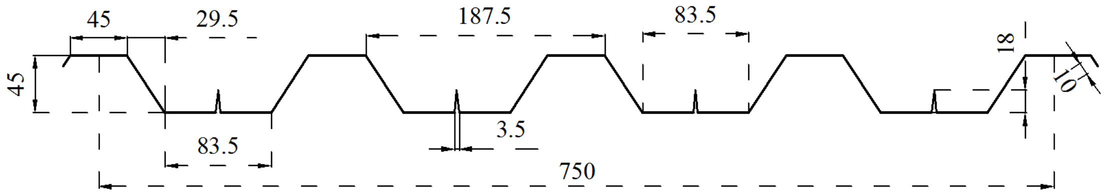

(All dimensions in mm)

Figure 2.12 Cross section of Peva 45

Table 2.1 presents the technical data of Peva 45 according to the manufacturer’s literature.

Table 2.1 Material properties of Peva 45

Nominal thickness (mm)	**Cross section (mm^2/m)**	**Weight (Kg/m^2)**	**Moment capacity (kNm/m)**		**Yield strength (MPa)**
			Sagging	**Hogging**	
0.8	1126	10.67	2.98	3.17	350
1.0	1422	13.33	3.21	4.36	350

b) Dry Board

In the PSSDB system, using dry board has two advantages. First, it provides a flat floor surface covering the corrugated PSS. Second, it helps enhance the stiffness and strength of the composite system. The attachment of dry board to the steel sheeting improves the in-plane shear and minor axis bending stiffness, and makes the system more suitable for use as a roofing component (Wan Badaruzzaman 1994). Attaching the dry board to the PSS, aside from creating a composite unit to bear the transverse load, avoids the instability of the steel sheeting and accordingly enhances the buckling strength of the sheeting.

Using dry board as a structural element was first considered by Wright and Evans in the proposal of the PSSDB system. The structural role of the dry board was then studied in depth in Universiti Kebangsaan Malaysia (UKM).

The improvement of stiffness in the PSSDB system, under the presence of the dry board, was investigated by Wan Badaruzzaman et al. (1999a) and found to be about 25% compared with that of the profiled steel sheeting alone. Another remarkable effect of the boarding in the PSSDB system is the enhancement of web crippling strength in the negative moment region by bracing the compression edges of the adjacent webs of the steel sheeting (Akhand 2001).

Different types of dry boards, such as plywood, chipboard, Cemboard, block board, gypsum-bonded particle board, fibre board, wood-cement board, and PRIMA*flex*, are locally available in Malaysia. Plywood and chipboard were initially proposed by Wright et al. (1989) to be used in the PSSDB system. However, PRIMA*flex* was used in this study due to its durability and remarkable resistance. It was first used in the PSSDB system by Awang (2007). According to Hume Cemboard Industries, PRIMA*flex* is autoclaved cellulose fibre reinforced cement flat sheet made of Portland cement, top-grade cellulose fibre, finely ground sand, and water. They have classified PRIMA*flex* as calcium silicate board. Superior fire resistance, high resistance to decay, termite and rodent attack, and most chemicals, weather resistance, good workability, structural strength, and ideal substrate for various types of coating are the advantages of PRIMA*flex* (Hume Cemboard Bhd 2007).

PRIMA*flex* in various sizes and thicknesses is available in the market. The thicknesses vary from 3.2 mm to 16.0 mm, the most applicable thicknesses for the PSSDB system being 9, 12, and 16 mm. The dimensions of the product for these thicknesses are 1220 mm × 2440 mm. Table 2.2 presents further structural details of the PRIMA*flex*.

Table 2.2 Material properties of PRIMA*flex*

Thickness (mm)	**Dimensions (mm)**	**Density-dry (Kg/m^3)**	**Modulus of Elasticity (N/mm^2)**	**Poisson ratio**
12.0	1220×2440	1300	8000	0.25

c) Infill Material

The main role of infill material is to act in the system as a non-structural component to improve the performance of the floor system with consideration of sound, vibration, thermal, and fire requirements (Wan Badaruzzaman et al. 2006). Moreover, some infill material can improve the structural performance of the system. Various internal infill and external protective materials, such as dry sand, rockwool, polyurethane, cellulose product, lightweight clay concrete, lightweight palm shell concrete, a protective lower layer of thin Cemboard, and cementitious fire spray coatings were explored by previous researchers, and serve as additional features to the basic PSSDB system (Wan Badaruzzaman et al. 1996).

Although implementing the abovementioned infill materials may not contribute to the flexural strength of the floor system, they may somehow increase the diaphragm (horizontal) load capacity of the floor. Using non-structural concrete as an infill material affects the free deformation of the steel sheeting and accordingly increases its bending strength (Wright 1993; Uy & Bradford 1994). A study of the effect of infill material on the PSSDB system was carried out by Wan Badaruzzaman et al. (1999b) using rockwool and sand as infill materials.

The effect of concrete infill and topping in the PSSDB system was later investigated (Wan Badaruzzaman et al. 2002; Shodiq et al. 2003; Wan Badaruzzaman et al. 2006; Wan Badaruzzaman et al. 2006) to explore the improvement of the stiffness of the system. The research included the effect of the topping as well, which was studied experimentally for the PSSDB simple spanning panel with and without infill and topping material. Concrete grade 30 was selected as the infill and topping material, and the obtained results showed 10 times improvement of the stiffness and flexural strength of the system. Shodiq (2004) also showed that the introduction of concrete infill into the PSSDB system reduces the mid-span deflection by up to 19% due to the enhancement of the flexural strength of the system. Furthermore, the fire resistance of the PSSDB system with concrete infill was improved to more than two hours compared with only 63 minutes of fire resistance in the system without any infill material.

For the current study, grade 30 concrete infill was used to investigate the structural contribution of concrete infill and topping in the improvement of the flexural capacity of the system given the membrane action.

d) Shear Connection

Shear connectors play the main role in the composite action between components in the floor. As the existing practical types of shear connections are incapable of transmitting entire horizontal shear forces, partial interaction occurs. Horizontal shear forces could be transferred between the components by one or some of the alternatives, such as mechanical or frictional interlock, stud connector, and deformation of rib ends. Incomplete interaction results in a different distribution of connector force and consequent over-design of connectors (Plum & Horne 1975), whereas in full interaction, the plane sections remain plane, and slip and slip strain throughout the beam are zero.

In the PSSDB system, horizontal shear forces are transferred by self-drilling and self-tapping screws from steel sheeting and dry board. The degree of composite action in the system is highly associated with the type of connector, material strength, size, and connector spacing and distribution. Self-drilling and self-tapping screws are used because of the cost of the preparation of prehole-type screws. Moreover, other problems such as misalignment, oversized holes, or misshaped prehole-type screws may create unsafe connections.

Wright et al. (1989) considered various types of fasteners, such as wood screws, nails, nuts and bolts, and self-drilling and self-tapping screws, at the inception of the PSSDB system. Among the investigated connectors, self-drilling and self-tapping screw was selected to transfer the horizontal shear between dry board and steel sheeting owing to some good advantages, such as being fixed from boarding side, no periling, and having moderate pull-out and shear resistance.

For this study, DS-FH 432 self-drilling and self-tapping screws were adopted. The diameter and length of this type of screw are 4.2 mm and 30.0 mm, respectively.

A push-out test was conducted to evaluate the shear modulus of the screw and the total shear capacity of the connections.

2.3.2 PSSDB System Applications

The PSSDB system is used in construction as composite slab and composite wall. Composite slab involves floor and roof applications. Two ways of construction, prefabrication and site assembly, have been suggested. Between them, prefabrication, due to some advantages, is preferred. Difficulty in handling the prefabricated unit, being heavier to transport than separate components, and feasibility to route the cable through the unit are some reasons. The PSSDB system has wide potential not only as a floor unit, but also as a load bearing wall and folded plate roofing system. PSSDB panels can conveniently be assembled to form a folded plate structure (Wan Badaruzzaman 1994; Awang et al. 2006).

The PSSDB system can be used for the following purposes:

- Temporary disaster relief shelter, because this system provides a fast, flexible, and simple construction method without the need for messy concreting work on site;
- Timber building frame system from simple dwelling units to buildings requiring high aesthetical values, such as chalets for resorts;
- Temporary working platform supported by scaffolds during construction stage replacing the conventional method of timber runner–plywood in the current construction trend; and
- Renovation work requiring safer, neater, and quieter working environments.

For practical purposes, the PSSDB system was originally named Bondek II/ Cemboard Composite Flooring Panel in a five-star hotel in Malaysia in 1997. It covered 5,000 ft^2 with a dead and imposed load of 2 kN/m^2 and 5 kN/m^2, respectively. The steel sheeting of the composite panel was Bondek II with 16 mm Cemboard as dry board, with 200 mm spacing of the screws. The panel was supported by C channels of mild steel 900 mm C/C. Lightweight concrete (1,000 kg/m^3) was used as infill to insulate noise.

The second practical case of the system was constructed in the Universiti Teknologi MARA tower in Malaysia in 1997. The PSSDB system was utilised to cover the 300 m^2 surface of the 13-story building in upper levels. Given the site constraints, the application of the PSSDB system was the only option. The panel was composed of 1 mm thick Bondek II, 16 mm Cemboard, and 100 mm spacing of the screws.

Another practical case was the construction of a three-story building in UKM in 2000. The PSSDB system was applied to all floors except the ground floor. The panel comprised 0.9 mm Peva 45 as profiled steel sheeting and 16 mm Cemboard with 200 mm screw spacing. The system was supported on reinforced concrete beams at 2 m C/C. The PSSDB system lowered the foundation size and overall cost of the building. The system was used in some other cases as well (Wan Badaruzzaman et al. 2003).

a) Floor Application

The first study on the PSSDB system was about its application as a floor in domestic and low-rise buildings. In composite slab application, the PSSDB system is classified as a concrete-steel slab. The dry board is fastened to the profiled steel sheet by self-drilling and self-tapping screws. Dry board, sheeting, and screws have key roles in bending stiffness. The PSSDB panel carries the out-of-plane bending and shear as structural floors. Adding the dry board enhances the stiffness of the system and consequently creates less central deflection in the composite slab. Moreover, using this method as an alternative for the traditional system could decrease the slab thickness of the 4 m span in domestic floors by 100 mm.

b) Roof Application

The boarding component in PSSDB panel could enhance the in-plane shear and minor axis bending stiffness of the panel compared with bare PSS; therefore, the PSSDB panel could be a proper alternative in folded plate structures (Wright & Evans 1987). As a folded plate structure, the PSSDB system carries both in-plane and out-of-plane bending and shear, which produces a strong, stiff, and efficient structure arising from its geometry and omits the internal bracing of traditional folded plate roof. Therefore, the use of the PSSDB system in folded plate construction to provide an improved form of roofing for domestic houses is considered to have remarkable potential. Such folded plate structure is also particularly suitable for use as an emergency shelter in a disaster relief situation ((Wan Badaruzzaman 1994; Ahmed 1999; Ahmed & Wan Badaruzzaman 2005). The capability of the PSSDB system to be used as a folded plate structure was first studied by Wan Badaruzzaman in 1994. Given the elimination of truss and supports in folded plate structures, the speed of construction is enhanced, which could be of great importance in domestic buildings and emergency shelters.

c) Wall Application

The axial load capacity of walls made from slender profiled steel sheet can be improved by the attachment of dry board because the board takes some portion of the applied load. Furthermore, dry board enhances the lateral bending stiffness of the composite wall to prevent early bucking. Therefore, the PSSDB system as a wall provides excellent axial, bending, and racking resistance. In composite walls, the steel sheeting is fixed at the time of assembling the steel frame of the building and improves the lateral resistance of the frame. Similarly, it provides necessary resistance to concrete pressure in construction. After construction, the composite wall acts as a shear or core wall for lateral stability and carries in-plane deformation. The investigations of PSSDB panels as walling units, under either pure axial or eccentric loading, show the similar failure that happens first by the distortion of screws, then by local buckling in weak wide compression flange, and finally by dropping the load (Wan Badaruzzaman et al. 1996).

2.3.3 Analysis of the Composite System

In past decades, the approach utilised to analyse profiled steel sheeting is the simple elastic beam theory. This approach is applicable to the low range of load that causes the steel sheeting to behave elastically. The theoretical results are in agreement with experimental results in terms of loading level, but for a higher level, the obtained result is no longer reliable, because this approach underestimates the stresses developed.

Goldberg and Leve (1957) proposed one method for analysing folded plates, namely, folded plate analysis. The applied load in this method is considered to be imposed on the edge of plates jointed together. This restriction was then removed by Evans (1967) to enable this method to consider the distributed loads applied normally to plates; therefore, the method became the suitable method for analysing the profiled steel sheeting.

The determined stresses along and across each plate in the structure can be used to check for plate buckling. In this method, effective width is converted to effective thickness; otherwise, effective plate width would leave a void in the centre of each compression plate, leading to unrealistic results. For profiles without groove stiffeners, this method proves ideal. However, for stiffened profiles, the number of plates increases because each stiffener must be approximated as an assemblage of plates, and then computing time increases (Wright & Evans 1986).

Normally, despite some restrictions and assumptions, the obtained result from linear analysis is acceptable for engineering application. In some cases, such as gross changes in geometry, permanent deformation, structural cracks, buckling, stresses greater than yield stress, and contact between the component parts, nonlinear analysis is compulsory. The reasons behind the nonlinear behaviour of structures can be classified into three groups: geometric, boundary, and material nonlinearity.

Newmark et al. (1951) derived and solved differential equations predicting the behaviour of two elastic beam elements connected longitudinally by a linearly elastic connection subjected to point load. This analysis includes the flexibility of the connecting medium in predicting deflections, and the slip between the surfaces of two elastic beams.

Marciukaitis et al. (2006) introduced a model for calculating the behaviour of the composite slab, which involves the profiled steel sheeting and in-situ concrete. Based on some investigations, the theory of built-up bars could be applied in composite slab for calculation of load-carrying capacity and deflection. The partial stiffness of the connection between layers, the effect of normal crack in the concrete layer, and the plastic deformation of compressed concrete have been considered to calculate the deflection of such slab.

Normally, in the floor slab under a service load, cracks are generated in the concrete, and plastic deformations develop in the compression zone of the concrete. The cracks inflict changes in the stiffness of cross-sections in the cracked floor areas. The influence of all these factors on floor stiffness is significant. The assessment of many of these factors for floor stiffness is not straightforward. Therefore, further experimental–theoretical investigation into the stiffness of floor slabs, especially in the connection area, and the development of methods for analysis are essential (Marciukaitis et al. 2006).

The behaviour of the PSSDB system is linear elastic with a small range of plastic until the failure point. The probable failure is due to the buckling of the upper flange of steel sheeting, whereas the induced tensile stress in the lower flange of the sheeting is under the yielding point of the steel. This buckling is dependent on plate width and stiffener geometry.

The design method for the PSSDB system introduced by Wright et al. (1989) is based on simple beam theory, and the introduced method by Wan Badaruzzaman (1994) is based on the folded plate method of analysis. The experimental results at ultimate load are always greater than the theoretical results because of the plasticity of the steel sheeting, which was not considered during theoretical investigation (Wan Badaruzzaman et al. 1996).

According to the experimental observations, the ultimate mode of failure of PSSDB floor panels is the buckling of the upper flange of the PSS. Therefore, by limiting panel deflection, safety against ultimate failure of the panels is assured (Ahmed et al. 1996).

2.4 SUMMARY

This chapter offered a general explanation about the theory of membrane action, including compressive and tensile membrane action. Yield line theory takes into account only moments and shears forces at yield lines in the slab and the in-plane forces are ignored. Considering the effect of membrane forces enhances the flexural strength of the floor by developing the arch action from boundary to boundary through restricting the horizontal movements of the boundaries. The fundamentals of membrane action development in the floor slab were reviewed. Furthermore, the components of the PSSDB system were separately considered. This chapter also provided the characteristics of the materials used in this study. Various applications of the system were discussed as well.

CHAPTER III

EXPERIMENTAL STUDY ON THE INTERACTION BETWEEN PROFILED STEEL SHEETING AND DRY BOARD

3.1 INTRODUCTION

Both qualitative and quantitative knowledge of the material properties are required to properly predict the behaviour of structures by the finite element package. Qualitative knowledge of the material properties is required to understand which of the physical and mechanical properties of the composite material are important for structural analysis and design and why they are important. Conversely, quantitative knowledge of the material properties is required to perform the analysis and predict the behaviour and structural capacity of the member. This information can be determined throughout the experimental studies.

This chapter focuses on the conducted experimental tests to determine the characteristics of the PSSDB components and the interaction between the profiled steel sheeting and dry board. These characteristics are important in the development of the nonlinear analytical model.

As mentioned earlier, the PSSDB system is composed of profiled steel sheeting and dry board connected by self-drilling and self-tapping screws. Peva 45, adopted as profiled steel sheeting in this thesis, is locally produced, and the required structural characteristics of the product are according to the manufacturer's literature. Stress-strain behaviour and other required characteristics of the PRIMA*flex*, chosen as a dry board component in this study, were provided by the manufacturer.

Using self-drilling and self-tapping screws in the PSSDB system have to be in a pattern of small spacing between screws in longitudinal and transverse directions.

Therefore, the developed horizontal shear between the components of the PSSDB system could be partly transferred due to the created incomplete or partial interaction. Full interaction between the elements is achieved in the case of maximum points of attachments between the components and sufficient stiffness of the connection. The achieved composite action in the panel depends on many criteria, such as the depth, shape, thickness, and strength of the steel sheeting, and on the type, strength, and thickness of the adopted dry board, as well as the spacing and types of the fasteners.

The practical space between the screws according to previous research (Ahmed 1999) is 200 mm along the longitudinal direction (i.e., major direction) of the steel sheeting to provide the required composite action in the panel. This space is applied in all models throughout this study.

The developed tensile forces in the screws due to the bending deformation of the panel are considered minimal; thus, connection shear behaviour could be achieved based on the assumption of the developed pure shear load in the connection. The tensile forces in the connectors are adequately low to guarantee not pulling out the screws. The failure of the connection in the PSSDB panel is mostly due to the shear forces rather than the withdrawal of the screws in connection due to the induced tensile forces in them.

The shear properties of the connection are preferred to be determined by conducting an experimental test on small samples. The shear modulus of connectors is the transferred shear forces per unit length of displacement due to the shear (Akhand 2001). Partial interaction between the components of the PSSDB panel is derived from a well-known experimental method of push-out test on the small sample size.

The achieved shear modulus of connectors from the push-out test is used in the developed analytical model to anticipate the structural behaviour of the PSSDB composite panel.

3.2 BRIEF HISTORY ABOUT PUSH-OUT TEST IN PSSDB

Previous research studies performed the experimental push-out test to identify the behaviour of connectors in the PSSDB system. The first test was conducted by Wright et al. (1989) along with the introduction of the PSSDB system. Subsequent researchers, such as Ahmed (1999), Akhand (2001), and Awang (2007), followed the procedure of the push-out test detailed in CP117 part 1 (1965) for the utilisation of various materials in this system.

The developed composite action between the profiled steel sheeting and dry board, due to the improvement of the floor section modulus, increases the capability of the PSSDB system to resist higher buckling stresses and consequently to produce larger stress block. Accordingly, the developed composite action improves the moment capacity (Wan Badaruzzaman et al. 2003).

Given that the connection between the main components of the PSSDB system depends to a high extent on the properties of the used materials, the push-out tests were performed for the adopted materials of Peva 45 and PRIMA*flex*. Although the noticeable number of push-out tests has been conducted to establish the behaviour of the connection between different types of the material in the PSSDB system by previous researchers, a push-out test for the combination of PRIMA*flex* and Peva 45 has not been previously performed. Self-drilling and self-tapping screws of type DS-FH 432 were used as connectors in this study.

The wet dry board (i.e. due to weather condition) normally affects the behaviour of the connection because of the appearance of crushing, bulging, and tearing in the boarding and therefore causes the minor softening of the connection strength. Given this phenomenon, the wet condition of the connection was considered in the PSSDB samples. Hence, the conducted experimental programme is composed of dry and wet conditions of the samples.

3.3 PUSH-OUT TEST SAMPLES

In the PSSDB panel with concrete infill, two types of connections must be considered: first, the connection between profiled steel sheeting and dry board, and second, the connection between the steel sheeting and concrete infill due to the presence of embossments inside the sheeting. Embossments are designed in the steel sheeting to minimise slippage between layers. The performed push-out test in this study focuses on the first type of connection in the PSSDB system. The second type of connections is not considered because of the availability of the results for this type in literature (Shodiq 2004) with the same grade of concrete (C30).

The push-out test samples considered in this study are according to the used material for the PSSDB panel, namely, 1.0 mm thick Peva 45 and 12 mm thick PRIMA*flex* as profiled steel sheeting and dry board, respectively. This test was conducted for the dry and wet conditions of the connection. As mentioned earlier, the same type of self-drilling and self-tapping screws of DS-FH 432 was used. Table 3.1 shows the considered groups of the samples of the push-out tests in this experimental programme.

Table 3.1 Details of samples for push-out test

Test group	**Steel sheeting**	**Dry board**	**No. of screws**	**Moisture condition**	**Sample identification**
G1	Peva 45 (1 mm)	PRIMA*flex* (12 mm)	8	Dry	PPDryS1 PPDryS2 PPDryS3
G2	Peva 45 (1 mm)	PRIMA*flex* (12 mm)	8	Wet	PPWetS1 PPWetS2 PPWetS3

The used materials for the push-out test and the other experimental work are all from the same batch of materials, from the stock in the concrete laboratory. The considered variable for the adopted material is only the moisture condition. According to the available thicknesses of the PRIMA*flex* sheets in the market, 9, 12, and 16 mm thick PRIMA*flex* are applicable in the PSSDB system. Referring to the literature (Akhand 2001), the thickness changes of the dry board and various types of screws do not have a remarkable effect on the connection stiffness; therefore, single thickness of dry board and a single type of self-drilling and self-tapping screws are considered in the experimental programme.

3.4 PROCEDURES OF THE TEST

The procedure for the push-test is similar to that used by previous researchers introduced in ASTM D1761 for the compression testing of timber joints for the lateral strength of fasteners. To create pure shear in the screws, two pieces of dry board were attached to both sides of the steel sheeting, as demonstrated in Figure 3.1. The dry boards on both sides were carefully screwed to the steel sheeting at the top and bottom flanges. Proper consideration was given to the alignment of the layers. The attachment of the dry boards to the steel sheeting was in a way that all the connectors resist the same amount of load during the test. Loading plate was used over the top side of the sample to apply the distributed load. As the figure illustrates, the bottom layer (dry board) is fixed and the upper layer (steel sheeting) is free to move smoothly in the vertical direction.

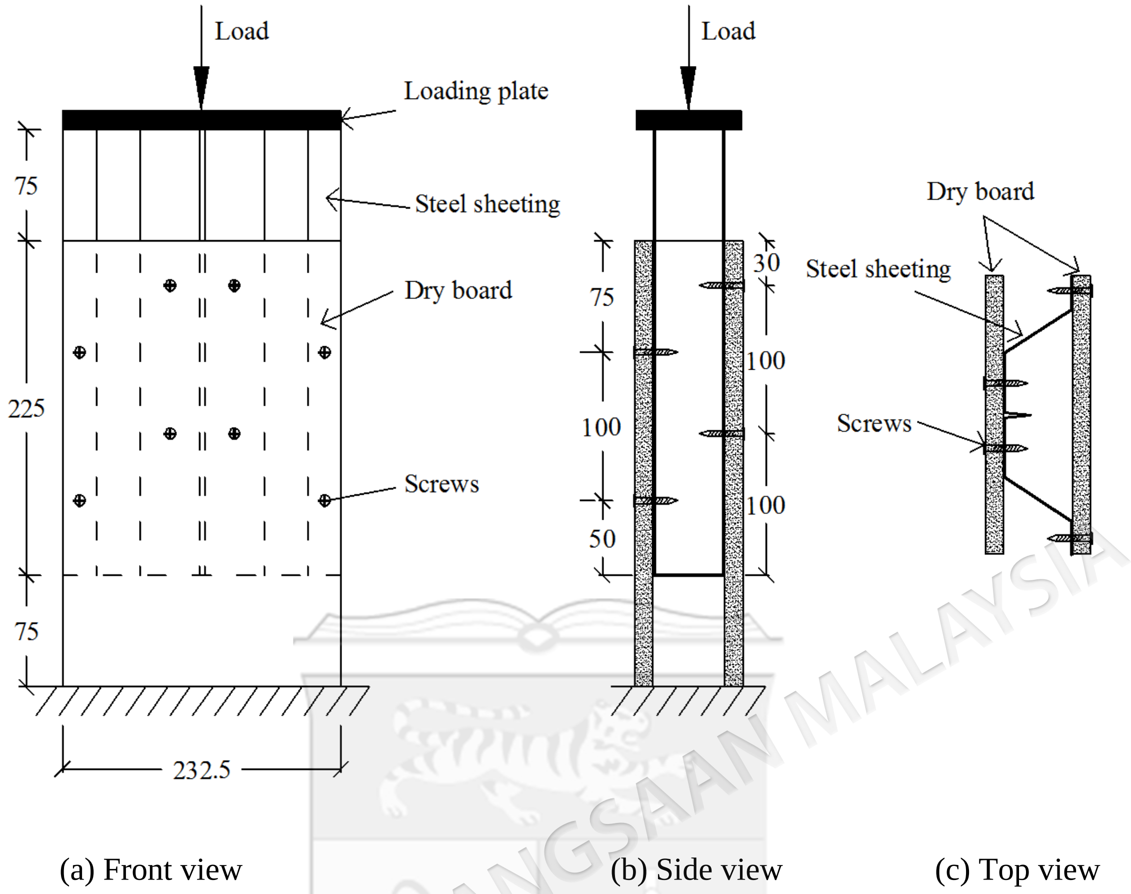

(All dimensions in mm)
Figure 3.1 Details of push-out test

3.4.1 Preparation of the Samples and Testing Rig

The small size samples for the push-out test were prepared in a way that measures the connection stiffness between the profiled steel sheeting and dry board. As the pure shear is assumed in the connection, special care was given to the cutting of the components and to the attachment of dry boards to the steel sheeting. Therefore, all the screws bear the equal amount of shear load developed between the layers during the loading.

The selected sizes of the sample were based on the width between the repeating troughs of the steel sheeting and the limitation of the testing machine. The width of the profiled steel sheeting was 232.5 mm, whereas the length was 300.0 mm. The selected size provided enough space to apply eight self-drilling and self-tapping screws in the sample, and each side of the sample contained four screws. The offset distance of the steel sheeting was 75 mm.

Zwick 100kN Proline Materials Testing Machine was used for the push-out test. High accuracy of the testing rig in measuring the applied load and the induced slippage between the layers can be mentioned as remarkable advantages of using this machine compared with the SINTECH universal testing machine (SINTECH, USA).

According to Table 3.1, two groups of samples were considered for the dry and wet conditions. The dried condition samples were kept at ambient temperature and with no special treatment. In accordance with experiment procedures in literatures (eg. Akhand, 2001), for the prepared samples to be tested in the wet condition, they were submerged in normal water with ambient temperature for 24 hours before the test. Ten minutes before the testing, the samples were drained to ensure no leaking of water during the test.

3.4.2 Conducting the Test and Observations

As mentioned earlier, the loading plates were used over the sample to apply the uniform distributed load. The samples were set in a way to be along the centre axis of the loading (see Figure 3.2). After checking all the alignments of the sample, the loading was started with a rate of 1 mm/min at all stages of loadings up to the failure of the sample. No setup modification was required for the testing machine. As the testing machine was digital, no special attention was required for the recording of data throughout the test, and the output results were provided in Excel files. As the loading increased, the screws gradually tilted, and the heads of screws bit the dry board.

Loading plates

Sample

Figure 3.2 Testing setup of push-out test

The test was continued with the tilting of the screws and the appearance of bulging in the PRIMA*flex* around the screw heads. Although the dry samples presented stiffer behaviour, the general behaviour of all the samples was almost the same. No sudden failure was observed in the samples, but the slippage was gradually increased with the penetration of the screw heads in the board. This ductile behaviour was observed for both groups of samples, but the biting of the screws to the board in the wet samples was more considerable (see Figure 3.3).

(a) Dry sample (b) Wet sample

Figure 3.3 Failure of the sample

The separation between the PRIMA*flex* and the steel sheeting was due to the penetration of the heads of screws inside the board in higher loads. In other words, the pulling out of the screws from the steel sheeting due to the induced tensile stress in the connectors was not observed. As described earlier, both groups of samples presented similar failure behaviour. The rate of loading throughout the entire tests was based on the displacement, and accordingly the same rate was applied for the initial and last steps of loading.

3.5 PUSH-OUT TEST RESULTS AND DISCUSSION

To analyse the connection behaviour between the fundamental components of the PSSDB system, the results achieved from the push-out test are discussed in detail. As mentioned earlier, the recorded displacement of the loading head of the testing machine was taken as an induced slip between the layers. Table 3.2 presents the summary of the results obtained from the test for both groups of samples. The tabulated loads in this table are the total load measured from the testing machine and the loads induced in each connector with the assumption of equally taking the vertical load on the sample. This table also presents the calculated average connector stiffness.

Table 3.2 Obtained results of the push-out test

Test group	Sample	Maximum load (N)	Connector stiffness (N/mm)	Average connector stiffness (N/mm)
G1	PPDryS1	25639	530.64	669.93
	PPDryS2	27056	844.10	
	PPDryS3	23066	635.06	
G2	PPWetS1	20096	436.17	476.56
	PPWetS2	20944	501.46	
	PPWetS3	18758	492.05	

Table 3.2 shows that the connector stiffness in the wet samples is considerably lower than those in the dry samples. For finite element modelling, the average connector stiffness of 670 N/mm was used for two tangential directions of the interface layer vertical to the connector axis.

The reported connector stiffness's by Akhand (2001) for two groups of the samples are provided in Table 3.3. The used materials were 1 mm thick Bondek II as profiled steel sheeting and 20 mm thick cement boded chipboard as dry board (T20). DX14 (4.2 diameter, 25 mm long) screws were used for connectors. These materials were used for the dried and wet conditions.

Table 3.3 Obtained results of push-out test from previous studies

Test group	**Sample**	**Connector stiffness (N/mm)**	**Characteristic stiffness value (N/mm)**
C1	T20/DX14/Dry/S1	809.3	710.4
	T20/DX14/Dry/S2	782.7	
	T20/DX14/Dry/S3	662.7	
C2	T20/DX14/Wet/S1	422.3	510.6
	T20/DX14/Wet/S2	622.3	
	T20/DX14/Wet/S3	512.6	

The values found for the connector stiffness in this thesis are very much similar in the same range as reported by Akhand (2001).

Figure 3.4 demonstrates the load-slip curves for all the considered samples of the two dry and wet groups. The provided results in the figure are based on the generated load at each connector. The samples with dry condition show stiffer behaviour compared with the wet samples. Although the obtained results are scattered for ultimate strength and its resultant slip between the samples, the behaviour of the samples after the ultimate point is predictable, and no sudden failure is observed throughout the tests. According to Akhand (2001), when cement board is used as a dry board, the behaviour of push-out samples is completely unpredictable due to the brittle nature of the boarding.

The scattered results may be due to the manual screwing of the dry board to the steel sheeting, which was expected to exert minor influence on the results because a sufficient number of screws were used in each sample. Despite the big difference in the achieved ultimate strength in the samples, the behaviours of the samples are almost similar up to 2 mm slip. The maximum reported slip in the PSSDB system is less than 2 mm (according to experimental observations), so the acquired connector stiffness is reliable for use in finite element modelling.

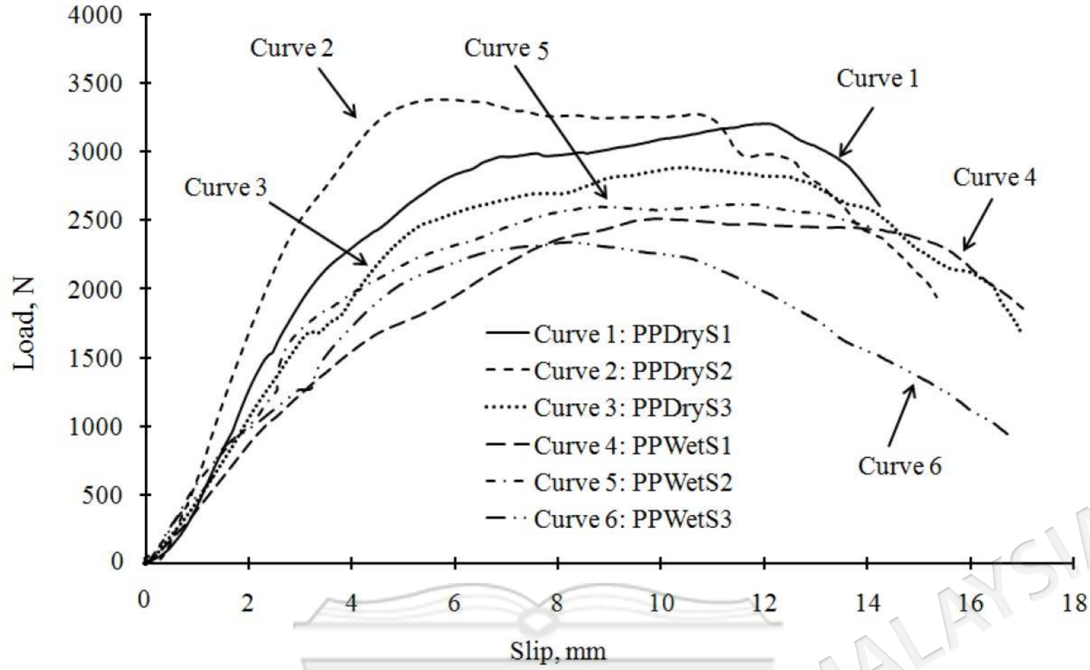

Figure 3.4 Load-slip curves for connectors

3.6 SUMMARY

This chapter discussed the measurement of the required experimental data for the development of the nonlinear analytical model. Push-out tests for the PSSDB components were performed in detail.

An experimental work was used to measure the connection stiffness between the basic components of the PSSDB system, namely, profiled steel sheeting and dry board. The test was performed for two groups of samples in dry and wet conditions. The result was 669.93 N/mm for the connection stiffness between the layers of the dry samples, and 476.56 N/mm for that of the samples in wet condition respectively.

According to experimental observations, the produced slips between the components are within the linear stage of the drawn graphs in Figure 3.4, therefore the connection stiffness was assumed linear in the finite element modelling. The average stiffness for the connectors in the developed finite element simulation was assumed to be 670 N/mm in both tangential directions on the interface layer.

CHAPTER IV

GENERATION OF THE FINITE ELEMENT MODEL FOR PSSDB FLOOR WITH SIMPLE SPAN

4.1 INTRODUCTION

This chapter describes the process of the development of nonlinear finite element model for the PSSDB floor. The structural component behaviour of the PSSDB system is discussed. The probable nonlinearities, method of loading, and boundary conditions in the modelling of the system are considered. Furthermore, methods to simulate the interaction between the layers in the composite floor are explained. Finally, the results achieved from the analysis are studied and compared with the experimental results.

4.2 FINITE ELEMENT IN STRUCTURAL ANALYSIS

Finite element modelling is a well-known numerical technique to provide approximate solutions for sophisticated problems by dividing them into small elements. Finite element analysis can be employed for simulation in different fields, such as structural, fluid mechanics, thermal, and electromagnetic analyses. Finite element was first used in aerospace industries for the development of new products. The popularity of the finite element method is mainly due to the development of computer facilities. In the past, performing tedious calculations due to the lack of computing machines was a daunting task for researchers; however, the recent development of computers has overcome this problem.

The finite element method provides an appropriate estimation of the structures' behaviours, as well as the equations for the analysis and design of the structural elements. Knowledge on finite element method leads to the effective analysis of complicated structures with accurate results.

Finite element has the capability to solve sophisticated problems. The most important advantages of this analysis technique are as follows:

- Finite element can be used to solve problems in any field.
- No limitation for the body shape and no geometric restriction exist.
- Finite element is applicable for any type of boundary condition and loading.
- The analysis is not restricted to isotropic material properties, and the material properties can vary between and inside the elements.
- Finite element can be used to solve problems with the combination of different mathematical descriptions and different behaviours.
- The actual body of the structure could be closely modelled.
- The obtained approximation of the results in finite element could be improved by making the mesh finer.

Conversely, finite element analysis has the following two disadvantages:

- The analysis of complicated problems is costly and time-consuming.
- The application of the finite element method does not require extensive knowledge; hence, the results obtained when limited knowledge is used may be unreliable.

Finite element packages provide the interface environment for users, so that all modelling processes can be performed in that area. Simulation is started by creating the model in the provided interface or importing it from the computer-aided design programme. To obtain accurate results, appropriate elements, loading techniques, boundary conditions, material properties, and stiffness matrix are important for the structural analysis (Cook et al. 2002). The final results obtained from the analytical model must then be verified with the actual structure.

4.3 COMPONENTS BEHAVIOUR IN THE PSSDB SYSTEM

The PSSDB system is composed of three main structural components, namely, profiled steel sheeting, facing dry board, and the connectors. Concrete as an infill material could assume the structural role in the system aside from its advantages in non-structural purposes. Defining the material properties in the developed finite element model is important to achieve the reliable prediction of the system's behaviour.

Linear finite element analysis of the PSSDB panel overestimates the flexural stiffness at all steps of loading. Nonlinear behaviour in the system is more likely to occur due to the appearance of the local buckling at flanges and webs of the steel sheeting. Moreover, the components of the PSSDB system exhibit materially nonlinear behaviour in the ultimate loading. Therefore, the nonlinear finite element method is considered in this research.

Implementing the finite element approach requires the application of proper elements to represent the real behaviour of the system. The accuracy of this method is highly dependent on the selective elements. The most essential factors that participate in the element selection can be obtained from the study of Ahmed (1999) as follows:

a. The selected element is required to represent the true bending deformation and in-plane deformation;
b. The element shape must be compatible to a given boundary geometry; and
c. The element should be efficient to minimise the computation time.

4.3.1 Profiled Steel Sheeting and Dry Board

This research employed Peva 45 and PRIMA*flex* as profiled steel sheeting and dry board in the PSSDB system. The properties of Peva 45 and PRIMA*flex* have been discussed in Chapter 2. The behaviour of Peva 45 is assumed to be ideally elastic-perfectly plastic for both tension and compression loading. The modulus of elasticity of Peva 45 is 210 GPa. Its yield strength and Poisson's ratio are 350 MPa and 0.3, respectively. The nonlinear stress-strain curve, provided by the manufacturer, is considered for the PRIMA*flex*. The modulus of elasticity and the Poisson's ratio of this material are 8.0 GPa and 0.25, respectively.

Profiled steel sheeting is the assemblage of thin plates that form a thin structure to perform jointly as a structural element. When the steel sheeting is subjected to the bending loads, the top flanges of the sheeting are responsible for resisting the compressive stress, so it is vulnerable to local buckling. Therefore, the stiffness of the section is accordingly decreased, whereas the induced tensile stress in the lower flanges is considerably lower than the ultimate tensile strength of the steel (Egilmez et al. 2007). In conventional concrete slabs, the concrete placed over the steel sheeting increases the bending capacity of the sheeting with the contribution of the concrete in carrying the compressive stress in the section.

In the finite element modelling of the profiled steel sheeting and dry board, thin finite thickness is assumed for the real component plates, and the idealised plates are assumed to be in the centroidal plane of the actual plate in a real structure.

The profiled steel sheeting is modelled as an assembly of isotropic plate elements, as demonstrated in Figure 2.12, whereas the orthotropic behaviour is achieved due to the geometry of the steel sheeting. The formation of the profiled steel sheeting produces some residual tensile and compressive stresses in the steel sheeting and may change in amount across the width of the sheeting. When the induced residual stresses in the sheeting are considered, the modelling becomes quite complex, so the stresses may not be considered for practical cases (Patrick & Bridge 1994).

The use of simple beam theory to analyse thin-walled structures can be traced back to earlier studies [e.g., Rockey and Evans (1969)]. This approach is applicable to low levels of load that cause the profiled sheeting to behave elastically. The theoretical results are in agreement with experimental results in that level of loading, but the obtained results are no longer reliable for higher levels of loading because this approach underestimates the stresses developed. The major inconsistency of this selection is that the beam element does not consider the local instability of the profiled steel sheeting (Ahmed 1999). The small thickness of the profiled steel sheeting must be dealt with in a similar manner as the thin-walled structures.

The nonlinear finite element approach is mostly employed for cold-formed steel sections rather than profiled steel sheeting (Akhand 2001). In-plane and out-of-plane deformations in sheeting should be considered. The plate elements are not applicable for geometrically nonlinear problems, so shell elements could properly represent this behaviour in the ABAQUS package.

Thin shell elements are considered in the ABAQUS/Standard only in cases when the transverse shear flexibility can be ignored and when the Kirchhoff constraint is precisely fulfilled. Thus, the shell normal remains perpendicular to the shell element reference surface. This phenomenon occurs in homogeneous shells when the shell thickness is approximately less than 1/15 of a characteristic length on the surface of the shell, such as the wavelength of a significant Eigen mode or the distance between supports.

Thin and thick shell elements are provided in the ABAQUS element library. A shell element that is applicable for both thin and thick shell elements is desirable due to the development of the large strain in the structure. In this study, S4R shell element was employed to represent the behaviour of profiled steel sheeting and dry board. S4R is a three-dimensional four-node doubly curved general-purpose shell with reduced integration and finite membrane strain. This element has six degrees of freedom per node that uses bilinear interpolation. The ABAQUS algorithm does not precisely calculate the normal to the nodes in the coarse mesh; thus, the fine mesh must be applied for a doubly curved surface (ABAQUS 2008).

Figure 4.1 demonstrates the used shell element in the developed finite element method to represent the behaviour of the profiled steel sheeting and the dry board in the PSSDB system.

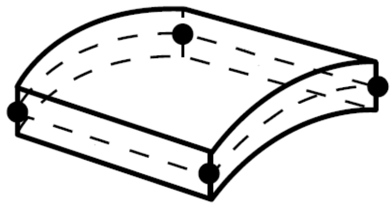

Figure 4.1 S4R element

4.3.2 Concrete

In the PSSDB system, concrete may be used as an infill or topping. Using concrete as an infill material improves sound and heat insulation, and has a structural function in the system. The presence of concrete infill in the system dramatically decreases the web crippling of the profiled steel sheeting in the internal supports. In addition, the concrete participates in carrying the induced compressive stresses above the neutral axis of the cross-section at mid-span, so it delays the occurrence of local buckling at top flanges of the steel sheeting, as proven by previous experimental research (Wan Badaruzzaman et al. 2002; Shodiq et al. 2003). Thus, concrete infill helps improve the structural performance of the PSSDB system.

When the composite slab is subjected to vertical loading, the interaction between the layers of the composite floor is responsible for transferring the developed horizontal shear forces. To ensure the structural performance of the concrete infill in the PSSDB system, some embossments have been placed in the troughs of the profiled steel sheeting.

The structural behaviour of the concrete infill is modelled by the three-dimensional, eight-node linear brick, with reduced integration, hourglass control, and solid element (C3D8R). Figure 4.2 demonstrates the adopted element as a solid element in this study.

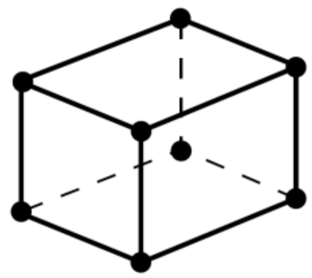

Figure 4.2 C3D8R element

The solid element with reduced integration was used to avoid the shear locking that may occur in the fully integrated elements. Shear locking causes the elements to exhibit stiff behaviour in the bending. This phenomenon only affects the fully integrated, linear elements when they are subjected to the bending loads. The edges of the quadratic elements are able to form curves, so shear locking is unlikely to occur in these elements. The fully integrated linear elements can only be used when the applied load produces small bending in the model. Using the first-order reduced-integration elements may cause the hourglassing problem in the analysis. Only one integration point is present in such elements, so element distortion may lead to zero strain at that integration point. Therefore, the analysis faces the problem of uncontrolled distortion of the mesh. This problem may be overcome by avoiding the concentrated forces and distributing the boundary conditions over the number of nodes (ABAQUS 2008).

4.4 NONLINEARITY IN FINITE ELEMENT METHOD

Although linear analysis is appropriate for the majority of engineering applications, studying the source of nonlinearity is inevitable to simulate the real behaviour of the PSSDB system, especially the last steps of loading. The reasons behind the nonlinear behaviour of a structure can be widely categorised in three groups as follows:

a) Geometric nonlinearity
b) Material nonlinearity
c) Boundary nonlinearity

The effects of residual stresses and some other minor nonlinear sources are not considered in this study.

4.4.1 Geometric Nonlinearity

Geometric nonlinearity may be due to large deflection/rotation or large deformation. This source of nonlinearity may result in stress-stiffening, buckling, collapse, and snap-through. The flexural stiffness of the structure is remarkably affected by the state of in-plane stress in the structure. The effect of a combination of in-plane stress and out-of-plane stress on the flexural capacity of the structure is known as stress stiffening, which mostly occurs in thin-structures (i.e., profiled steel sheeting) where the bending stiffness is considerably lower than the axial stiffness.

The remarkable changes in the body of the structure subjected to the loading cause the geometric nonlinearity. According to Ålenius (2003), in small-displacement analysis, geometric nonlinearity can be ignored. The buckling or the collapse may be the effect of some geometric nonlinearity. Local buckling and surface wrinkling can be considered as the other effects of geometric nonlinearity.

In the PSSDB system, geometric nonlinearity is the most probable source of nonlinearity. The behaviour of the PSSDB system is linear elastic with a small range of plastic in the first steps of loading. The probable failure in the PSSDB system is due to the local buckling in the upper flanges of steel sheeting, whereas the developed tensile stress in the lower flanges is far below the yielding stress of steel. The local buckling is dependent of the plate width and stiffener geometry.

4.4.2 Material Nonlinearity

When the material carries high stress levels, the material progressively presents disproportionate stresses and strains. Therefore, the plastic strain remains in the material when the stress is released. Material nonlinearity is considered in the analytical model by employing the nonlinear stress-strain constitutive model for all components of the PSSDB system. Table 4.1 provides details of the considered materials in this thesis.

Table 4.1 Details of the specimen

	Thickness / diameter (mm)	**Width & Length (mm)**	**Modulus of Elasticity (E, N/mm^2)**	**Ultimate strength (N/mm^2)**	**Weight of covered area (N/m^2)**
Profiled steel sheeting (Peva 45)	1.0	795×1730	200×10³	350	130.77
Self- drilling and self-tapping screw	4.2	30.0	----	----	----
Dry board (PRIMA*flex*)	12.0	795×1730	8030	22	172
Infill (Concrete grade 30)	Infill	Infill	25743	30	606.4

The Young's modulus were 25743, 8030, and 210 × 10³ N/mm^2 for concrete, PRIMA*flex*, and Peva 45, respectively. The Poisson ratios of the materials were 0.2, 0.25, and 0.3.

a) Constitutive Model for Steel

The material properties of the profiled steel sheeting (i.e., Peva 45) are orthotropic despite the isotropic behaviour of steel, due to the geometry of the steel sheeting. Some residual tensile and compressive stresses are induced in the steel sheeting at the time of its production from the coil sheet. As these stresses are unpredictable and have a minor effect (Patrick & Bridge 1994), they are not considered in the development of the nonlinear finite element model.

According to literature (Akhand 2001), the elastic–perfectly plastic model reflects the behaviour of the steel sheeting. Similar properties are considered for the tensile and compressive stresses of the steel sheeting. Figure 4.3 demonstrates the assumed constitutive model. The Young's modulus and the Poisson ratio of the steel sheeting are assumed to be 210000 N/mm^2 and 0.3, respectively.

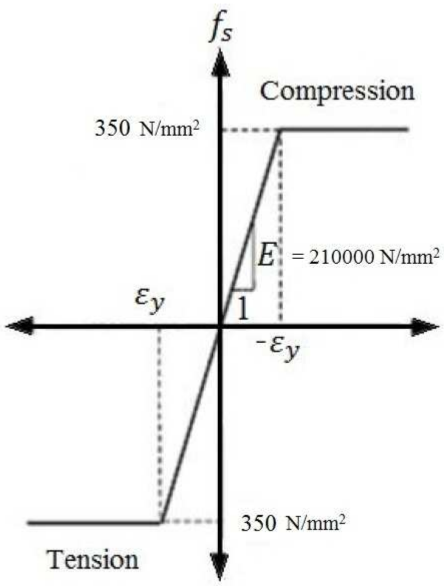

Figure 4.3 Profiled steel sheeting constitutive model

b) Constitutive Model for Dry Board

PRIMA*flex* with 12 mm thickness was utilised as a dry board in this study. The capability of the dry board to assume a structural function in the PSSDB system has been proved by previous researchers. The application of different dry boards causes different behaviours in the system. PRIMA*flex* exhibits better mechanical properties and higher strength compared with those of Cemboard, aside from PRIMA*flex*'s higher resistance in a moist environment.

The issued properties by the manufacturer for PRIMA*flex* are 8000 N/mm^2 modulus of elasticity and 0.25 Poisson's ratio. Isotropic behaviour was also assumed for the boarding. Figure 4.4 demonstrates the constitutive model released by the manufacturer. The stress–strain curve of PRIMA*flex* is almost linear and follows the short curve of plastic behaviour. The measured induced stresses in PRIMA*flex*, according to the results of the PSSDB experimental tests, are far below the elastic limit in its constitutive model. Therefore, linear part of the constitutive model was considered in the analytical model to represent the behaviour of material.

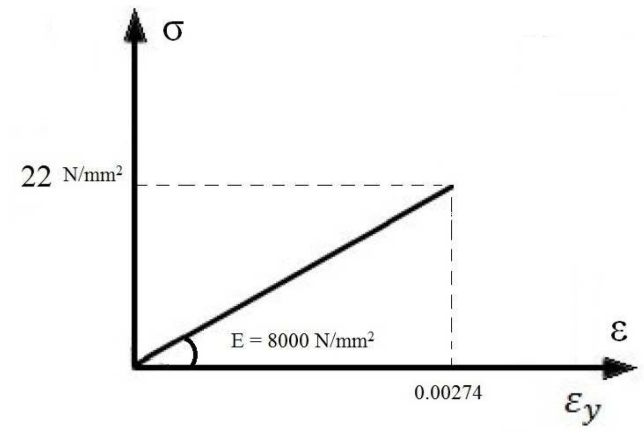

Figure 4.4 Dry board constitutive model

c) Constitutive Model for Concrete

In the ABAQUS, two failure mechanisms are assumed for the concrete, namely, compressive crushing and tensile cracking. The failure mechanisms can be derived from the Concrete Damage Plasticity option by defining *concrete compression hardening* and *concrete tension stiffening*.

The constitutive curve of the concrete for the uniaxial compression is assumed to be linear up to the point of initial yield stress. The plastic region starts from the point characterised by strain hardening and ends with ultimate strength and the falling branch of the curve known as softening of concrete (ABAQUS 2008). Strain softening can induce localised instability and non-unique solutions (Crisfield 1982). Therefore, strain softening can cause severe complexity of obtaining numerical convergence, particularly if the more reliable force norm convergence criterion is adopted (Crisfield 1982). The uniaxial tension of the concrete's stress–strain relationship is also assumed to be linear up to the failure point, which is followed by the beginning of the macro-cracking in the concrete.

Figure 4.5 shows the assumed constitutive model for the concrete in the nonlinear simulation. The Young's modulus and the Poisson ratio of concrete grade 30 were 26000 N/mm^2 and 0.2, respectively.

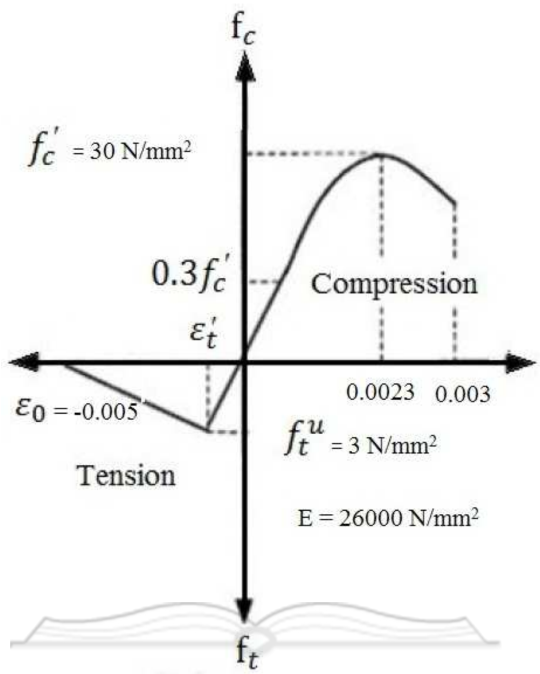

Figure 4.5 Concrete constitutive model

4.4.3 Boundary Nonlinearity

Boundary nonlinearity occurs in the analysis due to the changing boundary condition, contact or frictional behaviour. Nonlinearity in the model due to the boundary may have the following effects:

- Contact between the surfaces of the layers by load transfer
- Nonlinear external load
- Pressure load nonlinearities

In the perspective of PSSDB, boundary nonlinearity occurs in the simply supported slab subjected to the vertical loading. In the simply supported PSSDB slab, the slab ends rest on the supporting beam, so the downward movement of the ends is restricted. Boundary nonlinearity arises when the vertical load over the slab exceeds the specific point and the bottom flanges of the steel sheeting move upward. This movement is illustrated in Figure 4.6.

Figure 4.6 Upward movement of the boundaries in simply supported slab

Therefore, during simulation, restricting the vertical movement of the slab ends does not reflect the real behaviour of the structure, because the slab ends are not allowed to move upward when the slab carries the vertical load. To overcome this problem, normal contact interaction between slab ends and the supporting plate can be applied. This way, the boundary condition is assigned to the supporting plate. Although the surface-to-surface contact in the ABAQUS allows upward movement for the bottom flanges of steel sheeting, it restricts any downward movement of the slab ends.

4.5 LOADING

According to the literature (May et al. 1988), three methods of loading are mostly applied in nonlinear finite element analysis, namely, load control method, displacement control method, and arch length method. Many studies have used the load control strategy to achieve the load-displacement curve for comparison with experimental data. Application of load control produces some problems, including failure to predict the falling branch and the snap-through in the load-displacement relationship and instead comes up the horizontal line for the falling branch. Another problem in load control method is the inability to predict the closeness of the final converged increment to the expected collapse load.

The load control approach is not as beneficial as the displacement control method in nonlinear analysis, as observed when the applied load reaches the ultimate load of the structure. At this point of loading, each increment of load causes considerable increase in the corresponding displacements and leads to numerical convergence problems. Furthermore, load control method requires 40% more disk space on average, and its processing time is about 140% longer compared with the displacement control solution (Queiroz et al. 2007).

The nodal displacement control method is the option selected by many investigators to avoid the problems entailed in using the load control method. The displacement control consists of incremental procedure in the desirable component of the nodal displacement vector. This method also consists of an iterative step to correct the previously predicted solution. The displacement control method can follow the softening equilibrium paths and the equilibrium paths with weak load level variation. The proper choice of controlled nodal displacement is required.

According to Dall'Asta and Zona (2002), the best strategy for numerical applications is displacement control method. Although the arch length method could be applied instead of displacement control in case of numerical problems, the displacement method is still the best because of its displacement control capability in controlling structural evolution (e.g., control of mid-span deflection). This capability is even applicable in the case of weak load level variation as it happens near the ultimate load. Furthermore, this method can control the structural evolution in the softening equilibrium path and when the analysis encounters sudden load variation in the case of brittle failure of some materials.

4.5.1 Loading Method in the Developed PSSDB Model

The displacement control method was adopted in the developed nonlinear model because of its high capability. In this control method, if the concentrated load is applied to the structure, a direct relationship can easily be derived between the applied load and the displacement. In structural problems with remarkable nonlinear effect, finding the relationship between the applied distributed load and the associated displacement is difficult, especially for the plastic range. Thus, some strategies must be considered.

The four equal line loads of the loading beams adopted in the experimental test were utilised to simulate the uniformly distributed loading. The loading beams are arranged in such a way that the point load could be applied in the system, and then the loading beams transfer the four equal line loads to the model. Figure 4.7 demonstrates the arrangement of the loading beams in the experimental test.

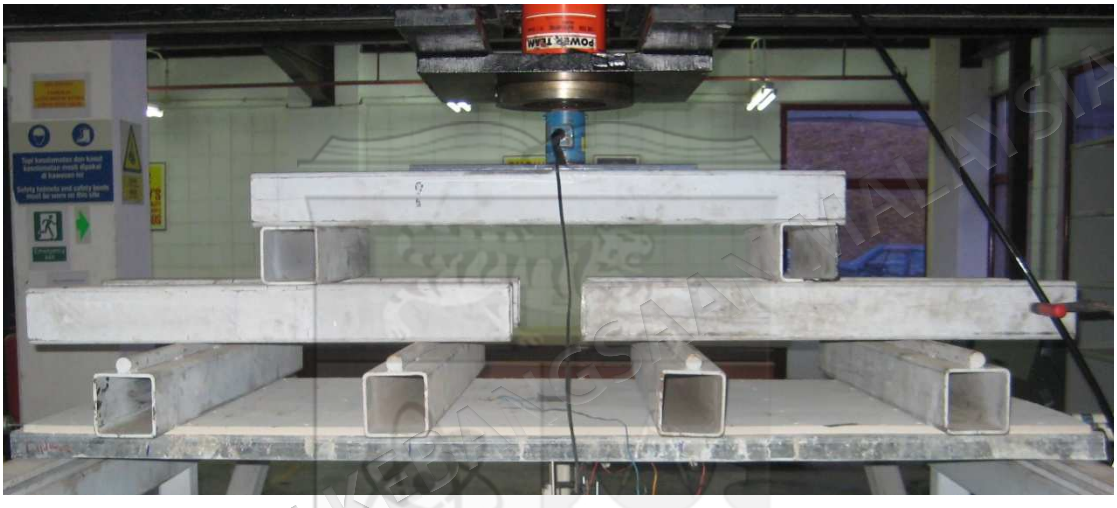

Figure 4.7 Four equal line loads in experimental test

The four equal line load strategy can be similarly adopted in the nonlinear finite element model, so the displacement control method could be easily applied by putting the displacement when applying the point load by a hydraulic jack. More details about the application of this strategy in the finite element model are presented in Figure 4.8.

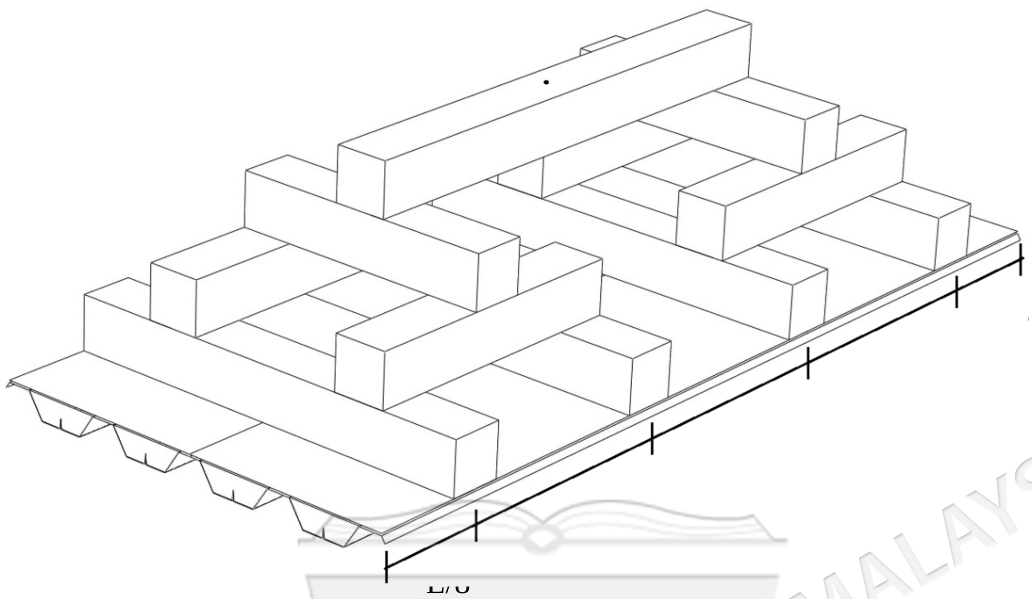

Figure 4.8   Loading in the finite element model

Figure 4.8 shows that the arrangement of the loading beams is precisely based on the experimental setup. The distances between the weightless loading beams were similar to those in the experiment and equal to L/4. The rigid element provided in the ABAQUS was used to model the load beams; therefore, the applied displacement at the demonstrated point was ideally transferred to the model.

The load beams in the model were lying on top of each other in the contact area. Surface-to-surface contact feature was applied to avoid the penetration of the beams. The lower loading beams rested over the dry board, and the same contact feature was used to transfer the applied displacement to the created model. To avoid the sliding of the loading beams, friction can be applied between the surfaces in large displacements of the mid-span. The simulated load beams can rotate during the analysis; hence, the applied displacement will be accordingly transferred to the model.

To obtain the load-displacement curve of the model's behaviour, the reaction force at the point of applying the displacement control and the deflection of interesting point (for instance mid-span) can be considered. The obtained reaction force in the displacement point can be taken as the total load exerted over the model.

4.6 BOUNDARY CONDITIONS

The membrane action is developed in the slab by restricting the horizontal movements and/or rotation of the slab at the boundaries. At the first steps of loading, avoiding the horizontal movements and/or rotation at the slab ends causes the formation of the arch from boundary to boundary, and hence improves the stiffness and flexural capacity of the slab (Zheng et al. 2008; Vulcu et al. 2010; Zheng et al. 2010). To examine the capability of the PSSDB system in the development of the membrane action and therefore benefit from the arching action, three types of boundary conditions are considered in the present study:

a) Simply supported boundary conditions
b) Pinned-pinned boundary conditions
c) Fixed-fixed boundary conditions

4.6.1 Simply Supported Boundary Conditions

Simply supported boundary condition along the specimen edges is considered for comparison. This setup indicates that the slab with simply supported condition is allowed to have outward or inward movements at the supports; therefore, the compressive membrane action is unlikely to occur in the slab. Accordingly, the load-bearing capacity of the slab is only due to the bending action (yield line theory) of the system. Figure 2.4 shows the contribution of the arching action in improving the flexural capacity in case of the development of compressive membrane action in the conventional concrete slab.

According to the experiment by Vecchio and Tang (1990), two large-scale slabs subjected to the concentrated mid-span load were considered. One slab had no limitation for the horizontal movement at supports, and the other slab was restricted for slab end horizontal movement. The obtained results from the tests showed relative lateral displacement of the slab ends without limitation on the horizontal movement.

In addition, high axial compressive forces were reported in the supports of the slab with restrained ends, which represent the formation of the compressive membrane action in the slab.

Figure 4.9 demonstrates the plan of considered supports in the first type of boundary condition. The lower flange of the steel sheeting rests over the surrounded frame, and the restriction of the movement in the slab for the pinned condition is applied to the lower flanges. Welding the lower flanges can guarantee the rigid restriction of the pinned end support for practicality (Figure 4.10).

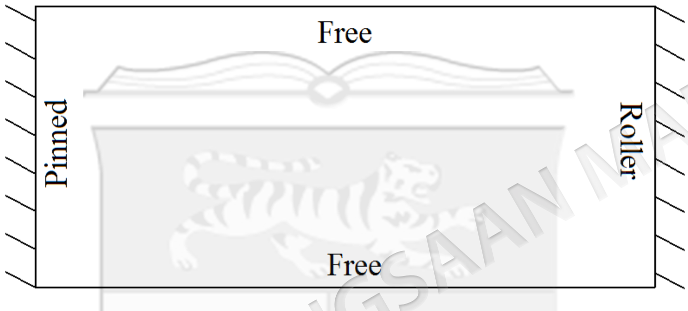

Figure 4.9 Simply supported boundary conditions

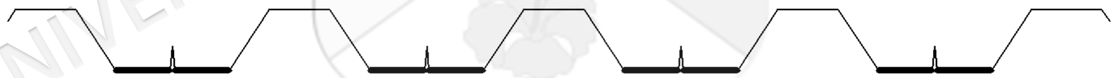

Figure 4.10 Details of the pinned boundary condition

4.6.2 Pinned-Pinned Boundary Conditions

Compressive and tensile membrane action could be developed in the slab by restricting the lateral translation and/or rotation of the slab ends. The pinned-pinned end condition is considered in examining the level of improvement of the flexural capacity of the slab. On the pinned-pinned end condition, the slab ends are free to rotate, whereas the horizontal movements at both ends are restricted for the development of the arching action in the slab.

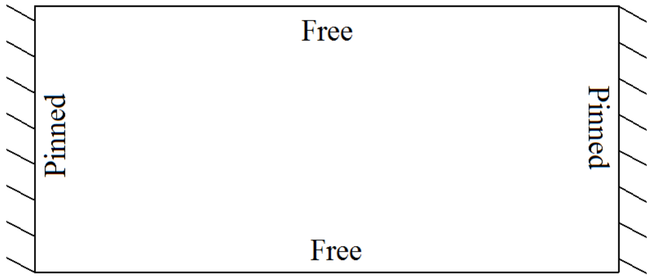

Figure 4.11 Pinned-pinned boundary conditions

Although the lower flanges of the profiled steel sheeting are restricted in the pinned-pinned end condition, the restriction of the bottom side of the concrete infill in the troughs of the steel sheeting ensures the formation of the arching action in the concrete. For practical purposes, the non-shrink grout could be employed to fill the gap between the concrete infill and the supporting frame.

4.6.3 Fixed-Fixed Boundary Conditions

According to the literature, fixed-fixed boundary condition has better function in the formation of compressive membrane action in the slab compared with the pinned-pinned boundary condition. Although the slab ends in the specimen with pinned-pinned end condition are allowed to rotate but restricted in horizontal movement, they are restricted in translation and rotation in the fixed-fixed boundary condition.

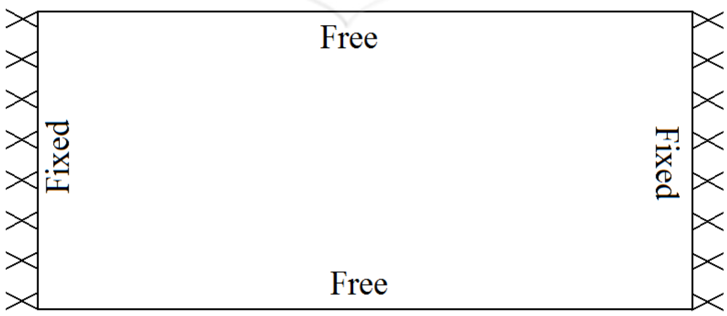

Figure 4.12 Fixed-fixed boundary conditions

Welding of the steel sheeting to the frames provides the rigid connection necessary to guarantee the restriction of horizontal movements. In the pinned-end condition, the lower flange of the steel sheeting is welded to the frame. However, in the fixed boundary condition, the lower and top flanges of the sheeting are attached to the frame by welding to ensure the absence of rotation at the ends of the slab (Figure 4.13). To restrict the end movement of the concrete infill, the non-shrink grout can also be considered.

For the modelling of the boundary conditions, the shell elements are allowed in the ABAQUS to restrict the translation and rotation, whereas the solid elements can be restricted at the nodes only for the translation. The limitation of the top and bottom sides of the solid elements prevents their rotation.

Figure 4.13 Details of the fixed boundary conditions

A quarter of the slab is considered in finite element analysis for time saving due to the symmetry of the applied load and the geometry.

4.7 INTERACTION BETWEEN THE LAYERS

In composite structures, the interaction between layers is important in transmitting the developed horizontal shear for combined performance. Considering the full interaction between layers produces no slip in the layer interface, which is not possible in reality. Conversely, assuming the absence of interaction between the components leads to the separate performance of the layers. Therefore, the obtained load-carrying capacity of the composite structure is not greater than the accumulated capacity of the individual components (Newmark et al. 1951). Figure 4.14 demonstrates the strain distribution of full interaction, partial interaction, and no interaction between layers of the structure, which are considered in simulating the real behaviour of the slab. As the figure shows, the dotted lines represent the partial interaction between the components.

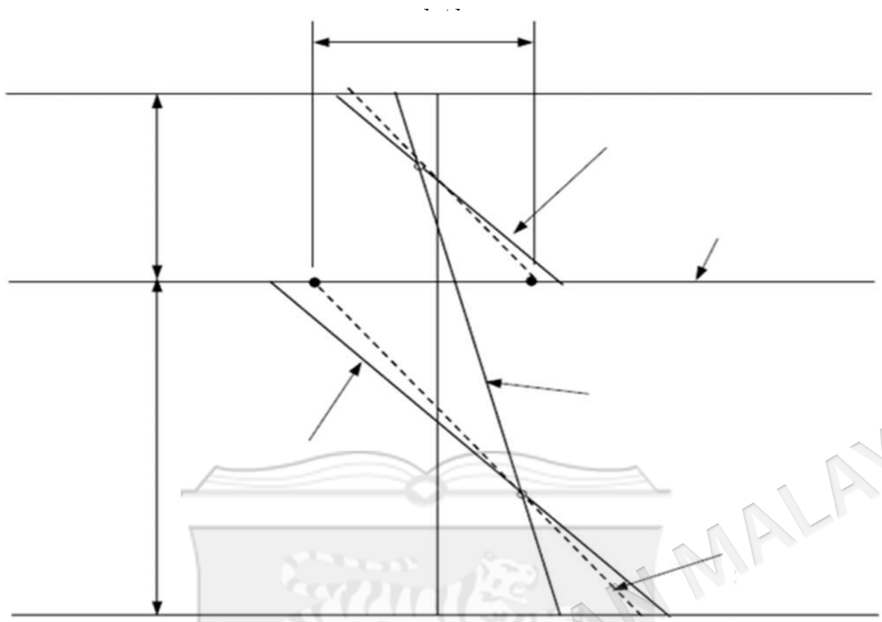

Figure 4.14 Strain distributions in composite section
Source: Ahmed 1996

4.7.1 Interaction between Profiled Steel Sheeting and Dry Board

The profiled steel sheeting and the dry board are used as the main structural components of the PSSDB system. The composite interaction between them is obtained by the self-drilling and self-tapping screws. Self-drilling and self-tapping screws are normally used as simple mechanical connectors because they are simple, quick to operate, and provide efficient and positive connection behaviour in composite structures.

The slip at the interface between layers and at the end of the PSSDB floor system is inevitable as a consequence of horizontal shear load development due to partial interaction. Incomplete interaction results in a different distribution of connector force (due to various position of connectors in span), and thus, over-design of connectors (Plum & Horne 1975).

To simulate the behaviour of the self-drilling and self-tapping screws as connectors in PSSDB, the Fasteners feature was employed. The Fasteners feature in the ABAQUS could be used to model point-to-point connections, such as a rivet, a bolt, or a spot weld. The fasteners are adopted in the selected points, and they are mesh-independent. Therefore, fining the mesh does not change the position of the fasteners. The first step is to create the attachment points at equally spaced intervals according to the positions of the connectors. The created connections should have the capability to represent the behaviour of the shear connections because the deformability and their properties in the longitudinal direction are highly important.

The provided element in the ABAQUS for this type of connection is CARTESIAN, as demonstrated in Figure 4.15. This element ensures the relative displacements and rotations that are local to the element. Twelve nodal degrees of freedom are presented in the connector element for the three-dimensional models to assist three displacements and three rotations in the element local direction of both ends of the element. The biaxial shear deformability of the self-drilling and self-tapping screws is simulated by applying the isotropic connector. Independent behaviour is achieved between the two nodes and three local Cartesian directions.

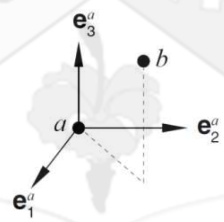

Figure 4.15 Connection type CARTESIAN
Source: ABAQUS 2008

The shear rigidities of the self-drilling and self-tapping screws for the two tangential directions are obtained from the push-out test. According to the test observations of the PSSDB floor, the slippage between the layers does not exceed 2 mm. Conversely, the obtained behaviour curve from the push-out test represents the linear behaviour for even larger displacement. Accordingly, considering the elastic behaviour for the connectors in the developed nonlinear model is reasonable (Akhand

2001). For the normal direction between the steel sheeting and the dry board, the rigid contact was defined to avoid the penetration of the layers.

4.7.2 Interaction between Profiled Steel Sheeting and Concrete

The strength of contact between concrete and profiled steel sheeting determines the behaviour and nature of failure in the composite section. Rigidity of contact has a remarkable role in effective action. Thus, decreasing the slip between concrete and steel sheeting in the contact plane could improve the composite action. Three stages in the contact between steel and concrete are remarkable: 1) the chemical bonds, 2) after the failure of the chemical bonds, and 3) after the failure of the mechanical bond provided by friction and shear studs. Deformability and the contact strength are affected by the shape of profiled steel sheeting, pre-compressing force perpendicular to the contact plane, and horizontal force restraining the transversal strain of concrete. When the pre-compressing force and concrete transverse strain restraining force between the concrete and steel sheeting increase, shear strength increases and shear strain decreases.

In the three stages of contact between the steel sheeting and concrete, the chemical bond fails before the service stage due to concrete shrinkage. Effective action would be achieved using a suitable shape of steel sheeting, such as Holorib-type sheeting. At the top of the main rib, the existence of a transverse rib improves the strength of the local pressure when the contact deforms. Furthermore, the dovetail shape of the ribs prevents separation and consequently improves the stiffness and strength of the composite section. In the support zone, due to the presence of reaction forces, the compression in the contact plane increases and leads to the enhancement of the mechanical bond and friction in contact. The failure of the slab in support is due to longitudinal cracks near the longitudinal ribs of the profiled steel sheeting. In conventional concrete slab, the magnitude of cracks is determined by the amount of horizontal and perpendicular reinforcements to the ribs. The transversal strain is prevented by these reinforcements.

The provided embossments in the profiled steel sheeting are responsible for transferring the developed horizontal shear forces between the steel sheeting and the concrete when the PSSDB floor is subjected to the bending loads. The embossments could either be simulated by the fasteners or by the tangential friction between the respective layers. Employing tangential friction results in the convergence problem in the analysis; thus, the Fasteners feature was used. Connection-type CARTESIAN was used for the Fasteners. The previously obtained stiffness rigidities of the connection between Peva 45 and the normal concrete (Shodiq 2004) were used in this study.

In addition to the tangential properties of the interaction, surface-to-surface contact was defined between the layers to ensure the absence of penetration. Concrete elements were selected as the master surface and steel sheeting elements were selected to function as the slave surface. The stiffer nature of the concrete may be the reason for the selection of it as master surfaces.

Likewise, the connection between the concrete and the dry board must be considered. No tangential friction was assumed between the surfaces, and only the normal surface-to-surface contact was defined. Similar strategies, such as steel sheeting and concrete, were assumed to minimise the contact penetration issue of the materials. Concrete was again chosen as the master surface and the dry board as the slave surface. The contact direction to the surface for the interaction between steel sheeting and concrete and between dry board and concrete has to be assigned carefully. If the normal direction was erroneously adopted, large over-closure and convergence difficulties may arise.

4.8 ANALYSIS

The development of computational devices has led to another popular method for partial interaction analysis in composite slab and beam. Finite element method is the extension of the matrix method of analysis of continuum structures. This approach includes the non-linearity of the connection behaviour and geometric and material non-linearity (Chin et al. 1993; Xu & Teng 1994), finite difference (Roberts 1985) or finite strip (Plank & Wittrick 1974; Uy & Bradford 1995) methods. Finite element approach is normally used for cold-formed, thin-walled steel sections, and is less used for thin-walled profiled steel sheeting. Some difficulties are encountered in modelling the profiled steel sheet slabs because of the section embossments and dimples, and because the profiled steel sheeting does not have a unique section in various cases.

4.8.1 Implicit or Explicit Analysis

The available methods of implicit and explicit finite element analysis in the ABAQUS are performed on the incremental load. At the end of each increment, the geometry of the structure may change or the material properties become nonlinear or yield. The stiffness matrix is regenerated after each increment of loading due to this reason.

The explicit analysis, unlike implicit analysis, does not perform the Newton–Raphson iteration to achieve the equilibrium of the internal forces and the applied external forces. In explicit analysis, the taken increments have to be quite small to achieve proper accuracy; otherwise, the solution deviates from the accurate solution. Given the huge number of increments, the analysis is time-consuming. Thus, the usage of this type of analysis is limited. For instance, explicit analysis cannot be used for problems with snap through or snap back. The analysis of the dynamic problems is computationally intensive; thus, explicit analysis is preferred in dynamic problems.

Conversely, the results obtained from implicit analysis are more accurate than those from explicit analysis. Moreover, bigger increments can be taken in implicit analysis. The drawback of this method is that the analysis must reconstruct the stiffness matrix in every iteration of the Newton–Raphson approach, which is computationally costly. Some approaches have been introduced to overcome this problem, such as the modified Newton–Raphson method (Crisfield 1996).

In the current research, the implicit type of analysis was selected in the development of nonlinear finite element modelling.

4.8.2 Nonlinear Finite Element Analysis

Unlike the finite element model of linear elastic behaviour, the modelling of nonlinear behaviour is much more intensive and requires special skills on the part of the analyst.

In this respect, excellent accomplishments in numerical techniques are necessary, but insufficient (Ramm & Stegmueller 1982).

The adopted procedure for the nonlinear finite element method is as important as the results obtained; therefore, the analysis procedure must be consciously selected.

In the linear analysis, four properties can be used for the linear problems:

a) Existence, which means at least one solution exists for the applied load;
b) Uniqueness, which means only one solution exists for the applied load;
c) Scaling, which means that when displacement (u) is obtained due to the application of load (F), the displacement (au) could be achieved due to the load (aF); and
d) Superposition, which means that when load (F) causes displacement (u) and load (G) causes displacement (v), the accumulation of the loads ($F+G$) causes the accumulation of the displacements ($u+v$).

However the issue for nonlinear problems is completely different in the following aspects:

a) Non-existence and non-uniqueness: For the applied load, none, one, or many displacements could be achieved. In the linear regime, the current value of the applied load causes the determined displacement, whereas in nonlinear problems, the unique solution of the obtained displacement depends on the entire load history.
b) No scaling: When load (F) causes displacement (u), then load (aF) may not cause a displacement (au).
c) No superposition: The accumulation of the loading may not result in the accumulation of the respective displacements.

In the nonlinear, static, structural problems could be dealt with the system of equations in the statement of the static equilibrium. In order to solve the nonlinear systems of equations, a variety of methods have been proposed in which the total applied load is divided into the smaller increments with the intention of obtaining the nonlinear solution path. At each load increment, an approximate solution is achieved. To obtain the accurate enough approximate solution, several iterations may be required.

Two available strong iterative methods are the Newton–Raphson technique and quasi-Newton technique. Both methods are incremental and iterative, and they are available in the ABAQUS/Standard. The difference between the methods is in the frequency of stiffness matrix calculation. In the full Newton–Raphson method, the stiffness matrix is generated in every iteration, whereas in the quasi-Newton method, the stiffness matrix is generated in every eight iterations (default value in the ABAQUS). This difference indicates that the quasi-Newton method saves computational effort when the numbers of iterations are the same. The most proper usage of the quasi-Newton method is when the system of equations is large, and the change in the stiffness matrix is unremarkable from iteration to iteration. Some examples of this situation may be dynamic analysis with implicit time integration and small-displacement analysis with local plasticity.

The incremental-iterative solution technique according to the Newton–Raphson method is utilised in the ABAQUS/Standard. This method is unconditionally stable, and any increment size could be taken. The Newton–Raphson finds the best displaced shape when the residuals are zero. The residuals demonstrate the magnitude and the distribution of the out-of-balance force at each degree of freedom.

$$R(u) = P - I \tag{4.1}$$

Where,

$R(u)$ represents the residuals, and P & I represent the external and internal forces.

When the calculated value of the residuals is greater than the predefined value, the structure is not in equilibrium at that position. Displacement correction is applied in the Newton–Raphson method to find the equilibrium position.

4.9 CONVERGENCE

The convergence in finite element analysis may have a variety of meanings, such as mesh convergence, convergence of nonlinear solution procedure, time integration accuracy, and solution accuracy.

In mesh convergence, increasing the number of elements leads the obtained results to approach the analytical results. At a certain level of refinement, no significant changes occurs in the resulting deflection and stresses, so they are considered as a converged solution for a particular loading, geometry, and constraint. Mesh convergence is applied for both linear and nonlinear finite element analysis. Some exceptions for the mesh convergence rule exist, such as singular solutions and localisation problems.

St. Venant's principle states that the developed local stresses in one region of the structure have no influence on the stresses elsewhere. Therefore, performing the test convergence in the region of interest in the model is possible by refining the mesh and retaining the unrefined and probably un-converged mesh elsewhere, provided they properly represent the geometry and an appropriate mesh transition is carried out. To achieve accurate solutions, converged mesh and proper convergence for the nonlinear solution procedure are highly important. Furthermore, engineering sense is required throughout the modelling, including material, boundary conditions, loads, and solution procedures. The proposed model is expected to predict the local buckling and stress distribution in the system; therefore, the actual distribution of mesh is essential, which could be obtained by convergence history and result. The proper result could be determined only by the trial and error approach (Akhand 2001).

The divergence of the solution in the ABAQUS simulation is due to many reasons, majority of which can be easily overcome. The main reason for the convergence problem in nonlinear simulations is an improper way of modelling in finite element. Some examples of the common mistakes in modelling that lead to the convergence problem are listed below.

- Defining multiple constraints in some points by contact conditions or boundary conditions;
- Not properly constraining the model;
- Incomplete or improper material properties; and
- Adopting the inadequate element for the problem.

The stress–strain relationship of concrete possesses the strain-softening falling branch. Strain softening may cause localised instability and non-unique solutions. Severe difficulty in obtaining the numerical convergence may be the notable consequence of this issue (Crisfield 1982).

Different features are provided in the ABAQUS to address the convergence issue, such as contact controls, stabilisation, automatic tolerances, convert SDI, contact interference, initial overclosure, and adaptive meshing. However, contact control and automatic stabilisation could not be simultaneously employed in the ABAQUS.

Contact directions of the surfaces must be cautiously selected; otherwise, large over-closures may result and fail to converge in the analysis. Likewise, frictional contact problems are more vulnerable to convergence difficulty than frictionless contact problems. A larger frictional coefficient generally causes more convergence problems in the analysis. The contact control and immediate onset of friction may be used to overcome the convergence problem due to contact.

The provided convergence criteria in the ABAQUS can be applied as required. In the PSSDB system, as the solution approaches the nonlinear region, the analysis slowly continues and more iterations are required to find the position in which the model is in equilibrium.

4.10 RESULTS, VALIDATION AND DISCUSSION

The proper selection of elements, loading techniques, boundary conditions, material properties, and matrix manipulation are important in analysing an actual structure. The obtained results from the finite element package must be verified by the experimental results of the same model. The recorded results obtained from the experimental test were used for verification and validation purposes. The identical model properties, boundary condition, and loading were employed in the developed nonlinear finite element model. The applied method of loading in the experimental test was precisely used in the developed finite element approach. A quarter section was used in the finite element modelling with the proper selection of boundary conditions due to the symmetric geometry of the PSSDB panel.

4.10.1 Finite Element Idealisation of the Model

Figure 4.16 demonstrates the finite element idealisation of the model and shows the experimental test. The quarter model was employed in the finite element model to save computation time.

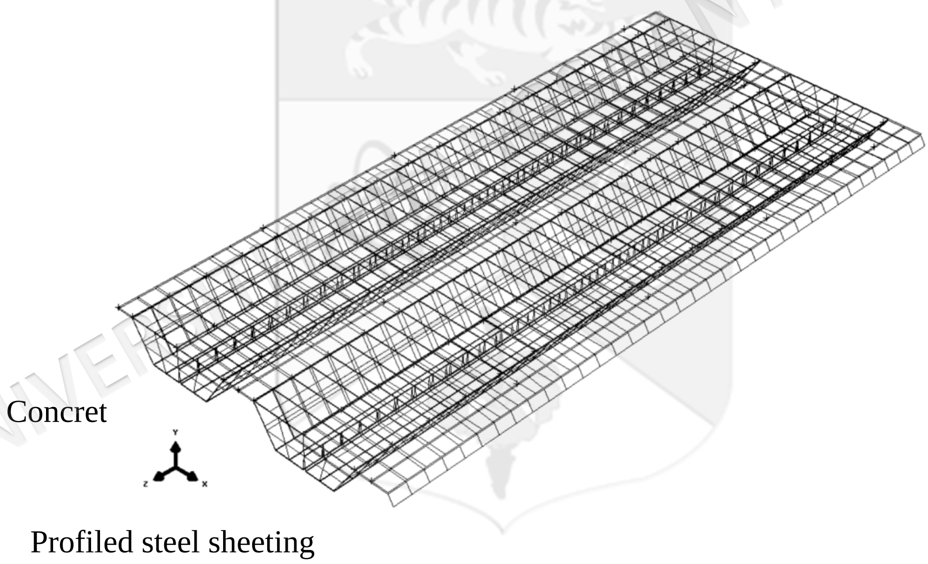

Figure 4.16 Finite element idealisation of the model

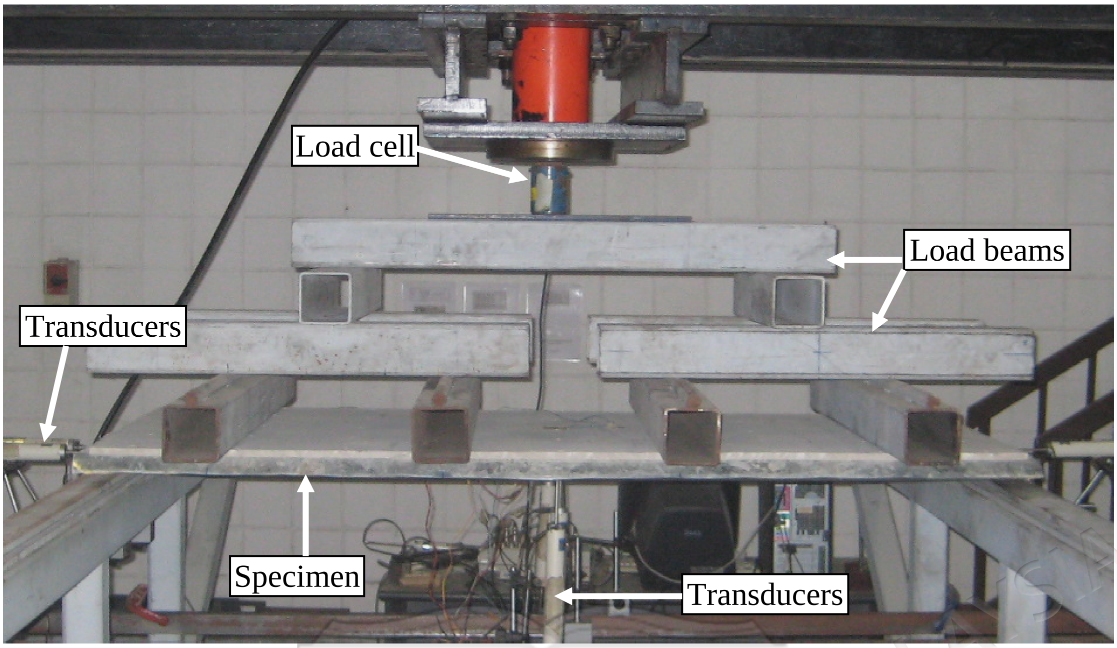

Figure 4.17 Experimental test of the simply supported PSSDB specimen

The discretisation model is in accordance with the above elements. A global mesh size of 25 mm was selected. The convergence test (Figure 4.18) showed that the selected mesh size was sufficiently small to obtain reliable results from the model.

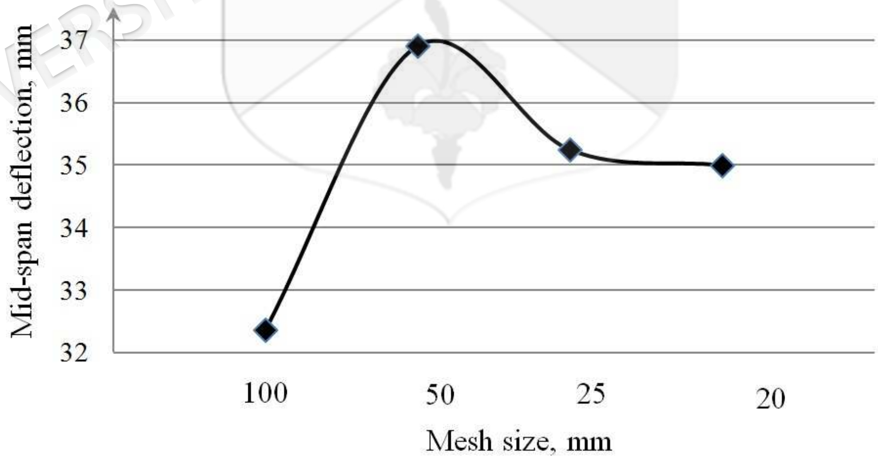

Figure 4.18 Convergence test

4.10.2 Load-Deflection Results

The experimental test results (explained in the next chapter) were used for comparison. The vertical load-mid-span-deflection curve related to the experimental test and nonlinear finite element modelling are presented in Figure 4.19. As the experimental graph shows, the behaviour of the PSSDB panel with simply supported boundary conditions is almost linear before the appearance of the local buckling at the top flange of the profiled steel sheeting in the middle region of the panel.

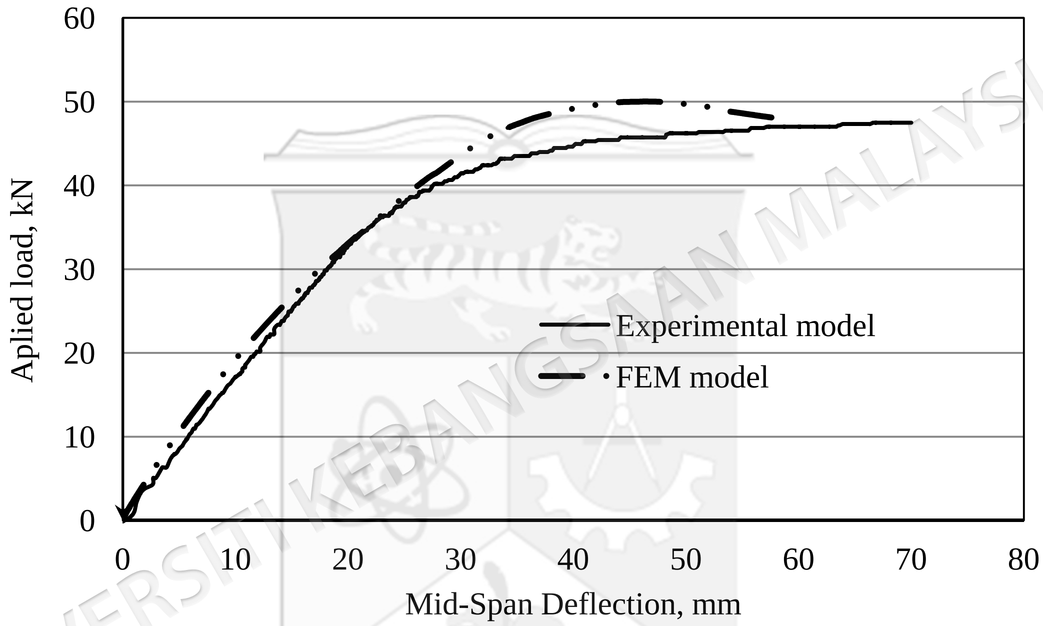

Figure 4.19 Load-deflection curves in FEM and simply supported experimental models

The load-deflection curve continues in the plastic region with no remarkable change in the applied vertical load. The limitation of the transducers in measuring the higher displacement caused the cessation of the test without achieving the tangible falling branch of the curve. Table 4.2 shows the ultimate load obtained from the finite element and experimental results.

Table 4.2 Mid-span deflection of experimental and FEM results

	Deflection (mm)	**Load (kN)**	**Difference**
Experiment	40	44.94	9.5%
FEM	40	49.21	

A minor discrepancy of less than 10% (see Table 4.2) was achieved in the obtained ultimate load-carrying capacity by the nonlinear finite element model and experimental test. This difference is lower than the maximum allowed variation of 15% in accordance with the standards (ASCE Standard 1984; American Iron and Steel Institute (AISI) 1996). Good agreement between the drawn curves can be seen in the figure for the elastic and plastic behaviour of the panels.

4.10.3 Horizontal Movement in the Supports

The mid-span vertical deflection of the simply supported floor under the bending load is associated with the horizontal movement of the floor at the supports. In the first steps of loading, the slab ends move outward. As the bending load increases, the slab ends move inward. Restricting the outward horizontal movement of the slab ends leads to the development of the compressive membrane action in the floor. Similarly, the generated inward movement of the slab ends is the consequence of the induced tensile membrane forces in the slab, which leads to the tensile membrane action when they are restricted. Figure 4.20 shows the horizontal movement of the slab ends in the floor.

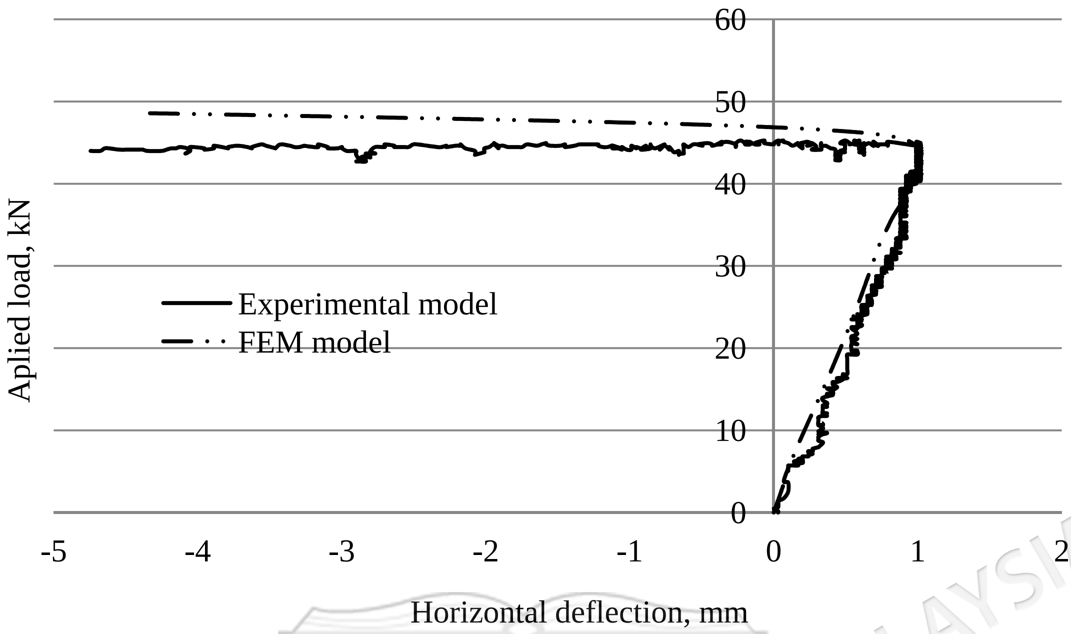

Figure 4.20 Load-horizontal deflection curves in FEM and experimental models

The recorded outward movement of the slab is about 1 mm, whereas the inward movement increases along with the increase of the mid-span deflection when the floor is in plastic phase. Good agreement between the achieved results of the experimental test and the nonlinear finite element model is demonstrated in the figure.

According to the curves in Figure 4.19 and Figure 4.20, the developed nonlinear finite element model can be employed for further research on the potential of the PSSDB panel to develop compressive membrane action.

4.10.4 Formation of Local Buckling at Webs and Top Flanges of Profiled Steel Sheeting

The early appearance of local buckling at the top flanges of the steel sheeting in mid-span causes failure of the floor. The induced stress in the lower flanges of the steel sheeting is far below the ultimate tensile strength of the steel, which indicates that the full strength of the steel is not attributed to the load-bearing capacity of the system. Figure 4.21 shows the formation of local buckling at webs and top flanges of the steel sheeting which leads to the main failure modes of the PSSDB system.

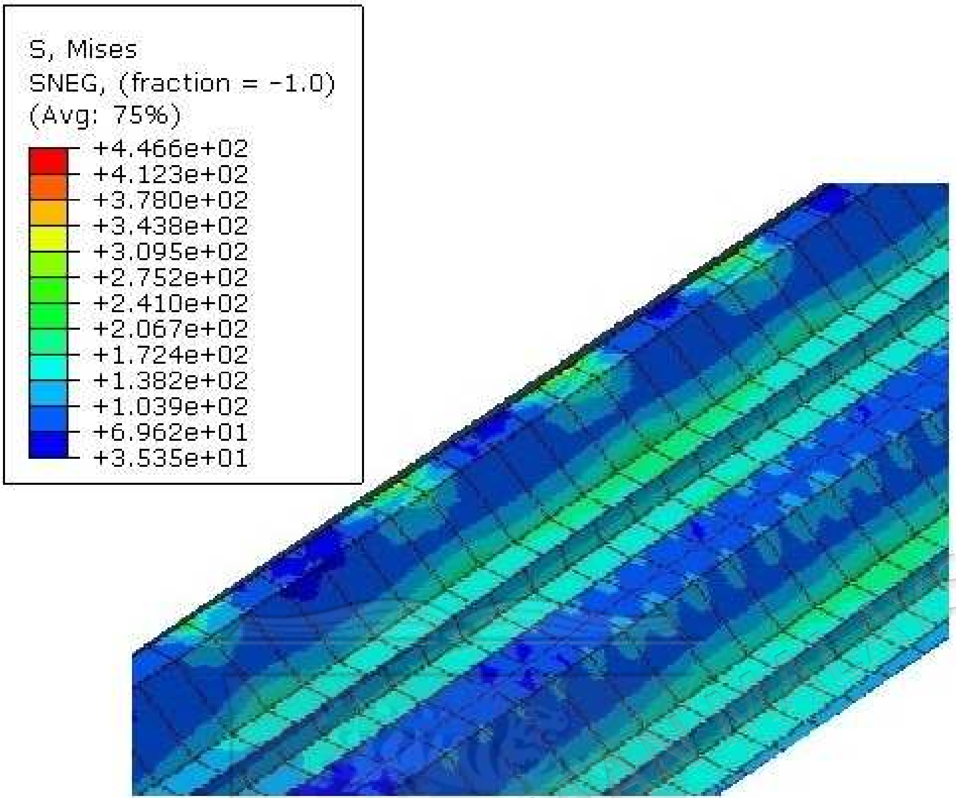

Figure 4.21 Formation of local buckling at top flanges and webs of the profiled steel sheeting

4.11 SUMMARY

To investigate the potential of the PSSDB floor system to develop compressive and tensile membrane action, a nonlinear finite element model using the ABAQUS was developed. The fundamental criteria, including material properties, element selection, method of loading, boundary conditions, and interaction between the components of the PSSDB floor for the development of the finite element model, were described in detail in this chapter.

The finite element results were verified and validated with the recorded experimental results (explained in the next chapter). The results achieved from the verified finite element modelling ensured that the generated horizontal movements at the supports of the PSSDB floor system can be considered as the sign for capability of the system to benefit from compressive membrane action, and thus experience higher rigidities and flexural stiffness. The developed nonlinear model was used for further studies in the next chapters.

CHAPTER V

EXPERIMENTAL STUDY ON THE BEHAVIOUR OF THE PSSDB FLOOR WITH VARIOUS BOUNDARY CONDITIONS

5.1 INTRODUCTION

The literature study in Chapter 2 presented the long list of experimental works conducted on floors. The aim of these studies was to investigate the contribution of membrane action in the improvement of the load-carrying capacity of floors. The development of compressive and tensile membrane action in the slab is strictly correlated to the lateral outward and inward movement of the slab ends. Thus, when one-way slab is subjected to vertical loading, the slab at the supported edges tends to move outward in the first steps of the loading. Further increase of the load causes inward movements of the slab ends. Therefore, limiting the outward and inward movements of slab against horizontal movement facilitates the development of compressive and tensile membrane action (Muthu et al. 2006; Qingxiang et al. 2010). This chapter focuses on the conducted experimental tests on the PSSDB floor slab with various boundary conditions.

5.2 EXPERIMENTAL PROGRAMME

In the experimental programmes performed in this chapter, the PSSDB floor with various boundary conditions was designed for the following purposes:

1) To measure the lateral translation of the simply supported specimen when it is subjected to bending load;

2) To consider the simply supported specimen as a control sample for the determination of flexural capacity enhancement;

3) To evaluate the stiffness and flexural capacity improvement for the specimen with pinned-pinned and fixed-fixed boundary conditions; and

4) To study the progressive collapse resistance of specimens with various boundary conditions.

The experimental test on the one-way PSSDB floor included simply supported, pinned-pinned, and fixed-fixed boundary conditions. One end of the simply supported specimen was considered as a pinned boundary condition, whereas the other end was considered a roller support to ensure the free movement of the PSSDB slab at the supports. In previous experimental tests by researchers on the PSSDB floor, the lateral movement of the slab was not considered. The supports were restrained against translation and/or rotation for specimens with respective boundary conditions.

Figure 5.1 schematically demonstrates the lateral translation of the slab at the time of mid-span deflection. The behaviour of the simply supported PSSDB floor under vertical loading should be determined to investigate the deferment of the local buckling formation in the top flanges of the profiled steel sheeting to the higher vertical load in case lateral translation is restricted. Restricting the boundaries against lateral translation leads to the generation of arching action in the slab. The developed compressive membrane action (arching action) is demonstrated in Figure 5.2.

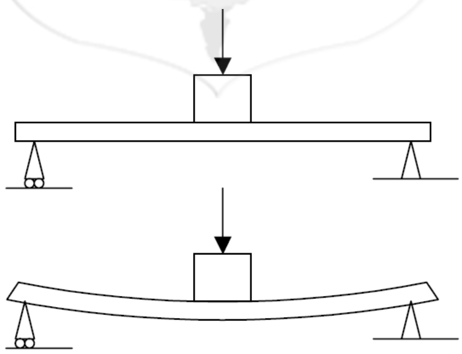

Figure 5.1 Unrestrained slab under the vertical loading

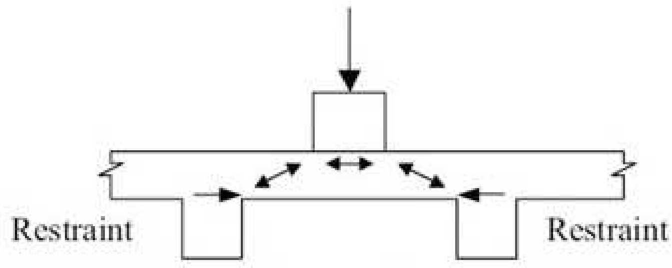

Figure 5.2 Development of compressive membrane action (arching action)

5.3 TEST SPECIMENS

Three specimens were tested in the experimental programme. For each boundary condition of roller-pinned, pinned-pinned, and fixed-fixed, one specimen was prepared. More details about the specimens are presented in Table 5.1. The specimen ID was used for the test specimens to show the boundary conditions.

Table 5.1 Specimens

Supports condition	**Length & width (mm)**	**Specimen ID**
Roller-pinned	1730×795	Roller-pinned-S1
Pinned- pinned	1730×795	Pinned- pinned-S1
Fixed- Fixed	1730×795	Fixed- Fixed-S1

5.3.1 Preparation of the Test Specimens

Locally produced material was employed to prepare the PSSDB floor specimens. 1 mm thick Peva 45 and 12 mm thick PRIMA*flex* were used as profiled steel sheeting and dry board, as shown in Figure 5.3. In accordance with the standard (DIN 18807 Part 3 1987), the minimum thickness of 0.88 mm could be used for major load-bearing elements on the floor. The selected width of the specimens was based on the width of

Peva 45, produced by the factory. More details about the cross-section of Peva 45 are presented in Figure 2.12.

.

(a) Profiled steel sheeting (Peva 45) stock

(b) Dry board (PRIMA*flex*) stock

Figure 5.3 Main components of the PSSDB system

To provide the pinned-pinned and fixed-fixed boundary conditions in the specimens, the C channel of mild steel was utilised. C channel was prepared to be used at the ends of the steel sheeting. Figure 5.4 shows that the bottom flanges of the steel sheeting were tightly clamped to the C channels, and spot welding was applied. Spot welding is an accepted welding method that can provide sufficient resistance in the overlapping metal sheet with the maximum thickness of 3 mm. The limited deformation of metal sheets in spot welding is the key advantage (Weman & Klas 2003). According to the standard (Steel Deck Institute (SDI) 2000), the minimum thickness of 0.71 mm for the steel sheeting is appropriate for welding. No weld washers are required. Proper current and voltage of the welding equipment are required to facilitate welding of the deck with no tearing.

Figure 5.4 Welding of the C channel to the Peva 45

Spot welding was applied for the attachment of C channels to the bottom flanges of both ends of steel sheeting in two specimens with pinned-pinned and fixed-fixed boundary conditions (see Figure 5.4).

After preparing the grade 30 concrete (see Appendix A), the troughs of Peva 45 sheets were filled with the concrete. The filled concrete was properly vibrated. The surface of the concrete was designed to completely fill up the troughs and to ease the attachment of the dry board. The specimens were kept with proper curing for 28 days, and then the PRIMA*flex* sheets were attached to Peva 45 using self-drilling and self-tapping screws (see Figure 5.5, Figure 5.6 (a)).

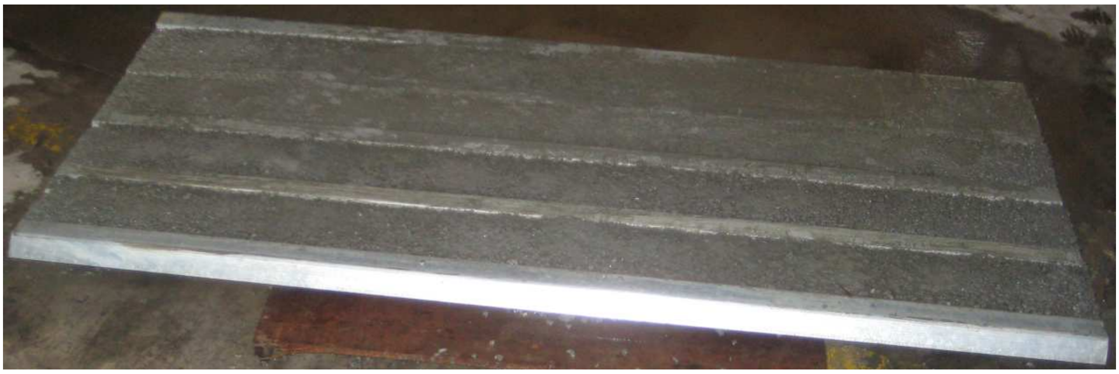

Figure 5.5 Before attachment of the dry board

Along with the casting of the mixed concrete inside the troughs of Peva 45, 150 mm × 150 mm × 150 mm cube samples of the concrete were taken for each specimen for the compression test (see Appendix B). After the samples had hardened, they were kept in water for 28 days.

The applied spot welding is responsible for restricting the horizontal movements of bottom flanges on the floors at both pinned and fixed boundary conditions. The number and the strength of the spot welds must be sufficient to resist the developed axial loads in steel sheeting at compression or tension. To restrict the rotation in the case of fixed boundary conditions, non-shrinkable grout (SikaGrout-215) was used, as shown in Figure 5.6 (c). Non-shrinkable grout contains some additives that expand during the stage of plastic and/or hardening to compensate for the shrinkage of the cementitious matrix.

(a) Specimen with simply supported condition

(b) Specimen with pinned-pinned boundary condition

(c) Specimen with fixed-fixed boundary condition

Figure 5.6 Preparation of the specimens

5.3.2 Specification of the Specimen Components

1.0 mm-thick Peva 45 and 12 mm-thick PRIMA*flex* were used as profiled steel sheeting and dry board, respectively. Grade 30 concrete in the troughs of the steel sheeting was used as infill material. Other specifications of the utilised material are presented in Table 4.1. The properties of the material are according to the manufacturer's literature. DS-FH 432 self-drilling and self-tapping screws with 30 mm length were used with screw spacing of 200 mm c/c for all specimens.

5.4 TEST EQUIPMENTS

The experimental programme was conducted in the structural lab in Universiti Kebangsaan Malaysia (UKM). The employed equipment is briefly described in the following sections.

5.4.1 Testing Rig

The testing rig with 300 kN capacity was made with mild steel C channels (300 mm × 300 mm × 9 mm) with dimensions of 4600 mm × 1200 mm × 2600 mm. The maximum load applied to the specimens in the entire experimental programme was about 70 kN, which was less than a quarter of the testing rig capacity. The experimental framework is demonstrated in Figure 5.7.

Figure 5.7 Testing rig

5.4.2 Data Logger

To measure the deflections and strains of the specimen during the test, transducers and strain gauges are required. The measuring instrument used to record the detected data by the sensors in the experimental programme was UCAM-20PC KYOWA data logger. The recorded data could be reviewed by the connection between the data logger and the PC (Figure 5.8). The data logger was carefully set according to the instruction in the catalogue. The accuracy of the recorded data by the data logger reached as low as 0.1 μm/m.

Figure 5.8 20PC KYOWA data logger

The main advantage of using the digital data logger rather than the analogue data logger is the ease of obtaining the results without the risk of mistake in transferring the data.

5.4.3 Transducers, Strain Gauges, and Load Cell

The induced movements in the specimen were measured by the transducers DT-100A (Figure 5.9 (a)) at different positions. DT-100A displacement transducers can be widely used for the measurement of the structural relative displacement or absolute displacement from a steady point. Vertical mid-span deflection and horizontal movement of the specimen at the boundaries were measured. The linear strain gauges (Figure 5.9 (b)) were applied to record the strains developed in the specimen under loading. More details about the positions of the transducers and the strain gauges are discussed in the test procedure section.

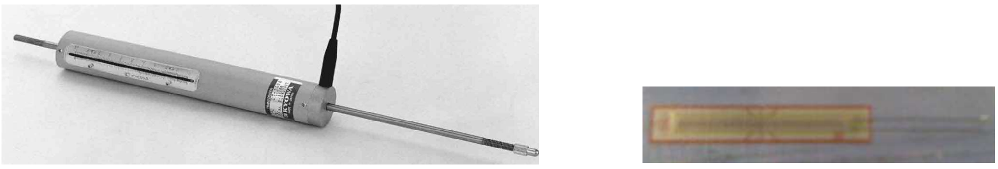

a) Transducer DT-100A b) Linear strain gauge 30 mm

Figure 5.9 The used transducer and strain gauge

The applied concentrated load by the hydraulic jack to the specimen was measured by the load cell with 1000 kN capacity. Figure 5.10 demonstrates the used hydraulic jack and load cell in the experimental programme.

(a) Hydraulic jack (b) Load cell

Figure 5.10 Loading instruments

The calibration coefficient of the load cell was accurately determined by applying a certain amount of load on it in the accurate compression machine. The accuracy of the transducers was accurately examined before application in the testing programme.

5.5 TEST PROCEDURE

Three specimens were tested in this study. One specimen was prepared for each boundary condition of roller-pinned, pinned-pinned, and fixed-fixed. The same general procedure was followed throughout the experimental tests. Some particular considerations were taken into account for the different boundary conditions clarified in the following section.

5.5.1 General Description

The supports in the testing rig were arranged in such a way that the centre of the specimen was aligned with the axis of the loading. Proper consideration was given to the setup of the specimen. To apply the uniformly distributed load on the specimen, the idea of load beams acting as equivalent line loads with equal amount was used. The applied concentrated load was transferred to the specimens in four equal line loads. Adjustment of the loading beams was performed with precise measurements to minimise the risk of un-symmetric loading. The loading beams were mild steel box sections, with the cross-section dimensions of 100 mm × 100 mm. The distances and the arrangements of the load beams are demonstrated in Figure 5.12. The load cell used to measure the applied load was located over the loading beams and exactly under the hydraulic jack.

5.5.2 Specimen with Simply Supported Conditions

In this experiment, one side of the specimen was considered a roller support to facilitate the horizontal movements of the specimens at boundaries. Positionss of transducers are shown in Figure 5.11.

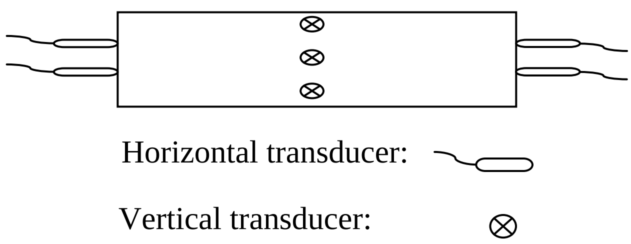

Figure 5.11 Positions of transducers in simply supported specimen

Seven transducers were installed, among which three were installed in the mid-span to measure the vertical movements and four were installed at both ends of the specimen to measure the horizontal movements. The transducers were properly installed to give a displacement that is as large as possible in the test due to the limitations.

Figure 5.12 (a) demonstrates the roller end of the specimen. The specimen ends are free to rotate.

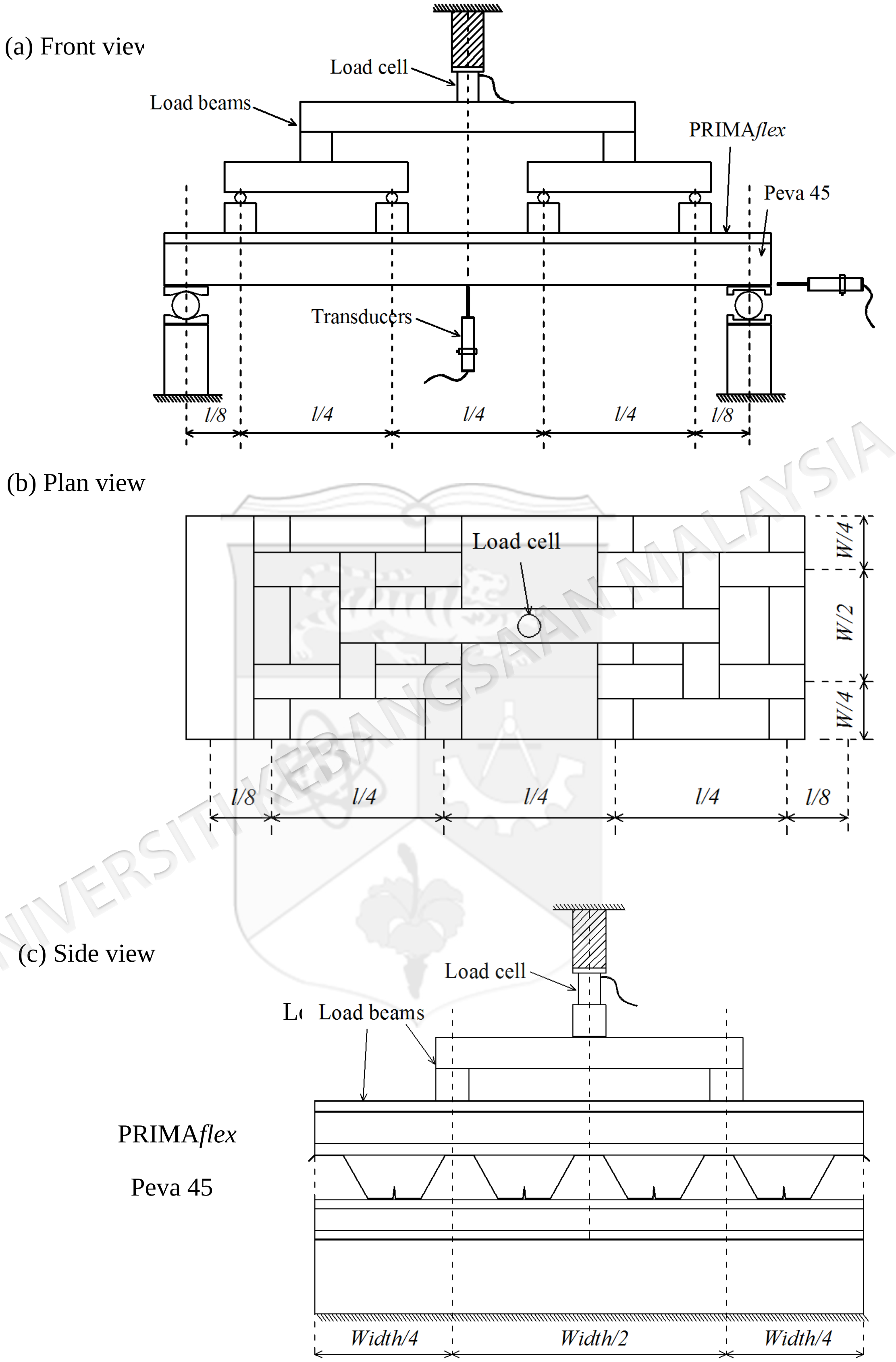

Figure 5.12 Test set-up

Three linear strain gauges were attached to the specimen to measure the strains developed in the specimen under vertical loading. The positions of strain gauges were in the mid-span of the specimen at the lower and top flanges of the steel sheeting and on the dry board (see Figure 5.13).

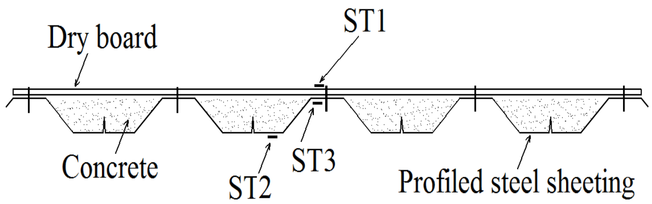

Figure 5.13 Positions of strain gauges in the simply supported specimen in mid-span

5.5.3 Specimen with Pinned-Pinned Boundary Conditions

C channels were used at both ends of pinned-pinned boundary conditions specimen due to the impossibility of welding on the testing rig. To limit the translation movements of the supports, lower flanges of C channels were welded to the supports in some spots. All the horizontal translations were avoided during the test due to the movements of the test rig elements. Five transducers were used to measure the generated vertical displacement at mid-span and to ensure the absence of horizontal displacements at both ends of the specimen. Aside from the installation of strain gauges at the mid-span, some strain gauges were properly installed near to the supports to measure the induced strain due to the development of compressive membrane action in the specimen.

5.5.4 Specimen with Fixed-Fixed Boundary Conditions

The installation of specimen with fixed-fixed boundary conditions was similar to the pinned-pinned conditions to restrict the horizontal movement. The rotation of the specimen must also be restricted, so the upper flanges of the C channel were also welded to the supports, aside from using the grout (previously explained). Other portable parts of the test rig were properly fixed. The transducers were installed in the mid-span and at boundaries similar to the pinned-pinned specimen. The strain gauge locations are shown in Figure 5.14. The strains near the supports at the top and bottom of the specimen were also recorded to study in-plane forces.

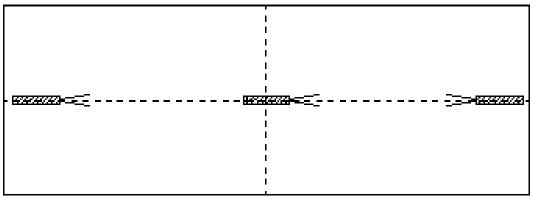

Figure 5.14 Positions of the strain gauges in the specimens with pinned-pinned and fixed-fixed boundary conditions at the top and bottom

5.6 LOADING PROCESS AND OBSERVATION

Once the calibration and installation of the equipment for recording the required data were completed, the employed electronic data logger was initiated to create the initial unloaded state of the model. Figure 5.15 illustrates the specimen and the equipment.

Figure 5.15 Testing of simply supported specimen

The progressive loading was started with the increment size of 200 N as a monotonic static load. Loading with the same increment was continued until the accumulated amount of the load was either about to exceed 80% of the predicted specimen ultimate load, or when the first plastic local buckling appeared at the top flanges of the profiled steel sheeting. From this point of test (starting point of inelastic range), the loading was further applied in such a way as to increase the 1.0 mm mid-span deflection after each step of loading. After the application of each increment, the amount of load must be held constant for at least five minutes or until the increase of the mid-span deflection is stopped. This interval was given to the specimen for micro deformation in the material. The loading process was continued beyond the maximum load and stopped once the mid-span deflection of the specimen approached the limit of the transducers. The digital data logger regularly recorded the data throughout the test.

Figure 5.16 Overall buckling of the specimen with simply supported boundary conditions

The failure of the specimen with simply supported conditions was the early appearance of local buckling at the top flanges and the webs of steel sheeting near the mid-span line. The local buckling eventually led to overall buckling, and thus, failure of the specimen. Figure 5.17 shows the formation of local buckling in the steel sheeting.

Figure 5.17 Local buckling in the profiled steel sheeting

The recorded lateral translation of the specimen ended when it was under vertical loading, which showed the outward and inward movements of the ends in the first and last steps of loading, respectively. Popping-out of the dry boards around the screws in the support area was another noticeable phenomenon in the specimens during the test because of the development of the slip between the profiled steel sheeting and the dry board. This phenomenon can be ascribed to the self-drilling and self-tapping screws, which were responsible for the transmission of the horizontal shear forces induced between the two layers of the PSSDB floor. Figure 5.18 shows the popping-out on the dry board following the inclination of screws in the support area. The developed slip in the floor was highest at the supports, and the popping-out of the dry boards was more expected in that area.

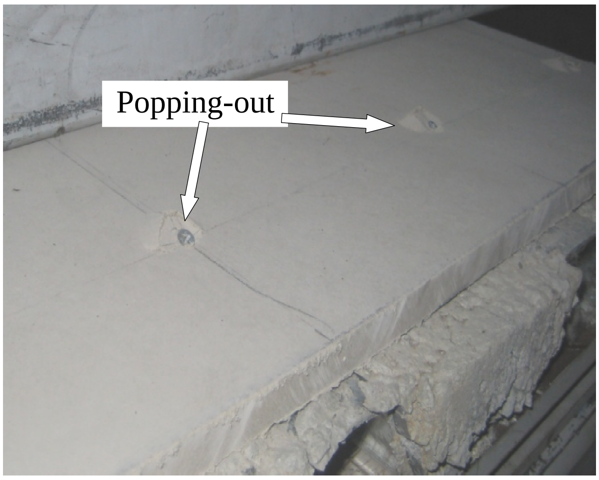

Figure 5.18 Popping-out of dry board around the screws in the support area

Similarly, the provided embossments in Peva 45 performed in the in-plane interaction between the steel sheeting and the concrete infill. The applied vertical load over the composite floor causes the development of horizontal forces, and the low tensile strength of the concrete facilitates the formation of cracks around the embossments at the support area of the specimen.

The interaction between the concrete and the steel sheeting is considered as partial interaction; thus, the slip between layers is unavoidable. Figure 5.19 shows the creation of cracks in the support area of the specimens and the slip between the layers of the composite PSSDB floor.

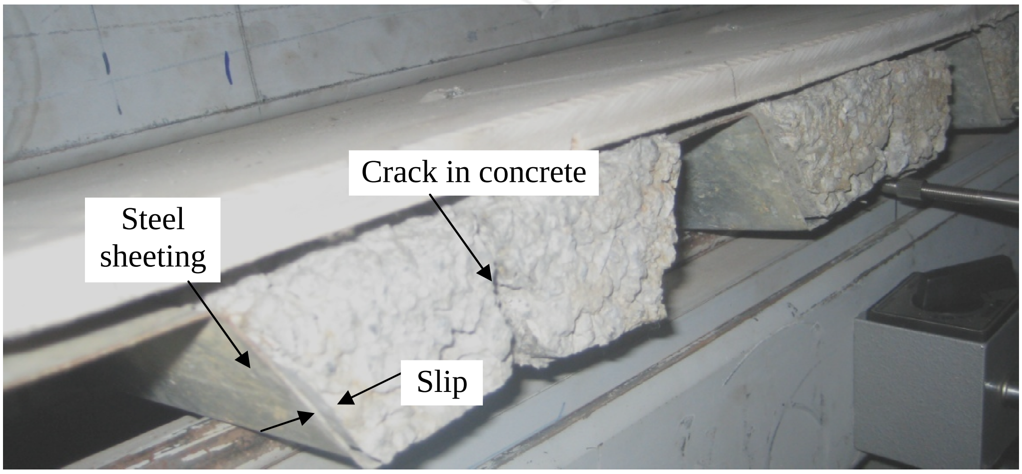

Figure 5.19 Cracks and the slip in the specimen

In the specimens with pinned-pinned and fixed-fixed boundary conditions, the specimen ends were not free to move horizontally, which led to the development of arching action in the specimens. Restriction of the horizontal movements delayed the appearance of plastic local buckling in the top flanges and webs of the steel sheeting near the mid-span.

The position of specimens with restricted boundaries in the testing rig was changed (Figure 5.20) to minimise the cantilever effect of the supports and reduce the lateral movements of the specimens. As the figure shows, the applied load from the hydraulic jack was transferred by a special loading device. Proper consideration was given to the alignment with the purpose of transferring the load through the centre line of the specimen.

Although the specimen with pinned-pinned boundary conditions was welded against end translation, the horizontal movements of the supports caused the recording of the horizontal translations in the horizontally installed transducers at the specimen ends. However, local buckling in the top flanges was still observed in the applied higher load. Loading of the specimen was performed exactly according to the aforementioned process. Sufficient time was given to the specimen in the plastic range after each load increment (1 mm mid-span deflection) to stop the increase of deflection.

Some horizontal movements were recorded in the specimen with the fixed-fixed boundary conditions. In addition, the specimen was not totally restricted against rotation at the boundaries despite welding the C channels at the top flanges to the supports. Rotation of the specimen ends occurred from the crack of the employed grout in the C channels. Welding of the top flange of steel sheeting to the support seemed necessary to avoid the rotation of the boundaries. The formation of local buckling in the specimen with this type of boundary condition was considerably delayed compared with both specimens with simply supported and pinned-pinned boundary conditions.

Figure 5.20 Setup of the specimens with restricted boundaries

Cracking of the grout in the C channel caused a slight rotation in the specimen ends. The generated tensile forces at the end of the second phase of loading caused the cutting of the spot welding at the top flange of the C channel, and accordingly led to the unexpected rotation of the supports. This occurrence could be the sign of the contribution of grout against the rotation of the specimen ends due to the high induced tensile stress in the flanges of the C channel. Although the concrete cracks at the end of the specimen were not visible, the small popping-out of the dry board in the support area showed the reduction of slip between the steel sheeting and the dry board when it is compared with those of simply supported specimen. According to the observations, the main failure mode of the restricted specimens was the formation of local buckling but at relatively higher load. However, for the higher mid-span deflections, the whole steel sheeting resisted the applied load due to the development of the tensile membrane action.

5.7 RESULTS AND DISCUSSION

5.7.1 Load Vertical-Deflection Curve

The load deflection curve obtained from the recorded results of the simply supported model (Figure 5.21) shows the linear behaviour of the specimen until the appearance of local buckling in the steel sheeting. Formation of the local buckling and material nonlinearity at the top flanges and webs brings the floor into the plastic range, and is known as the main cause of failure in the PSSDB floor system. The applied load follows the nonlinear track and finally reaches the horizontal line as a proof of the ductile behaviour of the PSSDB floor system.

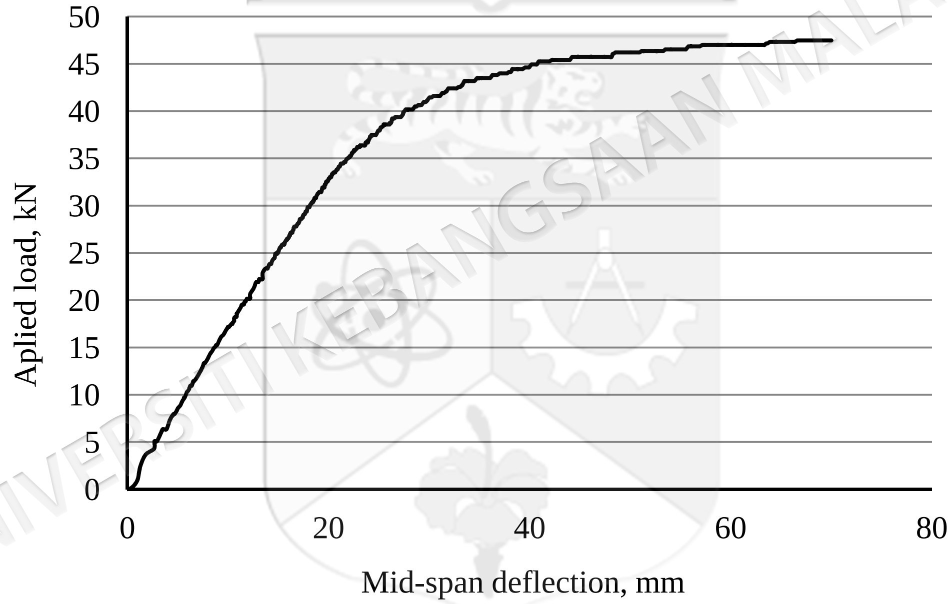

Figure 5.21 Load-deflection curve of a Model Roller-pinned-S1

The limitation of the transducers in measuring larger deflections does not allow the floor to present the falling branch of the load-deflection curve. When the plastic hinge is formed in the middle of the specimen, the applied load decreases and the specimen loses its stability.

5.7.2 Load Horizontal-Deflection Curve

Figure 5.22 demonstrates the applied vertical load against the horizontal deflection of the specimen at the roller support. The curve shows the outward movement of the specimen end for about 1 mm and then the inward movement of the ends begins. The measured data for the horizontal movement are based on the translation at one end of the specimen, whereas the other end was restricted against the lateral movement.

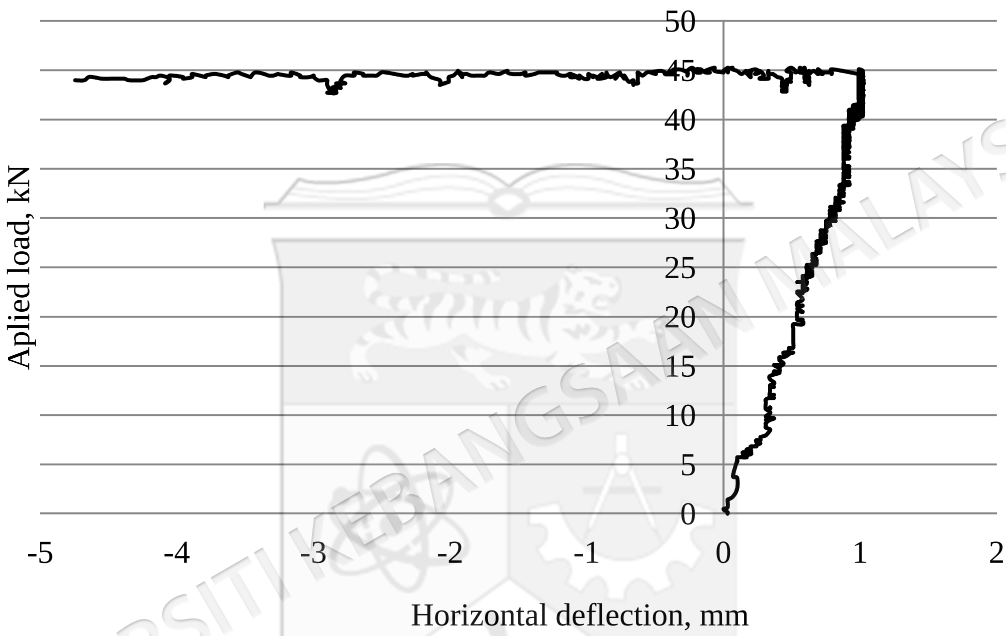

Figure 5.22 Relative lateral displacement of specimen at roller support

A comparison between Figure 5.21 and Figure 5.22 shows that the outward movement of the specimen ends occurs almost in the first phase of loading, which is fairly linear. Thus, the occurrence of local buckling and the material nonlinearity in the profiled steel sheeting initiates the inward movement of the specimen end and leads to a horizontal curve in the second phase of loading. When the outward movement tendency of the specimen is restricted under vertical loading, the compressive membrane action develops in the slab from boundary to boundary.

5.7.3 Distribution of the Strain in Profiled Steel Sheeting and PRIMA*flex* for the Simply Supported Specimen

The induced strains in the specimen were measured by strain gauges (properly attached to the specimen) in various locations (see Figure 5.13). Figure 5.23 demonstrates the recorded strains against the applied load in the simply supported specimen. The theoretical yield line of the steel in both compression and tension is also included in the figure. In addition, the yield line of PRIMA*flex* is shown in the figure.

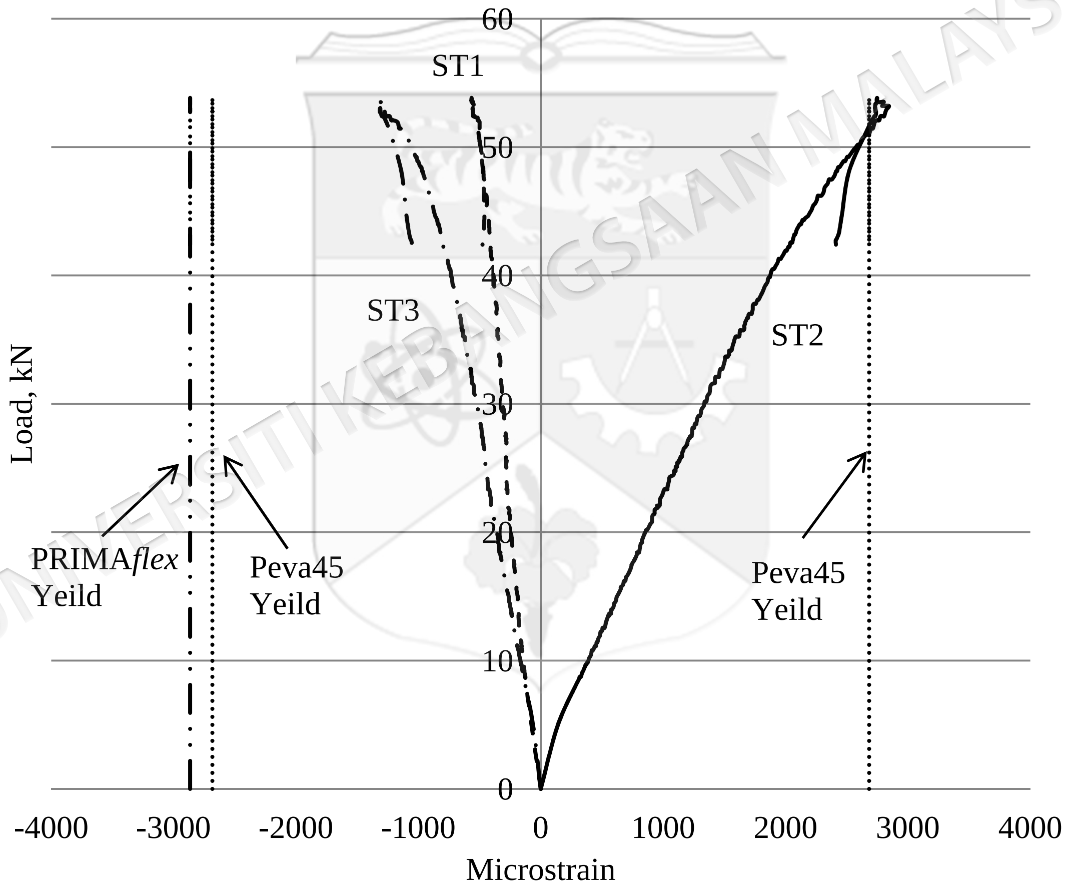

Figure 5.23 Distribution of the strain in the system for the simply supported specimen

The strain in the lower flange of the profiled steel sheeting (ST2) exceeds the yield line of the steel, whereas the recorded strain in the top flange (ST3) is far below the yield line, possibly because the formation of local buckling was not in the location of the strain gauge. Thus, local buckling in the top flanges of the steel sheeting does not let the stress in that region approach the full capacity of the steel. Furthermore, the drawn strain in PRIMA*flex* (ST1) shows a huge difference between recorded strain and the theoretical yield line.

5.7.4 Verification of the Nonlinear Finite Element Model with the Experimental Results

The developed nonlinear finite element model was verified with the experimental results obtained from the simply supported specimen. The verified finite element model was used for further parametric study on the membrane action effect on the PSSDB floor. Figure 4.19 and Figure 4.20 show the details of the agreement between numerical and experimental results (within 91% accuracy).

The experimental tests were conducted for the specimens with pinned-pinned and fixed-fixed boundary conditions as well. However, the results obtained from the specimens with these types of boundary conditions were inappropriate for verification as the restriction of translation and rotation of the boundaries in the respective boundary conditions was not fully achieved. Despite the incomplete boundary restraint, the bending stiffness and the load-carrying capacity of the specimens improved because of the partial development of their compressive membrane action. The results achieved from the restrained specimens tests are reported in the following sections.

5.7.5 Load-Vertical Deflection of the Pinned-Pinned Specimen

Regardless of the slight horizontal movements of supports, the load-bearing capacity of the specimen with pinned-pinned boundary conditions has improved due to the effect of the compressive membrane action. Figure 5.24 presents the results obtained from the experimental test on the specimen with pinned-pinned boundary conditions. The drawn results are the applied load against the mid-span deflection. The load-deflection curve of the specimen with simply supported condition is also included in the graph for the sake of comparison.

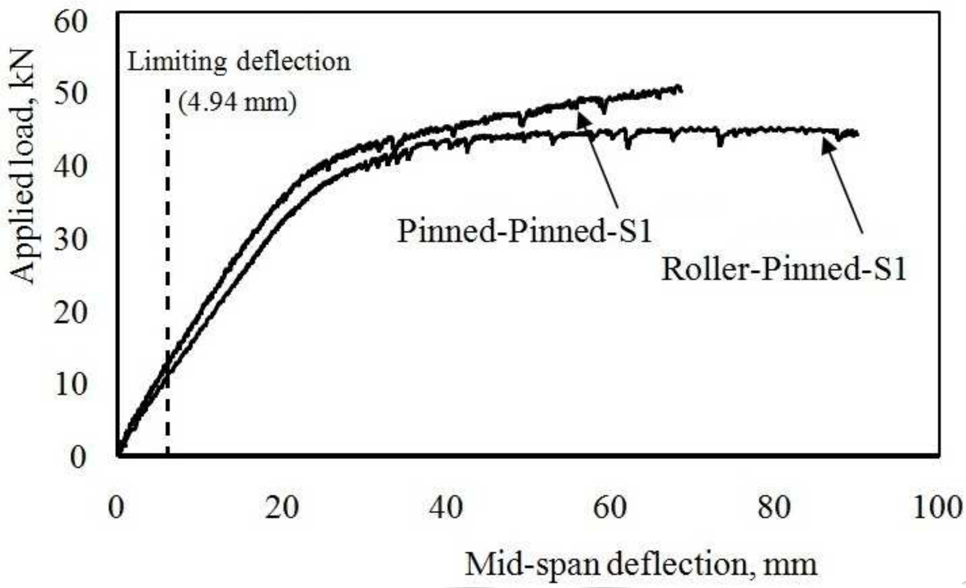

Figure 5.24 Load-deflection curve of Models, Roller-Pinned-S1, Pinned-Pinned-S1

The demonstrated results prove that restriction of the outward translation of specimen boundaries improves the flexural stiffness and load-bearing capacity of the specimen. This improvement is attributed to the arching action in the specimen. As the figure illustrates, due to the nature of the materials, ductile failure was observed in this type of specimen as well. As described earlier, the formation of the local buckling in the pinned-pinned specimen was postponed to the higher vertical load. The enhancement of the specimen is in both elastic and plastic regions. Given that the measurement of the mid-span deflection for larger displacement was limited to the transducers' maximum limit, the loading was stopped when the transducer hit the maximum level. The tensile membrane action is developed in the specimen for further applied loading.

5.7.6 Developed Strain in the Peva 45 for the Pinned-Pinned Specimen

In the specimen with pinned-pinned boundary conditions, due to the restriction of the horizontal movement at the boundaries, the in-plane stresses were induced in the profiled steel sheeting near the supports. Conversely, in the specimen with simply supported conditions, the generation of the horizontal movement leads to no in-plane stress in the sheeting at the support area. Figure 5.25 shows the in-plane strain in the lower flange of the profiled steel sheeting at the support area against the applied load.

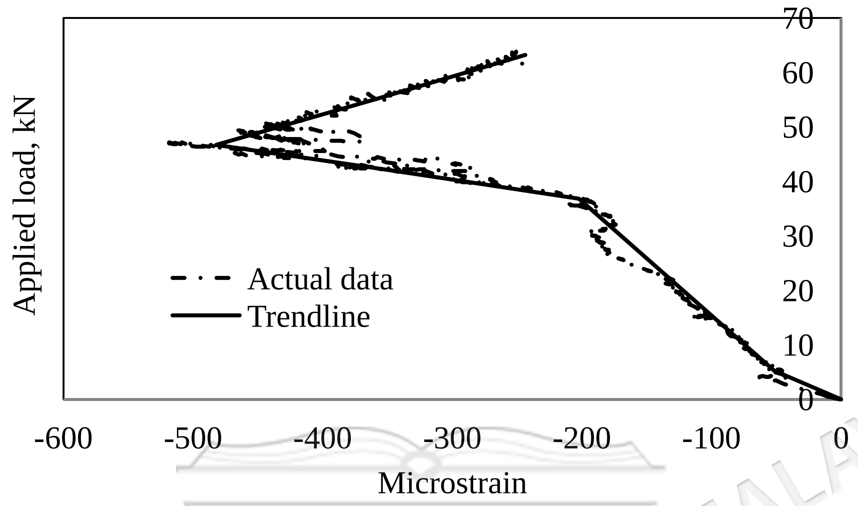

Figure 5.25 In-plane strain in the profiled steel sheeting at the support area for the Model Pinned-Pinned-S1

The trend of the strain in the graph illustrates the development of a compressive strain in the sheeting due to the formation of the arching action in the specimen. The compressive strain increases as the load increases. The developed stresses in the steel sheeting at the supports are taken by an adequate amount of spot welds. The reduction in the in-plane stress is due to the deformation of the arch configuration from boundary to boundary at larger displacement. Accordingly, the compressive in-plane stresses in the steel sheeting decreases to put the system in the tensile membrane action phase. The loading was stopped before the development of tensile membrane action due to the aforementioned transducer limitation.

5.7.7 Load-Vertical Deflection of the Fixed-Fixed Specimen

Restricting the end supports of the specimen against both rotation and translation is an essential factor in the fixed-fixed boundary condition. Figure 5.26 shows the obtained load-central deflection for various boundary conditions of simply supported, pinned-pinned, and fixed-fixed.

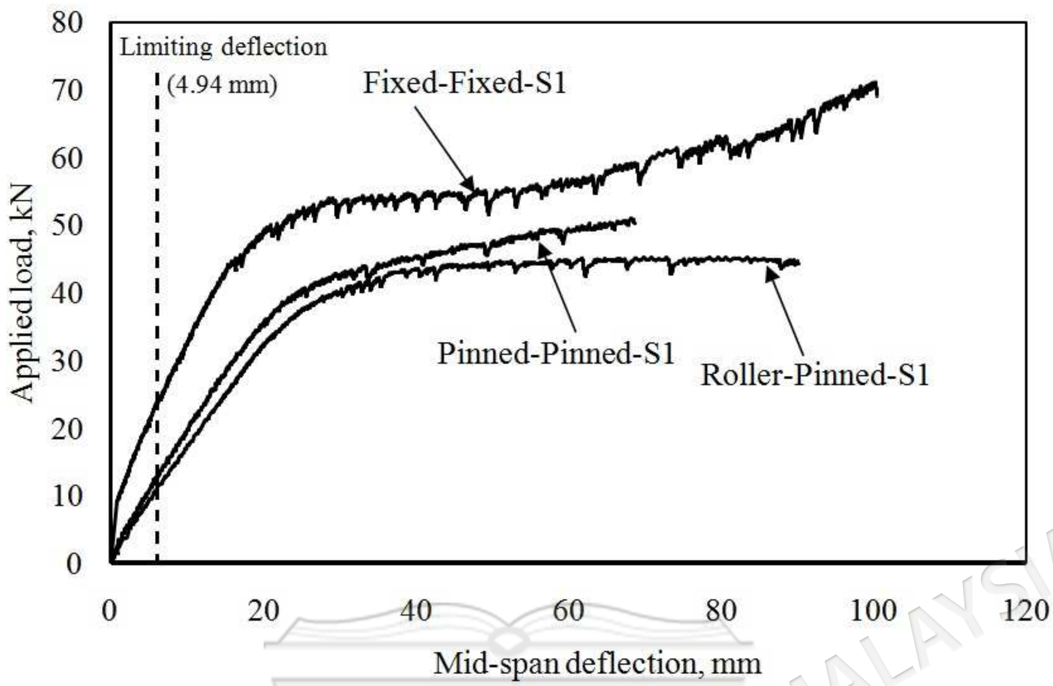

Figure 5.26 Load-deflection curve of Models, Roller-Pinned-S1, Pinned-Pinned-S1, Fixed-Fixed-S1

The achieved results show the enhancement of the flexural capacity of the specimen at different stages of the loading. As the figure demonstrates, the restriction of the rotation in the boundaries, in addition to the restriction of translation, paves the way for the better development of compressive membrane action in the system. Once the load reaches the ultimate load of the compressive membrane phase, the curve continues horizontally until the development of the tensile membrane action in the system. Further loading in the tensile membrane phase is carried only by profiled steel sheeting alone. The load in this phase is increased until the in-plane tensile stresses in the whole section of the steel sheeting reach the plastic range. To achieve the fully plastic section of the steel sheeting, sufficient spot welds must be provided in the supports.

5.7.8 Developed Strain in the Peva 45 for the Fixed-Fixed Specimen

Aside from the load-central deflection, the recorded strain at the support area of the steel sheeting in the bottom flange also can be considered as a proof for the development of the compressive membrane action (see Figure 5.27).

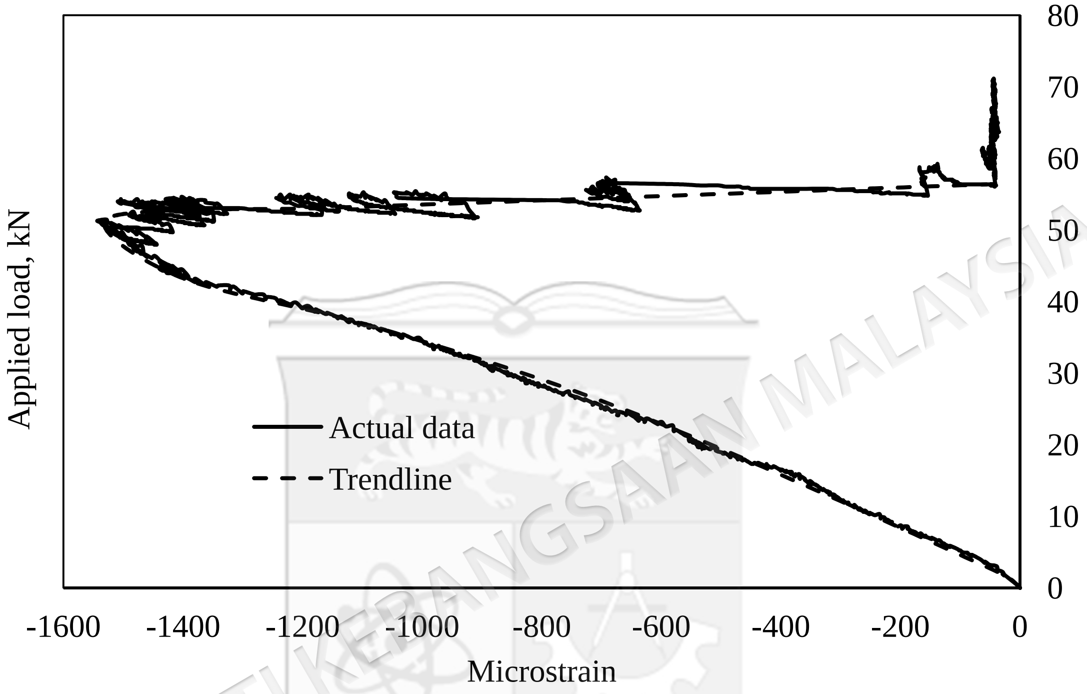

Figure 5.27 In-plane strain at bottom flange of profiled steel sheeting at support area for Model Fixed-Fixed-S1

Figure 5.27 illustrates the developed strain in the bottom flanges of the steel sheeting (at the support area) against the applied load. As mentioned in the description of the previous figure, the progressive load in the specimen caused the increase of in-plane stresses in the support area due to the formation of the arching action. The applied load increases up to the deformation point of the arch. The induced in-plane stresses then starts to decrease. The horizontal region of the load-deflection curve (see Figure 5.26) represents the deduction of the in-plane stresses. Further increase of the load is based on the development of the tensile membrane action, and thus the compressive in-plane stresses in the slab changes to tensile stresses.

The early appearance of the local buckling in the specimen with simply supported boundary conditions, as mentioned, is the main failure mode. Given the creation of plastic local buckling in some points at webs and top flanges of the steel sheeting, the in-plane stresses in the top flanges of the simply supported specimen (obtained from the recorded strains) are far below those of the compressive capacity of steel. Figure 5.28 shows the developed strain at the top flange of the profiled steel sheeting for both simply supported and fixed-fixed boundary conditions. According to the observation during the test, some small local buckling was seen when the load over the specimen was approximately 48 kN. This observation can also be recognised as the initiation point of the plastic behaviour in the system. The plastic behaviour was followed by the horizontal curve after the formation of local buckling and before the initiation of the tensile membrane action. The recorded strain for the fixed-fixed boundary conditions shows that the stress at the top flanges of the steel sheeting exceeds the theoretical yield stress of the steel, which is demonstrated in the figure. Conversely, the induced stress in the top flanges of the profiled steel sheeting in the simply supported specimen is far below that of the theoretical capacity of the steel sheeting.

Accordingly, the restriction of the specimen against the rotation and translation at the supports postpones the formation of the local buckling in the PSSDB system, and thus paves the way for employing the hidden capacity of the steel sheeting, is a fair conclusion.

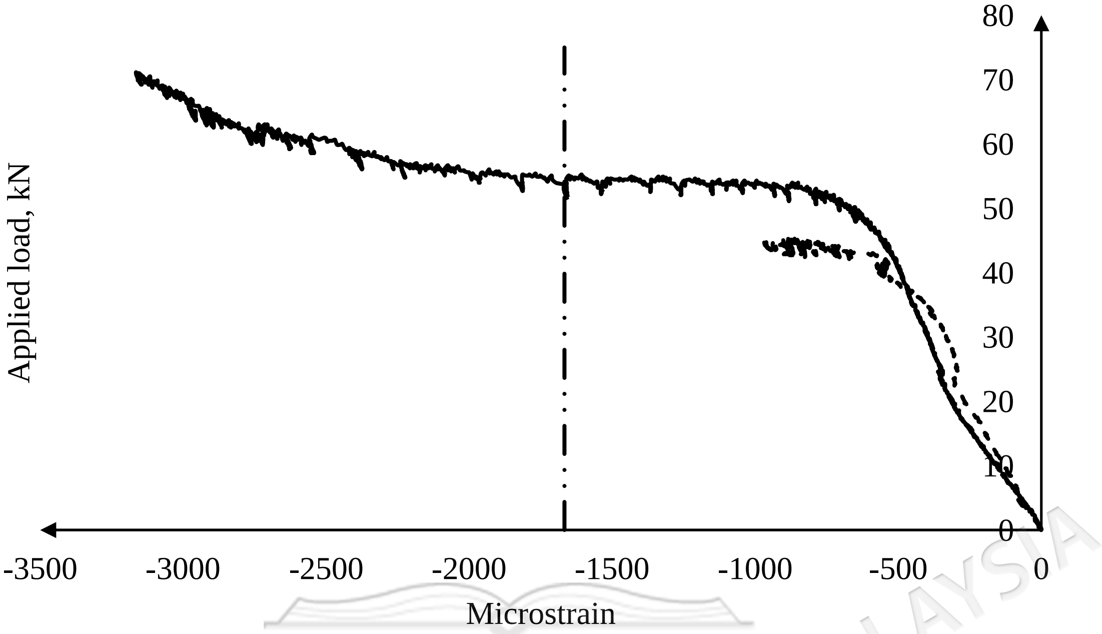

Figure 5.28 Strain at the top flange of the profiled steel sheeting for simply supported specimen and fixed-fixed boundary specimen

5.8 LOAD CARRYING CAPACITY OF THE SPECIMENS

The results obtained from the experimental programme for specimens under various boundary conditions are summarised in Table 5.2 for the comparison. The table includes the deflection limit load, which is the serviceability limit state deflection according to BS 8110 Part 1 (1997). Chapter 6 dis on limit in detail. The value of L/350 was used for the serviceability deflection in this study.

As the table shows, following the restriction of the rotation and the horizontal movement of the specimen ends, the deflection limit load improved by up to 27.38% and 147.86% for the pinned-pinned and fixed-fixed specimens, respectively. The enhancement of the specimen rigidity due to the development of the compressive membrane action is also presented in the table (see the calculations in Appendix C).

Table 5.2 Summary of the experimental tests results

Specimen	Dimensions (mm)	Deflection limit load (kN)	Improvement (%)	Rigidities (kN/mm)
Roller-pinned	1730×795	8.40	N/A	1.7
Pinned-pinned	1730×795	10.70	27.38	2.16
Fixed-fixed	1730×795	20.82	147.86	4.21

5.9 SUMMARY

This chapter focused on the conducted experimental programme on the PSSDB floor system with various boundary conditions to investigate the possibility of the formation of the compressive membrane action (arching action) in the PSSDB system. The main observations extracted from the carried out experimental study could be summarised as follows:

- The simply supported specimen test revealed that the vertical load over the PSSDB floor induces the horizontal movements at the roller support. Thus, the PSSDB floor has the capability to benefit from the formation of the arching action.

- The horizontal movements of the roller support in the simply supported specimen were restricted in the pinned-pinned specimen, and the partial development of the compressive membrane action was achieved. The improvement of the specimen load capacity occurred despite the slight lateral movements of the supports. A 27.38% improvement of the specimen load capacity was achieved. Meanwhile, the system had potential for the development of the tensile membrane action in the second steps of loading.

- In addition to the restriction of the lateral translations, the rotation of the specimen ends were also limited in the fixed-fixed specimen, and accordingly the load capacity of the floor was enhanced remarkably by up to 147.86%. The appearance of the local buckling at the top flanges of the steel sheeting was delayed to higher vertical load in the specimens with pinned-pinned and fixed-fixed boundary conditions.

CHAPTER VI

PARAMETRIC STUDIES ON PSSDB FLOORS WITH A SIMPLE SPAN

6.1 INTRODUCTION

This chapter focuses on the conducted parametric studies on the PSSDB floor to distinguish the effect of the concrete infill and components' thicknesses on the load-carrying capacity of the floor, as well as on the formation of the membrane action in the floor. In this regard, the previously validated ABAQUS model in Chapter 4 was employed. For comparison purposes, the serviceability limit state deflection provided in BS8110, 1997 was taken into account.

6.2 CODE REQUIREMENTS FOR THE DEFLECTION

The main aim of limiting the state design is to ensure that the structure will not become unfit for the defined applications during its design life. In other words, the structure does not approach the limit states. The structure could be unfit for use in many ways, such as excessive forms of bending, compression, shear, deflection, and cracking. All these mechanisms are limit states, and their effect on the structure must be measured separately. Among the mentioned limit states, the deflection and cracking mainly have an effect on the appearance of the structure, whereas other limit states such as compression, bending, and shear may cause the partial or complete failure of the structure. The limit states that have an effect on the appearance of the structure are termed as serviceability limit states; meanwhile, other limits causing the failure of the structure are categorised as ultimate limit states. However, the experience only provides judgment about considering the proper limit states in particular structures. The structure must be initially assessed for the most critical limit states, and then the remainder of the limit states must be checked. In the design of concrete slabs, the serviceability limit state of deflection is normally critical and is thus a central consideration (Arya 2009).

Codes of practice provide the permissible deflection for various types of floors. The controlling factor in many structures is deflection limitation rather than stress limitation. Calculation of the deflection presents the effect of the structural components in the system. However, the importance of controlling the deflection in the floors may be listed as follows:

i. Adequate stiffness is essential in the floor to minimise the deflections that may lead to damage to the other attached partitions, as well as the construction elements that are susceptible to damage in the large deflections.

ii. Noticeable deflection of the floor may cause a sense of collapse or safety concern among the occupants.

iii. The deflection is used as a measure of the undesirable vibration of floors; hence, it must be controlled.

In accordance with BS 8110 (see Appendix D), the visible structural members should not have sagging deflection larger than L/250, where L is either the span or the length of the cantilever. If the structural element is not visible, this limitation is normally not critical. Conversely, BS 8110 provides the limit of L/500 or 20 mm (whichever is lesser) for the brittle materials, and L/350 or 20 mm for non-brittle partitions or finishes. The provided criterion in BS 8110 (1997) is for the stiffness control of the floor system concerning the serviceability.

According to aforementioned criteria, the PSSDB floor falls into the second category and therefore, the serviceability limit state deflection for the considered floors in this chapter and in the next chapter was assumed to be L/350.

6.3 EFFECT OF CONCRETE INFILL

The main structural elements of the PSSDB system at the time of its inception were profiled steel sheeting and dry board. As described earlier, some infill materials were used with the intention of only improving the sound proofing and fire resistance properties of the system (Wan Badaruzzaman et al. 2003). Shodiq et al. (2003) first introduced the concrete infill in the system to fulfil both structural and non-structural purposes. The theoretical and experimental research conducted by him proved the effect of concrete infill compared with the original PSSDB system without infill. The mid-span deflection of the PSSDB floor was reported to be reduced by up to 19% due to the employment of the concrete infill in the steel sheeting.

The reasons behind the noticeable effects of the concrete infill may be the attribution of concrete to carry the compressive stresses in the section and partly overcome the weakness of profiled steel sheeting to resist the local buckling. The fire resistance of the system also increased to two hours compared with one hour of the system with no infill material.

In addition to carrying the bending load in the system, the concrete infill can resist the induced in-plane forces. The contribution of the concrete infill in resisting the in-plane forces may improve the possibility of arching action formation in the PSSDB floor system. This outcome can be achieved by limiting the slippage of the concrete infill in the troughs of the steel sheeting with restrained ends. To investigate the effect of the concrete infill in the development of the membrane action in the PSSDB system, the validated model in Chapter 4 was employed.

6.3.1 Models

Two different groups of models were considered for the PSSDB floor system with a practical length of 3000 mm and with and without concrete infill. Moreover, to explore the concrete effect, various boundary conditions were considered, including those of the simply supported, pinned-pinned, and fixed-fixed. The material properties are exactly in accordance with the material characteristics in Table 6.1. Table 6.2 presents information about the models and the dimensions.

Table 6.1 Details of the materials

	Thickness / Diameter (mm)	Width & Length (mm)	Modulus of Elasticity (E, N/mm^2)	Ultimate Strength (N/mm^2)	Weight of Covered Area (N/m^2)
Profiled steel sheeting (Peva 45)	1.0	795×1730	210×10^3	350	130.77
Self- drilling and self-tapping screw	4.2	30.0	----	----	----
Dry board (PRIMA*flex*)	12.0	795×1730	8030	22	172
Infill (Concrete grade 30)	Infill	Infill	25743	30	606.4
Topping (Concrete grade 30)	50	795	25743	30	1125

Table 6.2 Models for the concrete infill effect

Name of Models	Dimensions (mm)	Description	Boundary Condition
PSNIRP	3000×795	Practical Span with No-Infill and Roller-Pinned boundary conditions	Pinned Roller
PSNIPP	3000×795	Practical Span with No-Infill and Pinned-Pinned boundary conditions	Pinned Pinned
PSNIFF	3000×795	Practical Span with No-Infill and Fixed-Fixed boundary conditions	Fixed Fixed
PSWIRP	3000×795	Practical Span With Infill and Roller-Pinned boundary conditions	Pinned Roller
PSWIPP	3000×795	Practical Span With Infill and Pinned-Pinned boundary conditions	Pinned Pinned
PSWIFF	3000×795	Practical Span With Infill and Fixed-Fixed boundary conditions	Fixed Fixed

The pinned-pinned boundary conditions in the generated models are based on restricting the lower flanges of the steel sheeting against translation in the pinned models. The models with fixed-fixed boundary conditions were created by restricting the translation of the top and bottom flanges in the sheeting. In the models with concrete infill, the bottom sides of concrete in the troughs were limited against the outward movement in both pinned and fixed boundary conditions. For the purpose of practical applications, non-shrinkable grout can be employed after the installation of the PSSDB panel and welding of the steel sheeting flanges to the surrounding frames. Other features of the models such as the interactions and loading are according to the validated model.

6.3.2 Results and Discussion

The load-carrying capacities of the simply supported floors with and without concrete infill are presented in the form of applied load against the mid-span deflection in Figure 6.1. The serviceability limit states deflection (8.57 mm) according to the span length of 3000 mm is also presented in the figure.

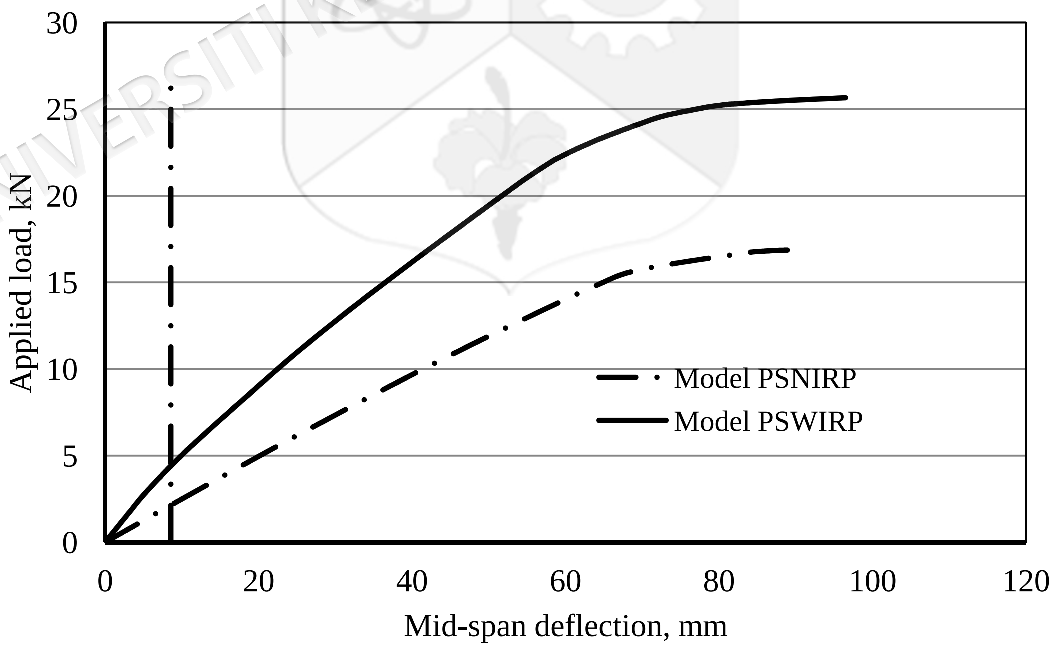

Figure 6.1 Load-deflection curves of Models PSNIRP and PSWIRP

The effect of concrete infill is shown in Figure 6.1. The flexural rigidity as well as the ultimate flexural capacity of the floor with concrete infill increased. More precisely, the obtained results of load-carrying capacities in the serviceability limit state deflection of 8.57 mm are 2.14 kN and 4.41 kN for Models PSNIRP and PSWIRP, respectively. The improvement of the load capacity due to the concrete infill is approximately 106%. The attributed reasons for this improvement were mentioned previously.

Concrete infill in the steel sheeting not only improves the pure bending strength of the simply supported PSSDB floor, but also contributes to enhancing the floor's flexural strength in terms of the development of the compressive membrane action. Figure 6.2 shows the load-deflection curves achieved from the models under consideration in Table 6.2.

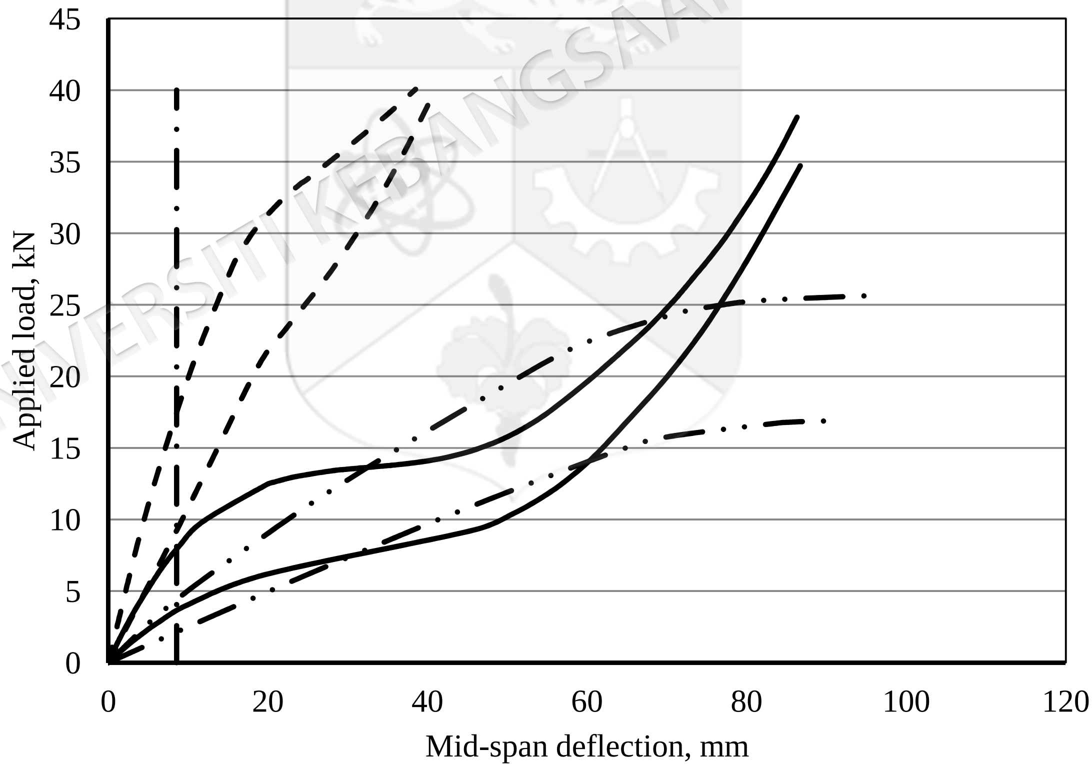

Figure 6.2 Load-deflection curves of Models PSNIRP, PSNIPP, PSNIFF, PSWIRP, PSWIPP, and PSWIFF

The development of compressive membrane action is apparent initially in the models with pinned-pinned and fixed-fixed boundary conditions due to the restriction of the movements at floor ends. The deflection limit load of the Model PSWIPP is almost close to that of the Model PSNIFF with different boundary conditions, which is attributed to the presence of concrete infill. In addition, the curve of models with pinned and fixed boundary conditions approach each other at the last steps of loading, which is the sign of taking the entire applied load by the steel sheeting in those models. The stiffer behaviour of the models with pinned and fixed-end conditions in the first steps of loading is also caused by the concrete infill, and as the compressive stress in the concrete reaches its crushing point, the models present the flexible behaviour in the last steps of loading to put the floor into the tensile membrane action. Notably, the concrete infill had a minor effect on the development of the tensile membrane action as the steel sheeting was the only load-carrying component in the last steps of loading.

Table 6.3 presents the results of serviceability limit loads and the rigidities of the considered models. The flexural capacity improvements of the PSSDB floors with pinned and fixed-boundary conditions are also presented in the table. The highest amounts of improvement are for the fixed-boundary conditions in which the rotations of the slab ends are restricted.

Table 6.3 Results for models with and without infill

Name of Models	Infill Status	Deflection Limit Load (kN)	Improvement (%)	Rigidity (kN/mm)
PSNIRP	No infill	2.14	N/A	0.25
PSNIPP	No infill	3.57	66.79	0.42
PSNIFF	No infill	9.23	331.53	1.08
PSWIRP	With infill	4.41	N/A	0.51
PSWIPP	With infill	7.93	79.97	0.92
PSWIFF	With infill	17.34	293.62	2.02

The induced membrane forces in the models with no concrete infill are shown in Figure 6.3. In the model with pinned-pinned boundary conditions, the developed compressive membrane forces turn to tensile membrane forces in the last steps of loading due to the arch deformation. To avoid the rotation of the floor ends in the fixed models, the top flanges are in tension, whereas the bottom flanges carry the in-plane compressive forces at supports. The reduction of the in-pane compressive forces due to the deformation of the arch has a noticeable effect on the rigidity of the Model PSNIFF when the central deflection of the floor exceeds 20 mm (see Figure 6.2, 6.3).

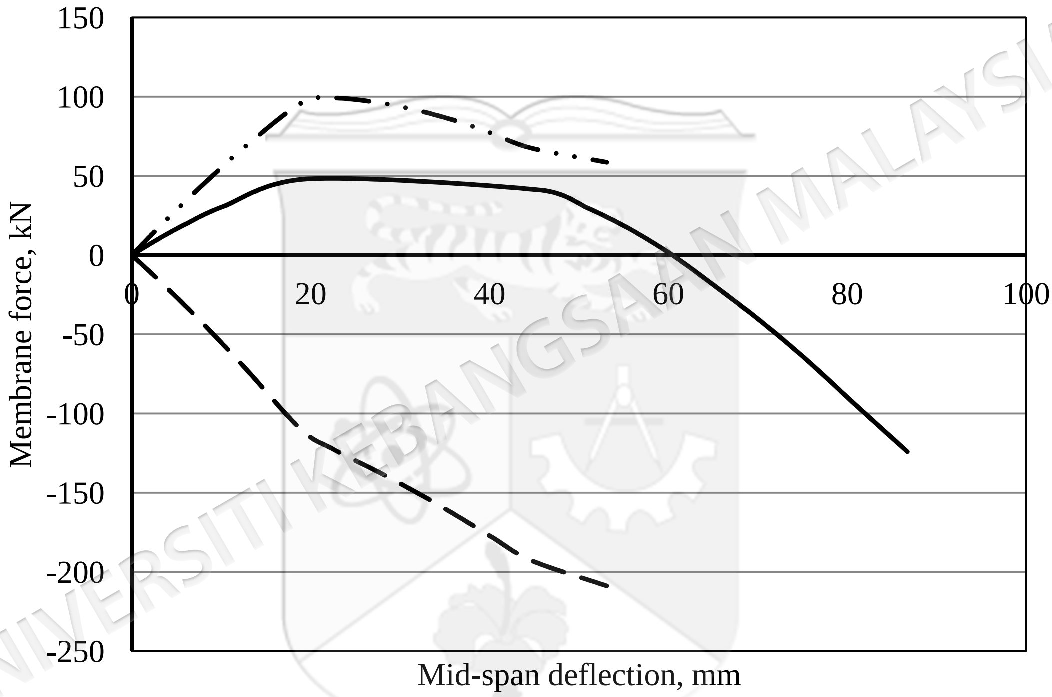

Figure 6.3 Membrane forces in Models PSNIPP and PSNIFF

Significantly, the drawn curve of membrane forces against the mid-span deflection for Model PSNIPP is almost flat in one part. That is, the formation of local buckling at the webs and top flanges of the steel sheeting in the mid-span smoothes the progress of the central deflection. Therefore, the compressive stress in the bottom flanges at supports does not increase further, whereas the concrete infill in the troughs of the steel sheeting delays the appearance of the local buckling, and accordingly the bottom flanges of the steel sheeting resist a higher amount of in-plane compressive stress. Figure 6.4 illustrates the developed horizontal load in the bottom flanges of the sheeting for the Model PSWIPP.

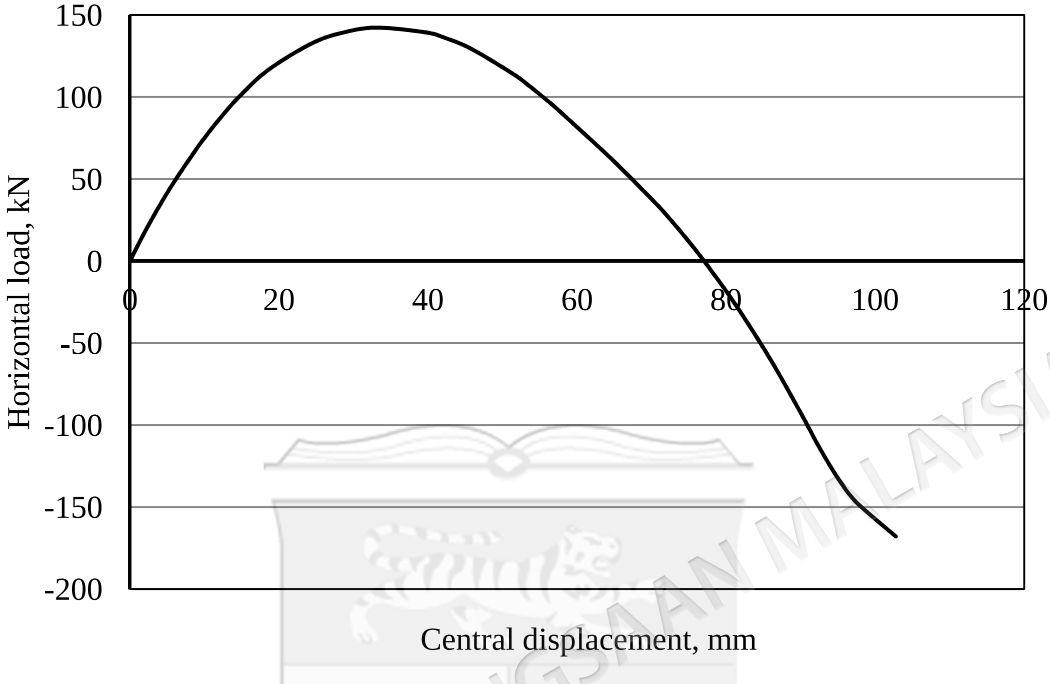

Figure 6.4 Horizontal Load at the Pinned Support-Central-Displacement Curve for Model PSWIPP

6.4 THICKNESSES EFFECT

To study the effect of material thicknesses on the development of the membrane action in the PSSDB floor, the available thicknesses of the PSSDB components in the market were considered for the parametric studies. Various boundary conditions were also assigned to the models. More details about the considered models are presented in Table 6.4.

Table 6.4 Models with various thicknesses of components

Name of Models	Dimensions (mm)	Material thickness (mm)		Boundary Condition
		Profiled Steel Sheeting	Dry Board	
P1D9RP	3000×795	1.0	9	Pinned Roller
P1D9PP	3000×795	1.0	9	Pinned Pinned
P1D9FF	3000×795	1.0	9	Fixed Fixed
P1D12RP	3000×795	1.0	12	Pinned Roller
P1D12PP	3000×795	1.0	12	Pinned Pinned
P1D12FF	3000×795	1.0	12	Fixed Fixed
P1D16RP	3000×795	1.0	16	Pinned Roller
P1D16PP	3000×795	1.0	16	Pinned Pinned
P1D16FF	3000×795	1.0	16	Fixed Fixed
P0.8D12RP	3000×795	0.8	12	Pinned Roller
P0.8D12PP	3000×795	0.8	12	Pinned Pinned
P0.8D12FF	3000×795	0.8	12	Fixed Fixed

6.4.1 Results and Discussions

The results obtained from analysis show that changing the dry board thickness has a minor effect on the floor performance for the entire considered boundary conditions. In other words, replacement of the dry board with the thicknesses of 9, 12, and 16 mm does not noticeably affect the results, whereas changing the profiled steel sheeting's thickness has a remarkable influence on the PSSDB floor's behaviour. For comparison purposes, the load-deflection curves of all models are demonstrated in Figure 6.5.

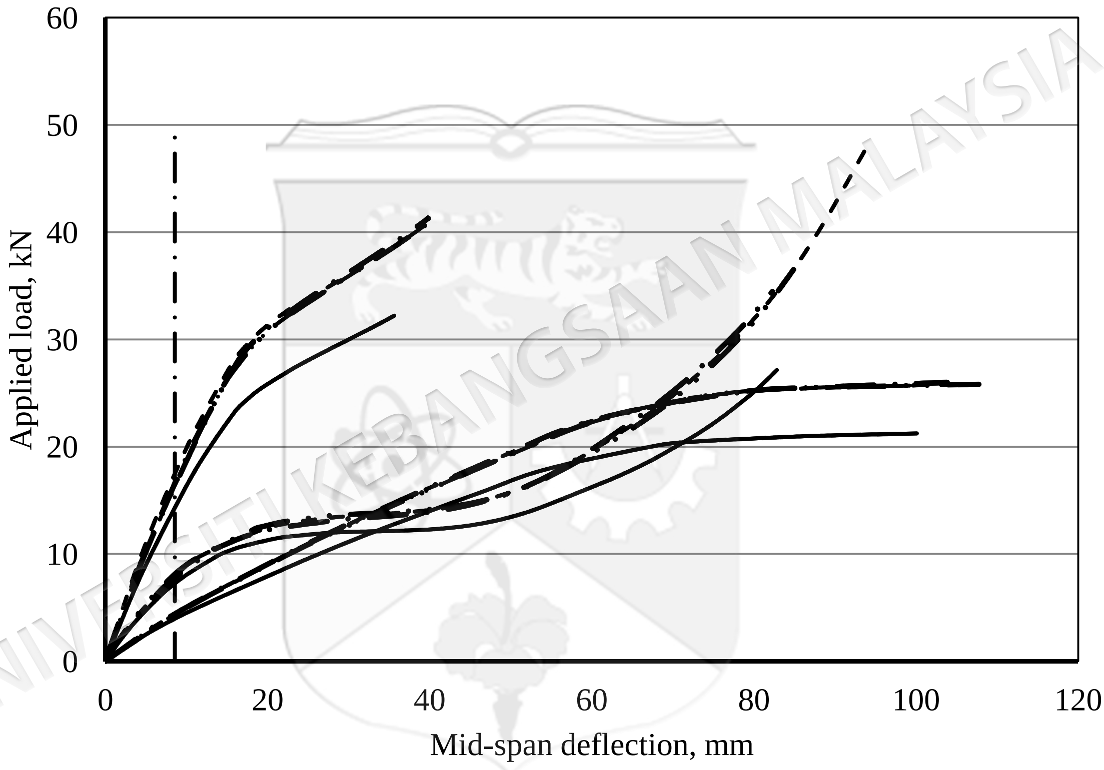

Figure 6.5 Load-deflection curves for different thicknesses

As the figure shows, only the lessening of the profiled steel sheeting's thickness reduces the rigidities and load-carrying capacities of the PSSDB floor restrained with different boundary conditions. The similarity in the behaviour of the floor with various thicknesses of the dry board may have economic significance.

Table 6.5 presents the rigidities and the serviceability limit load for different models, in addition to the improvement of the load capacity due to the compressive membrane action.

Table 6.5 Results of models with various thicknesses

Name of Models	Material thickness (mm)		Deflection Limit Load (kN)	Improvement (%)	Rigidity (kN/mm)
	Profiled Steel Sheeting	Dry Board			
P1D9RP	1.0	9	4.35	N/A	0.51
P1D9PP	1.0	9	7.76	78.30	0.90
P1D9FF	1.0	9	16.28	274.16	1.90
P1D12RP	1.0	12	4.40	N/A	0.51
P1D12PP	1.0	12	7.93	79.97	0.92
P1D12FF	1.0	12	17.34	293.65	2.02
P1D16RP	1.0	16	4.40	N/A	0.51
P1D16PP	1.0	16	7.92	79.89	0.92
P1D16FF	1.0	16	16.46	273.57	1.92
P0.8D12RP	0.8	12	3.96	N/A	0.46
P0.8D12PP	0.8	12	7.23	82.61	0.84
P0.8D12FF	0.8	12	14.29	260.81	1.67

The analogous rigidities of the models with the same thickness of the profiled steel sheeting for the correspondent boundary conditions proved the claim of insignificant effect of the dry board's thicknesses on the results. The improvement of the load-carrying capacity due to the arching action for all of the considered models was almost similar.

According to the table, the deflection limit load reductions due to a decrease in the steel sheeting's thickness were about 10%, 8.8%, and 17.60% for the PSSDB floor with various boundary conditions of simply supported, pinned-pinned, and fixed-fixed. The reduction in the floor's load capacity was almost the same for the simply supported and pinned-pinned panel. The conclusion that the tensile strength of the steel sheeting had a significant influence on the development of the compressive membrane action in the fixed-fixed panel is a fair one. The reason for the higher reduction in the fixed-fixed panel is that the tensile strength of the steel also contributes to the rotation's restriction of the floor ends. Figure 6.6 shows the overall buckling of Model P1D12RP.

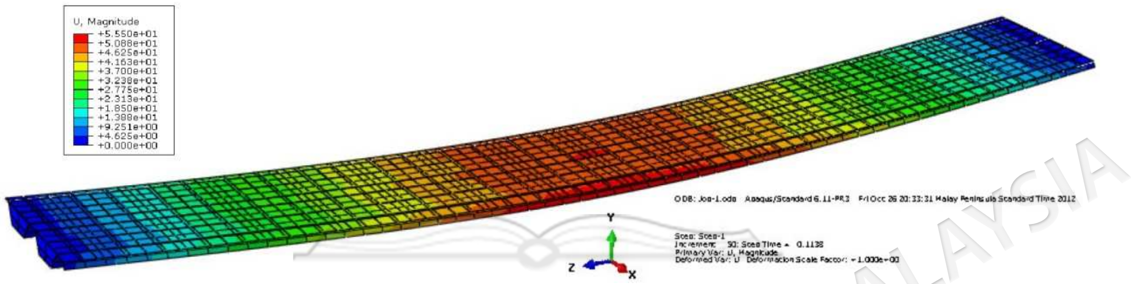

Figure 6.6 Overall deflection of the Model P1D12RP

6.5 SUMMARY

This chapter has focused on the parametric studies on the PSSDB floor to investigate the effect of the concrete infill as well as the various thicknesses of the PSSDB basic components. The following conclusions can be drawn from the conducted studies in this chapter.

- The results achieved from the analysis showed the remarkable effect of the concrete infill in the development of the compressive membrane action, whereas it did not have a perceptible effect on the tensile membrane action.

- The load-carrying capacity of the PSSDB floor was reduced to a significant extent due to the change in the profiled steel sheeting's thickness from 1.0 mm to 0.8 mm. This effect was observed for the various types of boundary conditions. The highest reduction was in the fixed-fixed panel at about 17.60%.

- Varying the thickness of the dry board did not have any effect on the results.

CHAPTER VII

PSSDB FLOORING SYSTEM FOR PRACTICAL APPLICATIONS

7.1 INTRODUCTION

This chapter focuses on the improvement of load-carrying capacity in the PSSDB flooring system for practical applications by considering the potential of the system to develop the membrane action in the floor. The development of the membrane action was considered in the PSSDB system with the infill for practical span without topping, as well as with topping over the full-length and half-length of the dry board. The continuous configuration of the PSSDB floor was also considered. The verified nonlinear finite element model for the PSSDB floor without topping, with conducted experimental work by the authors (explained in detail in previous chapters) was used to predict the effect of different boundary conditions on the performance of the system with practical applications.

The long list of studies about the various aspects of the PSSDB system provides valuable insights into employing the system for the practical applications in real buildings. Some remarkable studies in this regard can be mentioned as follows: water proofing, fire resistance, vibration, effects of various infill materials and finishing, noise and insulation transmission behaviour, continuity of the spans, and construction procedure and costs.

7.2 APPLICATIONS OF THE PSSDB SYSTEM

As briefly described in Chapter II, the applications of the PSSDB system are inclusive of floor, roof, and wall applications. The system was initially conceived as an alternative to the existing timber joist floors (Wright et al. 1989). The remarkable advantages of the PSSDB system, which leads to the popularity of the system, include shorter construction time, lightness and portability, need for semi-skilled labour, simplified utility installation, better structural integrity, reduction in labour time and cost, simplicity in construction method, minimum material wastage, and not requiring formwork (Surat et al. 2008).

The original purpose of the development of the system was to serve as the flooring and walling unit construction in the domestic scale buildings. The system carries the load in the form of out-of-plane bending and shear for the flooring applications, and it resists the in-plane deformation and shear in the walling applications. The application of the PSSDB system was further improved by assembling the panels in the form of folded plate configuration. Serving as a folded plate structure, the PSSDB system is capable of taking both out-of-plane and in-plane bending and shear. The application of the folded plate configuration is broadly utilised in long-span construction for economic and architectural reasons.

One example of the practical application of the PSSDB system is the annex classroom block for Sekolah Kebangsaan Teluk Mas, Melaka. This project included two standard classroom modules with the size of 9 m × 7.5 m. Locally available materials were used for the components of the system, such as Bondek II, Cemboard, and self-drilling and self-tapping screws. The constructed roof of this building is mono pitch roof for economic reasons and for the practicality of installation. The most challenging task was reported to be on the roof construction without rafter or truss, as well as the limitation of the dry board size. The PSSDB panels have a proper load-bearing capacity in the wall applications (Surat et al. 2008).

Extensive research was conducted on the wall application of the PSSDB system (Benayoune 1998; Benayoune & Wan Badaruzzaman 2000; Mangesha 1992; Mohd Shokory & Wan Badaruzzaman 2000). The PSSDB system acts as a membrane and resists the in-plane forces and shear. The structural performance of the system in different applications largely depends on the properties of the structural components of the system, namely, profiled steel sheeting, dry board, and concrete as an infill material. Moreover, the degree of interaction between the components is highly important, and may be either a partial or full interaction depending on the spacing of the connectors and their properties. Given that the PSSDB system for the wall applications plays an intermediate role in transferring the load from the floor to the foundation, the study of its structural behaviour is valuable in predicting the ultimate load-carrying capacity for the wall with and without opening.

In the practical applications of the PSSDB system as a roofing panel, the normal position of the dry board in the system is unsuitable for use in actual buildings. The reason is that the material of the dry board loses strength and shows bulging in volumes in the wet conditions even if the water-proofing layer is used to prevent direct exposure to hot and dry weather. The reverse position of the dry board was suggested to overcome this problem. Based on this proposal, the inside flat surface of the panel eliminates the need for the suspended ceiling.

7.3 PREVIOUS WORK ON PSSDB SYSTEM WITH TOPPING

The application of the topping in the PSSDB system was first studied by Shodiq et al. (2003) in the flooring system (Figure 7.1). Using the concrete as an infill material and topping was reported to increase the spanning capacity of the PSSDB system. The presence of concrete also improves the fire resistance and soundproofing characteristics of the PSSDB floor.

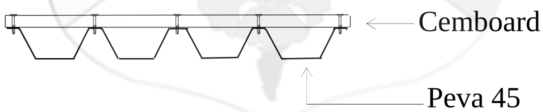

(a) Standard PSSDB panel

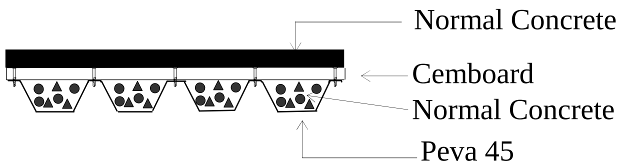

(b) Concrete infill and covered PSSDB panel

Figure 7.1 Cross section of specimens

Source: Shodiq et al. 2003

Shodiq et al. (2003) conducted an experimental test on two specimens (see Figure 7.1) in which one was made with the basic components of the PSSDB system (without infill and topping concrete), and the other one was prepared with normal concrete (grade 30) as an infill material and topping with the thickness of 25.4 mm. The uniform loading was applied to the specimens using steel blocks (0.2 kN). The incremental loading at each step was 1.33 kN/m^2, which was applied manually up to 6.67 kN/m^2. The maximum load was kept constant for about an hour, and then the specimens were unloaded at the same increment to zero load.

The results achieved from the conducted experiment showed that the stiffness of the basic PSSDB system remarkably increased in case of using concrete. The influence of concrete infill was also observed in preventing the early appearance of local buckling in the top flanges of the steel sheeting. The topping concrete improves the second moment of the cross-section. In addition, the concrete infill and topping enhances the composite modulus of elasticity in the system. The remaining deflections after the unloading of both specimens showed that the specimen with basic components has more plastic deformation compared with the specimen with infill and topping concrete. The maximum deflection for the same amount of load for the specimen with infill and topping concrete was reported to be one-tenth of the specimen prepared with the basic components of the PSSDB system (see Figure 7.2).

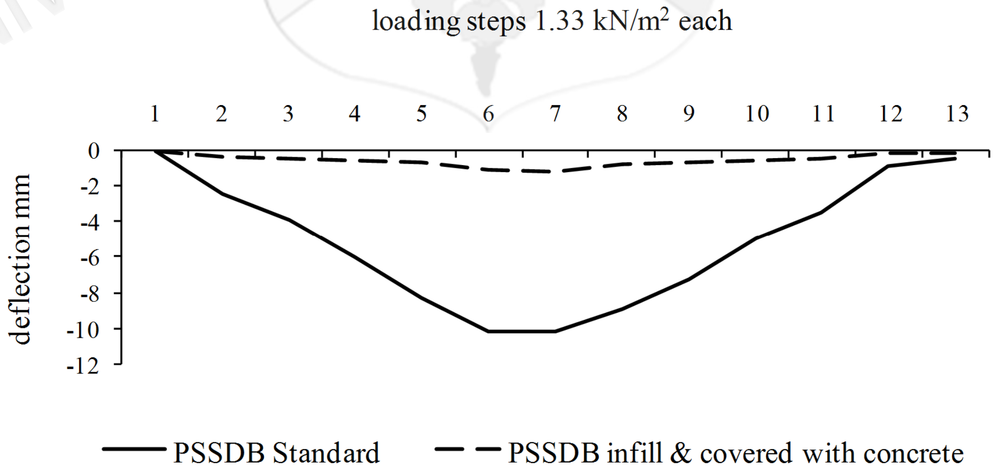

Figure 7.2 Graph of load against mid-point deflection

Source: Shodiq et al. 2003

7.4 PRACTICAL LENGTH OF PSSDB FLOOR AND TOPPING

The nonlinear finite element model was developed for the PSSDB floor with topping over the full- and half-length dry board and in a practical span length to study the effect of the membrane action on such floors. As mentioned earlier, the verified analytical model was employed in this regard. The span length of 3000 mm and the width of 795 mm were considered for the practical applications of the PSSDB system.

7.4.1 Analytical Models

Considering the practical length of the PSSDB flooring system is significant in proving the capability of the system for the practical applications and the development of membrane action in such a span with the restricted boundaries. The material properties of the PSSDB components in the entire models are according to the defined properties in the verified model as shown in Table 6.1. The width and length of the “dry board” in Models with half-dry board are 795 mm × 865 mm.

For the sake of comparison, three groups of models were considered with the practical span length. Table 7.1 presents the details about the models. The first group was the PSSDB floor without topping, the second group was with topping (50 mm thick), and the third group was with topping and half dry board in the middle of the span. All groups were considered with various boundary conditions of simply supported, pinned-pinned, and fixed-fixed. The half dry board in the middle of the span is proposed for practicality and economics purposes.

Table 7.1 Table of Models for practical span and topping

Name of Models	Dimension (mm)	Description	Boundary Condition
PSRP	3000×795	Practical Span with Roller-Pinned boundary conditions	
PSPP	3000×795	Practical Span with Pinned-Pinned boundary conditions	
PSFF	3000×795	Practical Span with Fixed-Fixed boundary conditions	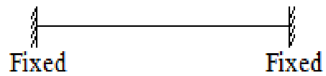
PSTRP	3000×795	Practical Span with Topping with Roller-Pinned boundary conditions	
PSTPP	3000×795	Practical Span with Topping with Pinned-Pinned boundary conditions	
PSTFF	3000×795	Practical Span with Topping with Fixed-Fixed boundary conditions	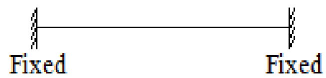
PSTHRP	3000×795	Practical Span with Topping and half-dry board with Roller-Pinned boundary conditions	
PSTHPP	3000×795	Practical Span with Topping and half-dry board with Pinned-Pinned boundary conditions	
PSTHFF	3000×795	Practical Span with Topping and half-dry board with Fixed-Fixed boundary conditions	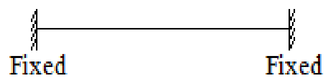

7.4.2 Practical Span Length

The model with the simply supported condition (PSRP) for one-bay span was considered under the progressive loading and up to the failure load of the model. The results achieved from the theoretical models with different boundary conditions were compared in Figure 7.3. Restricting the in-plane translation of the slab ends led to the formation of the arch in the slab strips from boundary to boundary. As Figure 7.3 shows, the flexural rigidities of the slab improved for the boundary conditions of pinned-pinned and fixed-fixed. The improvement of flexural rigidities is due to the development of the compressive membrane action in the slab. In the higher mid-span deflections, the load-carrying capacity of the slab was enhanced due to the development of the tensile membrane action in which the slab falls in the catenary action, and the entire applied load is taken by the profiled steel sheeting.

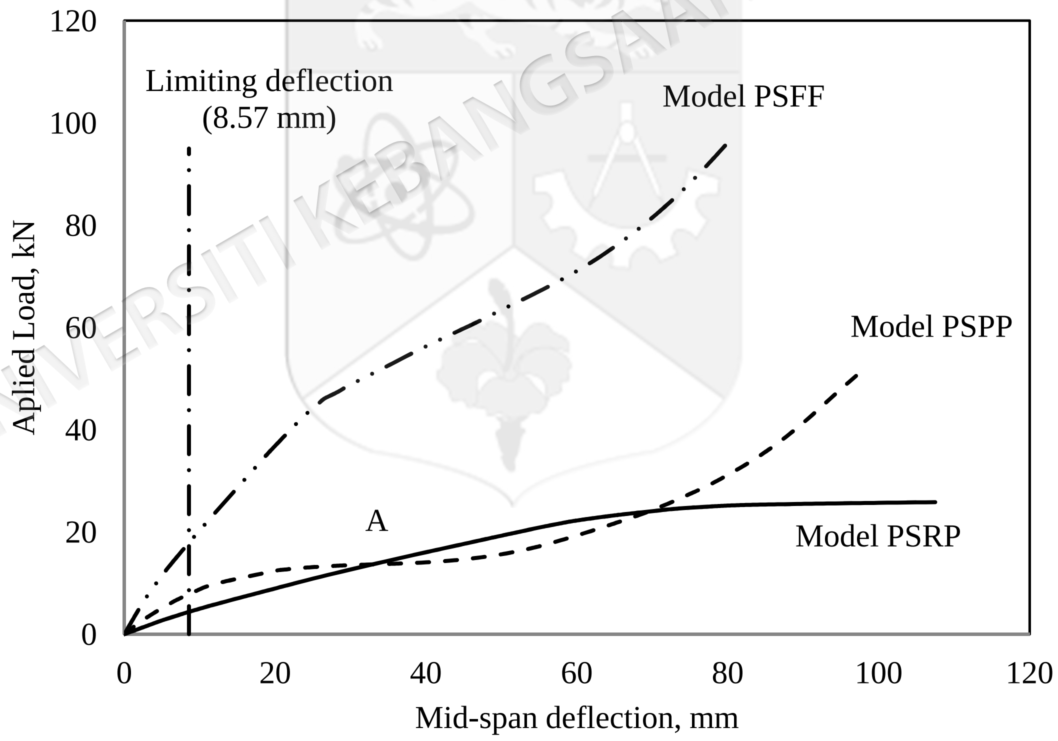

Figure 7.3 Load-central-deflection curves for Model PSRP, PSPP, and PSFF

Conversely, preventing the rotation in addition to the horizontal movements of the slab at boundaries further improved the flexural rigidities of the PSSDB flooring system, and accordingly the load-carrying capacity of the floor improved in both low and high central deflections.

The horizontal load (obtained from finite element modelling) is induced at the boundaries of the slab due to the development of the membrane action in the slab. Figure 7.4 demonstrates the developed horizontal load against the mid-span deflection achieved from the nonlinear finite element model for the model with pinned-pinned boundary conditions (Model PSPP). The in-plane forces at the first steps of loading are increased due to the development of the compressive membrane action. The maximum level of the in-plane forces is associated with point A in Figure 7.3. After this point, the in-plane forces are decreased in a way that the compressive membrane forces shift to the tensile membrane forces in the slab. Accordingly, the tensile membrane action develops in the slab. A summary of the results, including the deflection limit, rigidities, and improvement of the flexural capacities, is presented in Table 7.3.

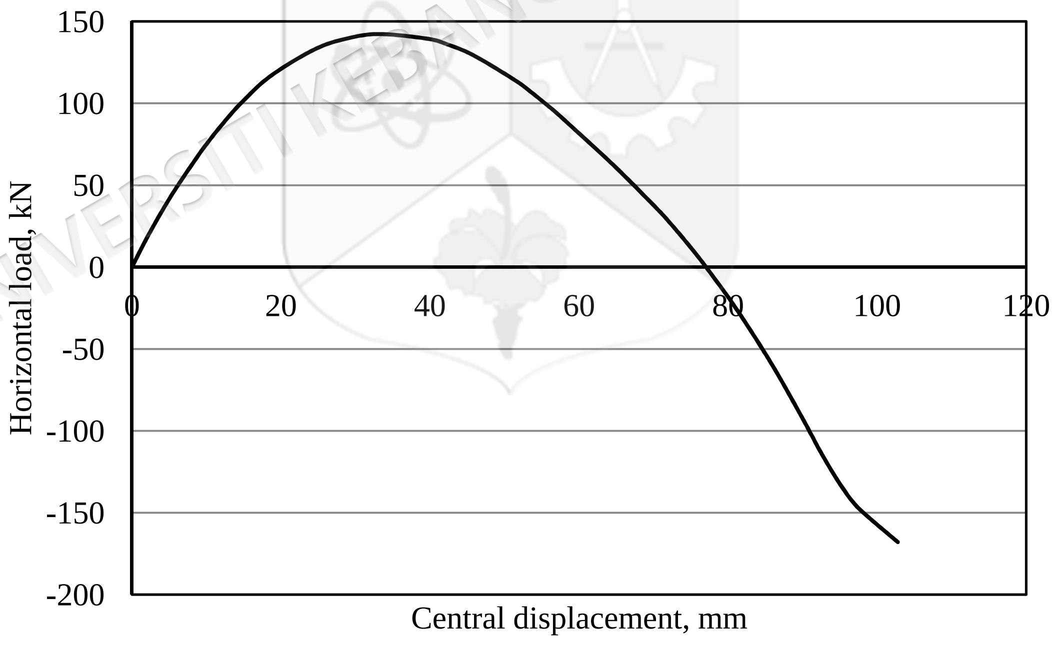

Figure 7.4 Horizontal loads at pinned support-central-displacement curve for Model PSPP

Figure 7.5 demonstrates the stress trajectory along the span of Model PSPP. The arch is visible from boundary to boundary of the floor. As it was previously mentioned, the developed arch between restricted supports of the floor is along the induced compressive membrane forces which form in arch shape. Compressive membrane forces in the floor are shown in figure. The developed arch is highlighted for better demonstration.

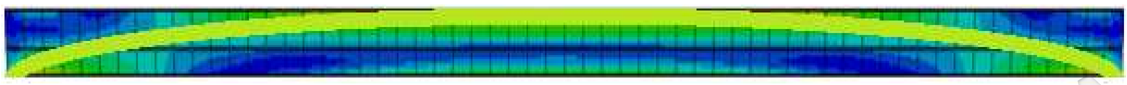

Figure 7.5 Stress trajectory along the span of Model PSPP

7.4.3 Practical Span with Topping and Full-length Dry Board

The considered model with a practical length of 3000 mm was covered with the topping concrete of grade 30. The assumed thickness for the topping was 50 mm. The topping concrete over the PSSDB floor, as mentioned earlier, was suggested by previous researchers (Shodiq et al. 2003) with the intention of increasing the compression part in the section to ensure the resistance of the compression stresses along with the dry board. The introduction of the topping concrete to the PSSDB system also leads to an increase in the overall thickness of the slab to fulfil the fire insulation requirements. Figure 7.6 illustrates the details of the dimensions and the applied materials in the PSSDB floor with topping. The material properties were employed according to the previously described properties in Table 6.1. The screw spacing and the thickness of the profiled steel sheeting and dry board are identical according to the other models in this study.

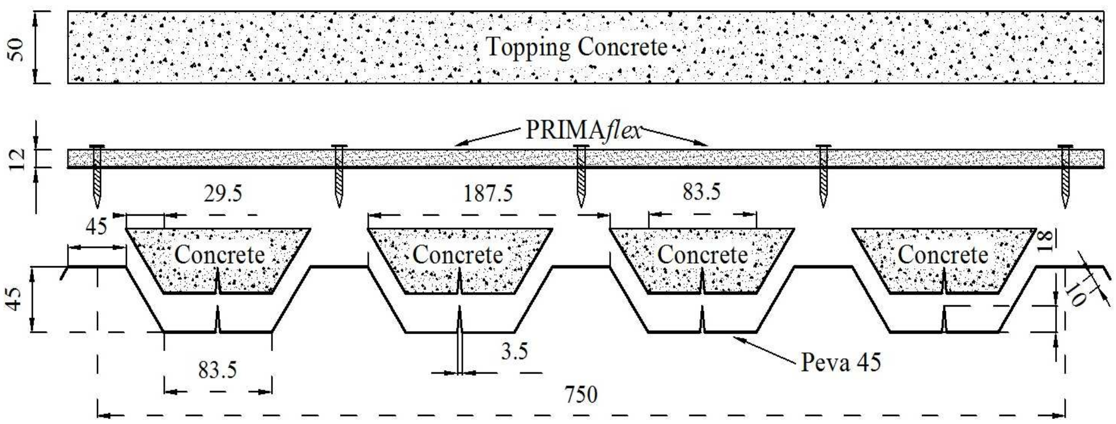

(All dimensions in mm)

Figure 7.6 Cross-section of Model PSTRP, PSTPP, PSTFF (with separated parts)

The PSSDB floor with topping was studied with various boundary conditions of simply supported, pinned-pinned, and fixed-fixed in the developed models of PSTRP, PSTPP, and PSTFF, respectively. Table 7.1 presents more details about the considered models. The simulation methods for the models with topping were implemented according to the aforementioned procedures. The nonlinear model was developed to examine the effect of the membrane action in the PSSDB slab covered with topping concrete in terms of the restriction of the translation and/or rotation of the boundaries of the slab subjected to the vertical loading. As the thickness of the slab increases, aside from improving the flexural capacity of the slab with simply supported boundary conditions, the possibility of developing the compressive membrane action in the slab with restricted ends against translation and/or rotations in the PSTPP and PSTFF Models is also expected to increase.

The load-central-deflection curves achieved from the analysis of the models with various boundary conditions are demonstrated in Figure 7.7. The presence of the topping concrete had a notable influence on the bending strength of the system, as expected, even for the simply supported model (Model PSTRP).

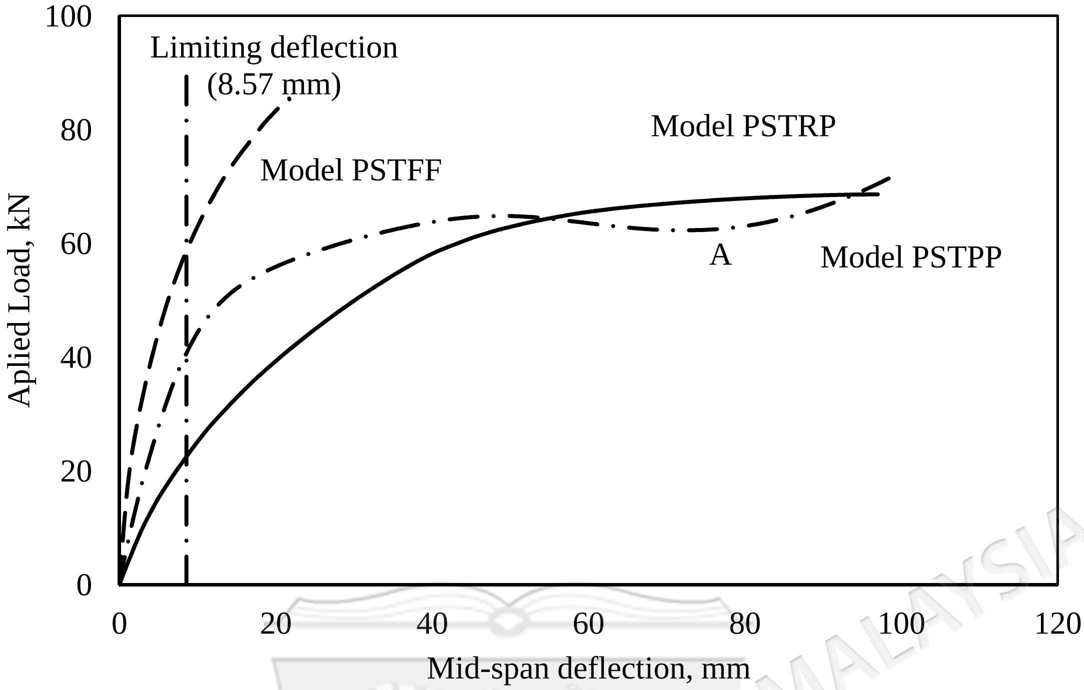

Figure 7.7 Load-central-deflection curves for Models PSTRP, PSTPP, PSTFF

Restricting the lateral translation and/or rotations in the models with pinned-pinned and fixed-fixed boundary conditions (Model PSTPP and PSTFF) remarkably enhanced the rigidities and flexural capacity of the system in the first steps of loading. Higher thickness of the slab and the development of the compressive membrane action from boundary to boundary are the reasons for this phenomenon. In Model PSTPP, once the developed compressive membrane forces exceed their maximum level (see Figure 7.8 and Figure 7.7), the load-carrying capacity of the slab decreases up to the point A that the compressive membrane forces approach zero and turn to the tensile membrane forces. At this point, the tensile membrane action comes into picture, and the improvement of the load capacity of the slab is attributed to the formation of the catenary action and the tensile strength of the profiled steel sheeting in the slab. The negative value of the horizontal load demonstrated in Figure 7.8 represents the development of the tensile membrane action.

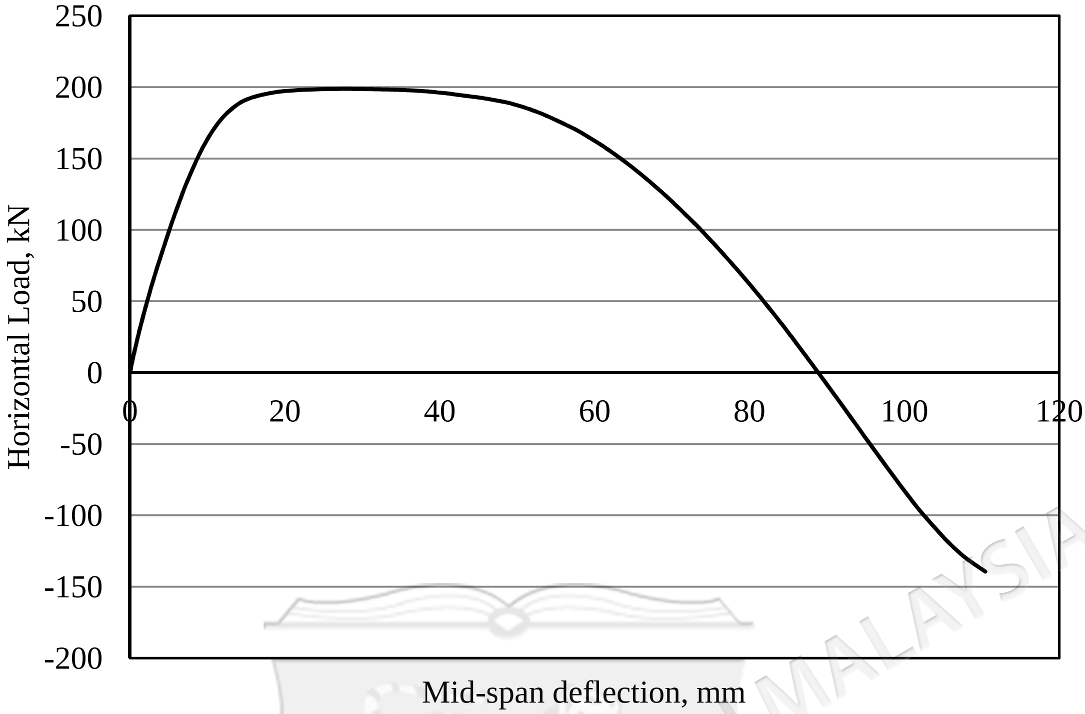

Figure 7.8 Horizontal loads at pinned support against central-displacement curve for Model PSTPP

The arching action develops from boundary to boundary of the slab strips, and therefore the compressive stress induces along the created arch. The additional flexural capacity of the slab due to the compressive membrane action is ascribed to the formation of the compressive arch in the slab. To study the induced compressive stresses in the developed arch, the stress at the top flange in the mid-span and mid-width of the slab was considered. Figure 7.9 demonstrates the stress at that point against the mid-span deflection for Model PSTPP. The compressive stress in the top flange of the profiled steel sheeting increases until the maximum level is reached, and once the slab falls in the tensile membrane action, the compressive stress at the top flange decreases. The turning point of the membrane stress in the top flange happens almost at the time of the initiation of tensile membrane action in the load-deflection curve (see Figure 7.8 and Figure 7.9). This outcome means that the created arch in the slab deforms, and the additional load-carrying capacity of the slab due to the compressive membrane action is eliminated. As the figure shows, once the applied load increases in the higher mid-span deflections, the compressive stress in the top flanges approaches zero, and the entire section of the steel sheeting carries the applied load in the slab.

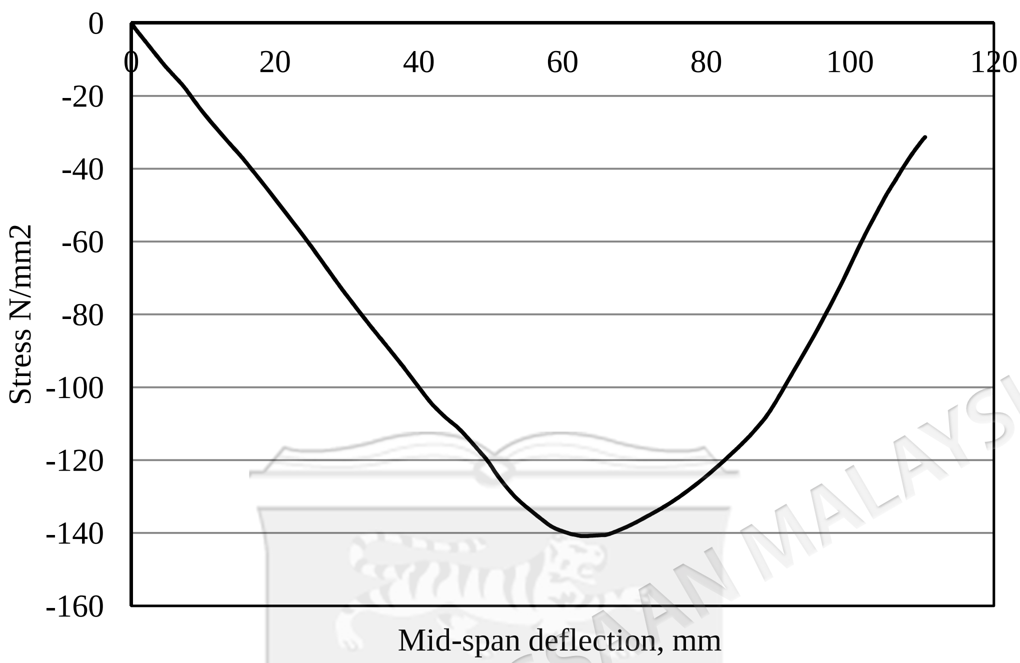

Figure 7.9 Developed stresses in the top flange and at the mid-span of the profiled steel sheeting for Model PSTPP

7.4.4 Practical Span with Topping and Half-length Dry Board

The practical floor with the span length of 3000 mm was then considered with a half-length dry board in the middle of the floor. As Figure 7.10 demonstrates, topping concrete rests over the dry board in the middle of the floor, whereas there is no dry board on the sides of the floor and the topping concrete lies over the profiled steel sheeting. The reasons for considering this type of floor may be as follows:

a. The bending strength of the bare steel sheeting increases due to the position of the dry board in the middle; therefore, no propping is required for the larger span length.

b. The topping concrete on the sides of the floor has better interaction with the steel sheeting due to the embossments on the troughs of steel deck.

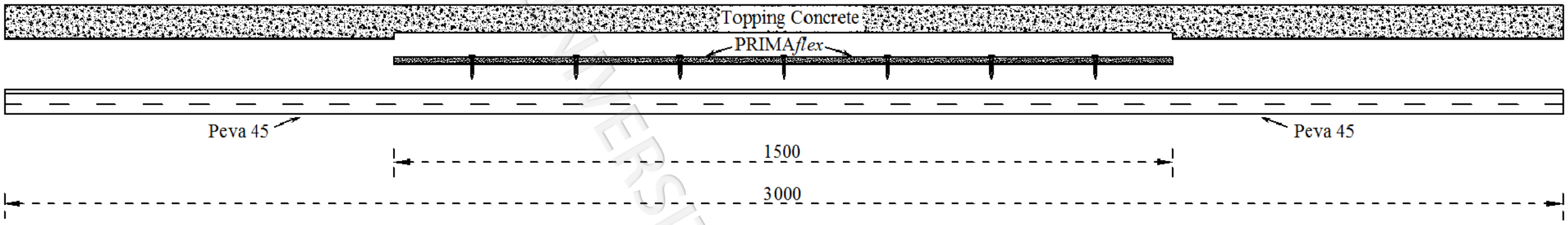

(a) Side view of the floor

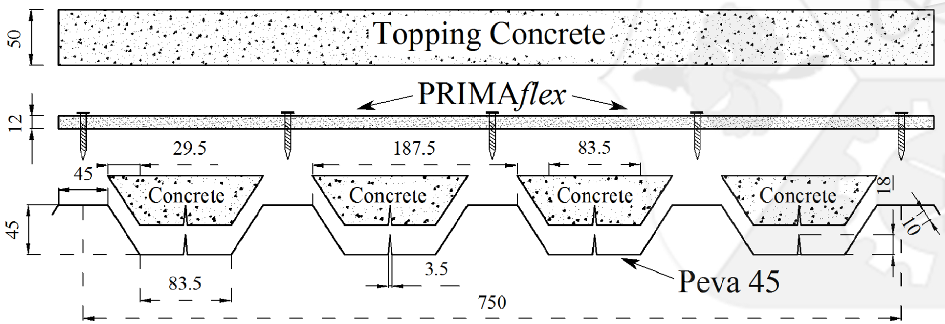

(b) Cross section of the floor in the middle

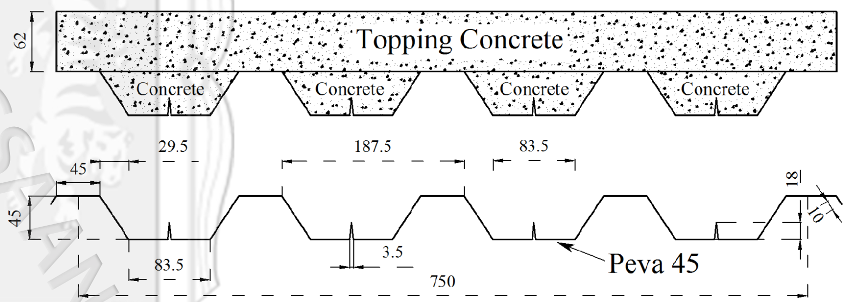

(c) Cross section of the floor at sides

(All dimensions in mm)

Figure 7.10 Practical span with topping and half-length dry board (with separated parts)

Details about the models under consideration are presented in Table 7.1. Models PSTHRP, PSTHPP, and PSTHFF are with the various boundary conditions of simply supported, pinned-pinned, and fixed-fixed, respectively. Given that the considered models are one-way slab, the floor with simply supported boundary condition (Model PSTHRP) does not benefit from the development of the arching action. In contrast, for the models with restricted boundary conditions (PSTHPP and PSTHFF), the rigidities and flexural capacity of the slab are enhanced. Notably, the fixed-fixed boundary condition is provided in the model by restricting the movement of the upper and lower flanges of the steel sheeting. The load-central deflection for the models and the effect of restricting the rotation and/or horizontal movement of the slab ends are clearly demonstrated in Figure 7.11. The falling branch of the Model PSTHPP is due to the softening behaviour of concrete in its constitutive model.

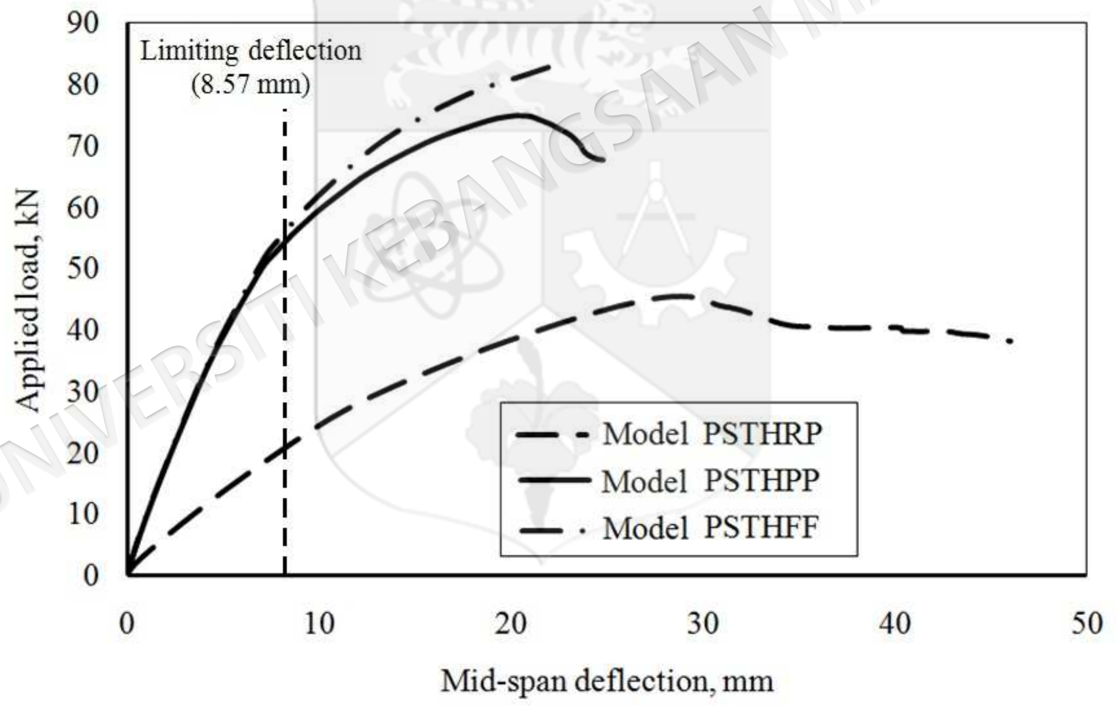

Figure 7.11 Load-central-deflection curves for Models PSTHRP, PSTHPP, and PSTHFF

In the first steps of loading, the obtained results for the model with pinned-pinned boundary condition are almost identical to those from the fixed model. As the load increases, the fixed model shows better performance due to the limitation of the rotation at the ends. To clarify the reason for this outcome, the horizontal movements of the floor end at different depth of cross section are drawn in Figure 7.12.

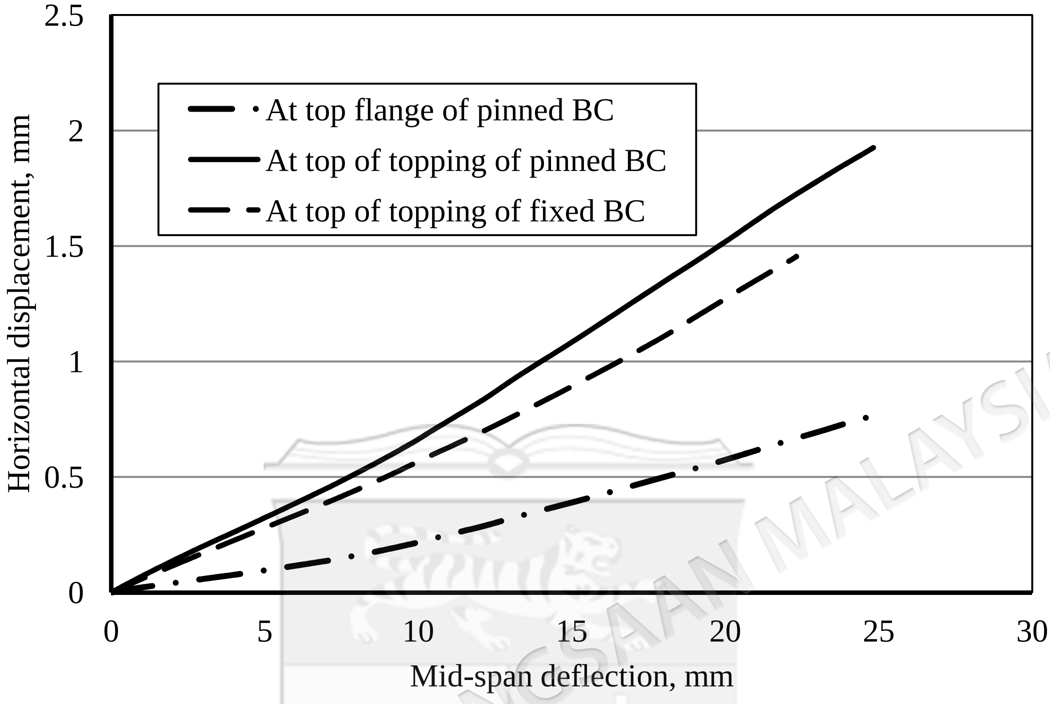

Figure 7.12 Horizontal displacements in the floor end at different depths

According to the figure, the rotation of the floor at the supports for the Model PSTHPP is due to the lateral translation of the upper flanges and topping. Although the upper flanges were restrained against movement, the topping of the Model PSTHFF had some movement. The horizontal movement of the fixed and pinned models at top of topping are almost close in the first steps of loading, and the deviation between them starts in the higher steps of loading. Accordingly, the bigger rotation of the slab with pinned ends at the supports leads to a slight reduction in the compressive membrane action effect, and thus a lower ultimate capacity of the slab.

7.5 CONTINUOUS PSSDB FLOOR

In the construction stage, the PSSDB floor is mostly constructed in continuous form over two or more supports. Thus, the PSSDB floors can be considered as a continuous floor. The continuous floor is mostly preferred to the simply supported floors due to its constructional and structural advantages. Some of these advantages are as follows:

a) The continuous form of construction decreases the construction stages, and therefore increases the construction speed. It also reduces the amount of structural components for the installation or construction, and therefore reduces the construction volume.

b) With the specific limits of deflection, the continuous floor benefits from higher span-to-depth ratios. This advantage leads to an increase in the allowed span length with the proper factor of safety, and therefore is preferable from an economic perspective.

c) A higher fundamental frequency of vibration is achieved in case of continuous floor, and therefore the movement of people creates less vibration in such floors.

d) In case of using rational methods for fire conditions in design, the continuous floor is more appropriate than the simply supported floor (Patrick 1989).

Meanwhile, the continuous floor also has some disadvantages as follows:

a) The analysis of the continuous floor is complicated compared with that of the simply supported floor, and more approximation is necessary in the analysis process for the continuous floor.

b) The design of the continuous floor involves a more complex combination of loading compared with that of the simply supported floor due to the interaction between the spans.

With conventional concrete, the application of the compressive membrane action in the continuous slab and beam floors allows the designer to deduct the intensity of the reinforcement of the panel from the intensity required by Johansen's yield line theory. However, for the same ultimate loads and the concrete dimensions, more steel would be required for the supporting beams of the panel to facilitate the development of the compressive membrane action, compared with that of the supporting beams of the panel according to yield line theory. To economically use the compressive membrane action in the slab, the reduction in the reinforcement in the panel should be greater than the extra reinforcement in the supporting beams. The extra reinforcement in the supporting beams of the panel is designed to develop the compressive membrane action required to tie the reinforcement (Park 1965).

The profiled steel sheeting in the positive bending of the composite slab is responsible for providing the flexural reinforcement to the concrete, whereas for the case of negative bending in the continuous slab, the steel sheeting absorbs the compressive stress. In the continuous slab with profiled steel sheeting and plain concrete, extra flexural reinforcement is required for the strength limit state. Therefore, using the profiled steel in the simply supported slab is more appropriate than in the continuous composite slabs (Bradford et al. 2012).

Another remarkable point about the continuous slab is that its deflection is lower than the similar simply supported slab when it is under the action of load. Obtaining a benefit from the edge continuity makes the slab strong enough to sustain the punching load. The improvement of the punching load capacity of the continuous slab because of the edge continuity may be attributed to the effect of the in-plane restraint in the slab (Alam 1997).

In addition, the continuous slab performs better in the case of structural fire resistance than the simply supported slab, which is attributed to the moment redistribution phenomenon in which alternative means resist the load after the formation of the first plastic hinge (Lim 2003).

The continuous slab in the PSSDB system was first studied by Akhand (2001) through experimental and analytical approaches. The inelastic strength of the PSSDB system is more economical to use, particularly for the continuous floor. However, the effect of the membrane action in the PSSDB continuous floor has not been considered yet.

The effect of the membrane action in the continuous PSSDB floor was investigated on the two-span slab. The reason behind the selection of the two-span slab may be attributed to the fact that as the elastic support moment and the shear in the two-span continuous structure are the largest, the load-carrying capacity of the two-span structure is less than the capacity of the multi-span sheeting. In addition, when considering the plastic analysis, the rotation capacity at the internal support of the two-span slab is equivalent to that of a multiple-span slab (Akhand 2001).

At the internal supports of the slab, as the cross-section of the steel sheeting exceeds the yield stress of the material, the cross-section of the PSSDB floor starts to collapse gradually and form a partial plastic hinge. The collapse of the section may happen even without formation of the complete plastification in the cross-section of the internal support. Figure 7.13 illustrates the two-span slab under consideration in this study.

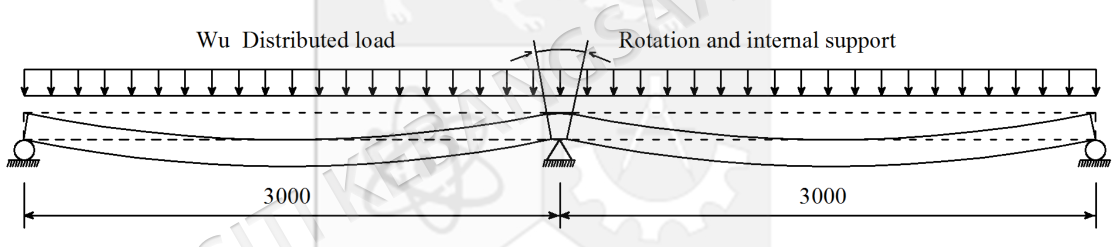

(All dimensions in mm)

Figure 7.13 Two-span model for Model C2SRPR

Source: Bryan and Leach 1984

The nonlinear numerical model was developed based on the symmetry axis of the middle support. Table 7.2 presents the details about the studied models. The horizontal translation of the roller supports (see Figure 7.13) in the Model C2SPPP was restricted, whereas for Model C2SFPF, both the translation and rotation of the roller support were restricted. The material properties used in the created models are reported in Table 7.2.

Table 7.2 Table of Models for the continuous slab

Name of Models	Dimension (mm)	Description	Boundary Condition
C2SRPR	6000×795	Continuous 2-Span with Roller-Pinned-Roller boundary condition	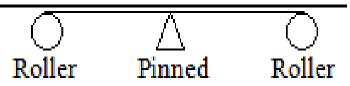
C2SPPP	6000×795	Continuous 2-Span with Pinned-Pinned-Pinned boundary condition	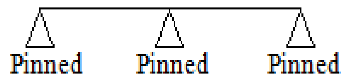
C2SFPF	6000×795	Continuous 2-Span with Fixed-Pinned-Fixed boundary condition	

The load-deflection curves achieved from the analysis of the continuous slab are illustrated in Figure 7.14. The applied load in the figure is for one span of the continuous slab. The rigidities and the flexural capacities of the Model C2SRPR and Model C2SPPP are relatively low in the first steps of loading.

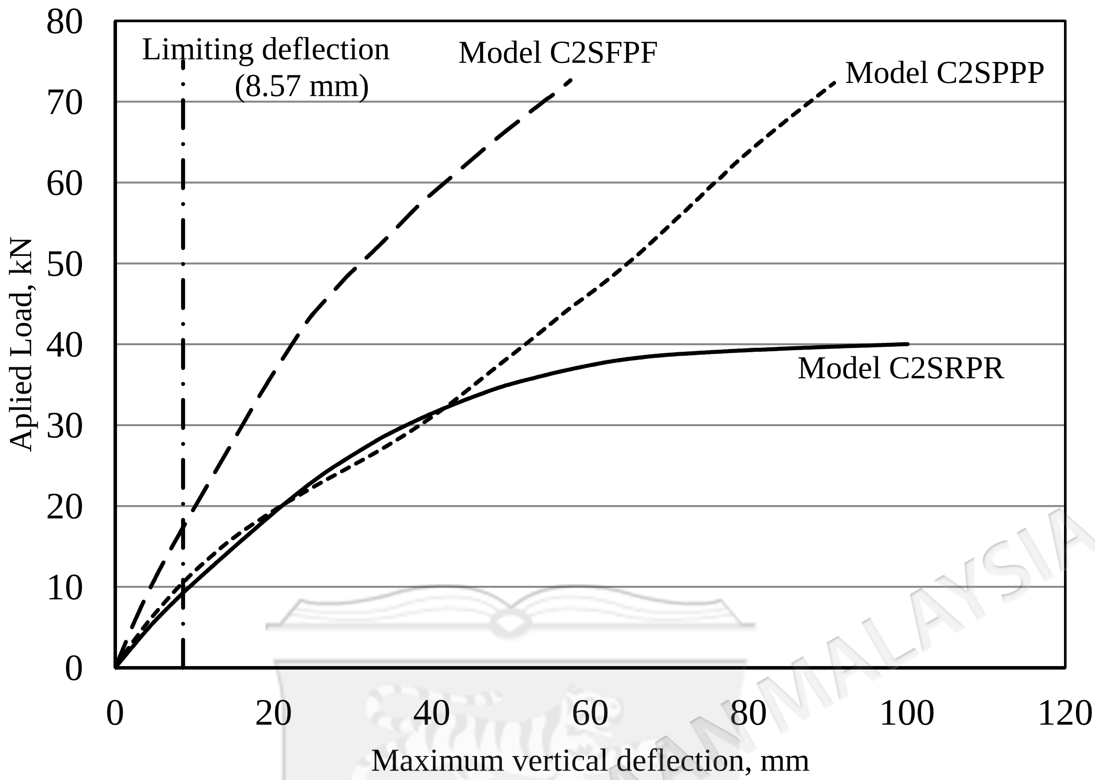

Figure 7.14 Load-maximum-deflection curve for Model C2SRPR, C2SPPP, C2SFPF

The restriction of the horizontal translations of the roller supports in Model C2SPPP does not remarkably improve the flexural rigidities in the first steps of loading. In other words, the compressive membrane action does not develop in the model with pinned boundary condition. As mentioned previously, the key prerequisite for the development of the compressive membrane action in the restricted supported slab is the generation of the horizontal displacement at the roller end in that slab with simply supported boundary conditions.

Figure 7.15 shows the applied load against horizontal deflection at the roller support of the continuous PSSDB floor with simply supported boundary conditions (C2SRPR). The maximum outward horizontal movement was 0.42 mm, which was almost less than half of the outward movement achieved from the experimental model. As the outward horizontal movement of the slab decreases, the formation of the arch between boundaries of the slab is unlikely to happen.

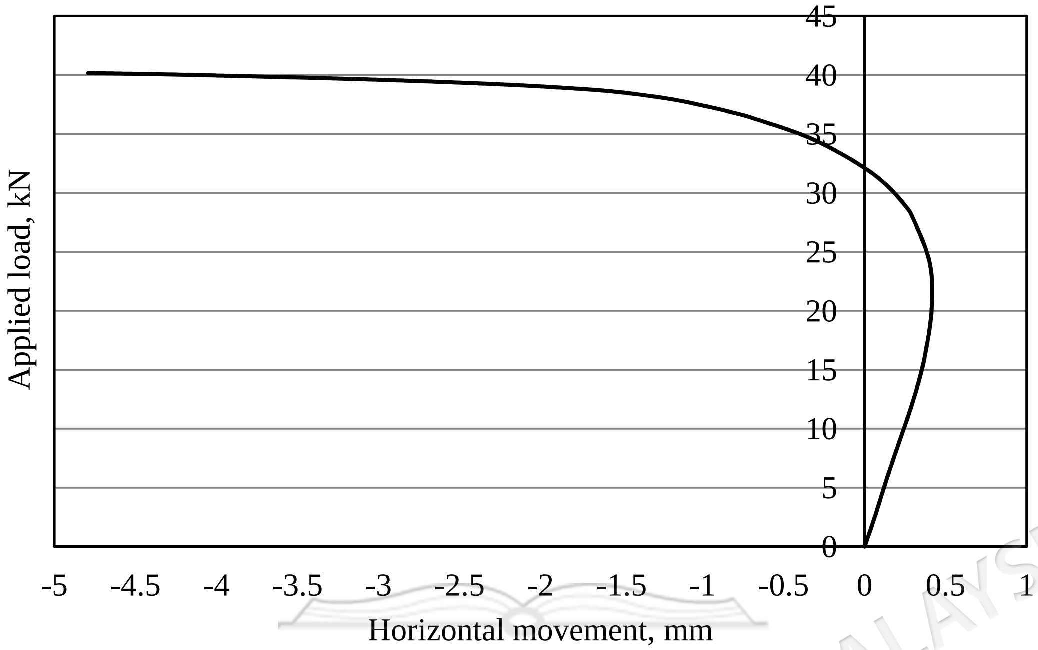

Figure 7.15 Load-horizontal deflection of Model C2SRPR

The restriction of the horizontal translations of the roller supports in the Model C2SPPP does not improve the flexural rigidities in the first steps of loading; nevertheless, due to the formation of the tensile membrane action in the higher steps of loading, the load-carrying capacity of the Model C2SPPP improves (see Figure 7.14), and the rigidities of the model become dramatically higher than those of the model with simply supported boundary conditions.

According to Krauthammer (2008), the development of the compressive membrane action in the slab is more likely to happen if the outward motion and rotation of the supports are sufficiently restrained. The restriction of the slab ends rotation (Model C2SRPR) had a great effect on the load-carrying capacity of the slab in both the first and second steps of loading (see Figure 7.14).

In addition, when the tensile membrane action is considered, the profiled steel sheeting is responsible for carrying the applied load. The slopes of the curves for the Model C2SPPP and Model C2SFPF in the second part are almost the same; this outcome is attributed to the fact that in both models, the steel sheeting is only in charge of carrying the applied load.

Table 7.3 Table of results for the models considered in this chapter

Name of Models	Span Length (mm)	Deflection Limit Load (kN)	Improvement (%)	Rigidity (kN/mm)
PSRP	3000	4.36	N/A	0.51
PSPP	3000	7.82	79	0.91
PSFF	3000	17.83	309	2.08
PSTRP	3000	9.27	N/A	1.08
PSTPP	3000	10.54	80	1.23
PSTFF	3000	17.33	161	2.02
PSTHRP	3000×795	21.46	N/A	2.50
PSTHPP	3000×795	55.38	158.09	6.46
PSTHFF	3000×795	57.25	166.84	6.68
C2SRPR	(2×)3000	22.46	N/A	2.62
C2SPPP	(2×)3000	40.5	14	4.73
C2SFPF	(2×)3000	58.55	87	6.83

7.6 SUMMARY

The developed three-dimensional nonlinear finite element models were employed to examine the development of the membrane action in the practical applications of the PSSDB flooring system. The analysis was conducted for the practical span with and without topping, as well as for the continuous configuration. The following conclusions can be drawn from the analysis results:

- In the PSSDB floor with practical length and without topping, preventing only the horizontal movement of the slab ends did not notably improve the performance of the floor in the first steps of loading, whereas the contribution of the tensile membrane action enhanced the flexural capacity of the system in the last steps of loading. Conversely, restricting both horizontal movements and rotation at the supports dramatically improved the structural performance of the floor.

- The application of topping concrete on the PSSDB flooring system enhanced the flexural capacity of the floor even with the simply supported boundary conditions. The development of the membrane action in the PSSDB floor with topping concrete improved the capability of the system for the pinned-pinned and fixed-fixed boundary conditions for both the first and last steps of loading.
- In models with the topping and half-length dry board, the formation of the compressive membrane action increased the load-carrying capacity of the slab in both models with pinned-pinned and fixed-fixed boundary conditions.
- The pinned-pinned boundary conditions in the continuous configuration of the PSSDB floor also did not improve the load-carrying capacity of the PSSDB floor in the first steps of loading, whereas the second part of the curve showed the better performance of the floor because of the development of the tensile membrane action in the profiled steel sheeting. Conversely, preventing both horizontal translation and rotation of the floor at the supports remarkably increased the structural performance of the PSSDB floor with continuous configuration.

CHAPTER VII

GENERAL CONCLUSIONS AND RECOMMENDATIONS

8.1 INTRODUCTION

This research investigated the capability of the PSSDB floor system to benefit from the development of the membrane action to increase the flexural capacity of the system. The theory of membrane action is composed of two phases, namely, compressive membrane action and tensile membrane action. When the slab is subjected to the vertical loading, in the first steps of loading, the compressive membrane action develops in the slab provided that the horizontal movement of the slab ends is appropriately restricted. The reason is the formation of the arching action from boundary to boundary. Extra strength of the slab due to the development of the compressive membrane action can be accumulated with the pure bending strength of the floor obtained from yield line theory. Given an increase in the mid-span deflection of the slab, the arch deforms and the tensile membrane action comes into the picture. This phase of membrane action normally happens in the second phase of loading, and the applied load can further increase until the rupture point of the elements responsible for carrying the tensile stresses in the slab.

To investigate the potential of the PSSDB floor, experimental and numerical studies were conducted. The experimental programme included the specimens with various boundary conditions. The validated finite element model was used for the parametric study on various applications of the PSSDB floors. The serviceability limit state deflection stated in the BS 8110 (1997) was used for comparison purposes.

8.2 SUMMARIES OF CONCLUSIONS

The obtained outcomes and findings based on previously conducted research can be summarised as follows:

8.2.1 Interaction between Peva 45 and PRIMA*flex* in a PSSDB Floor

i. The values of shear connection stiffness between Peva 45 and PRIMA*flex* for two different environmental conditions of dry and wet were 669.93 N/mm and 476.56 N/mm, respectively.

ii. The behaviour of the connection in all the samples was ductile, and no tearing of the components was detected.

8.2.2 Finite Element Investigation on PSSDB Floor with Simple Span

i. Good agreement was achieved between the developed non-linear finite element model and the experimental results.

ii. The achieved horizontal movement from the numerical studies for the simply supported model ensured the capability of the system to develop the membrane action.

8.2.3 Experimental Study on the Behaviour of the PSSDB Floor with Various Boundary Conditions

i. The horizontal movement was observed in the simply supported specimen at roller support compatible with that of the finite element results in the previous chapter.

ii. Despite the slight lateral translation of the supports, the partial development of the compressive membrane action achieved as much as 27.38% improvement in the pinned-pinned specimen.

iii. The restriction of the rotation in addition to the lateral translation contributed to the better development of the compressive membrane action in the specimen with the fixed-fixed boundary conditions. The load-carrying capacity of the specimen was improved by up to 147.86%.

iv. The local buckling formation in the top flanges of the profiled steel sheeting was postponed to a higher vertical load.

8.2.4 Parametric Studies on PSSDB Floor with Simple Span

i. The development of the compressive membrane action in the PSSDB floor with concrete infill is mostly attributed to the concrete. The concrete infill contributed to the formation of the arching action from boundary to boundary in the floor.

ii. The load-carrying capacity of the PSSDB floor remarkably decreased following the reduction in the profiled steel sheeting's thickness. The load capacity of the simply supported and pinned-pinned panels decreased by about 10% and 8.83%, and the fixed-fixed panel experienced 17.60% reduction.

iii. The effect of changing the thickness of the dry board was unnoticeable on the load-carrying capacity of the panel. This finding has economic significance.

8.2.5 PSSDB Flooring System for Practical Applications

i. Preventing the lateral translation of the PSSDB floor with practical length improved the flexural capacity of the floor by up to 79% in the first steps of loading, and the development of tensile membrane action in the second steps of loading enhanced the load-carrying capacity of the floor in line with the tensile strength of steel sheeting. On the other hand, the load capacity was improved by up to 309% in the floor with fixed-fixed boundary conditions.

ii. Topping concrete over the full-length of the dry board improved the flexural capacity even in the simply support floor. The development of the arching action in the floor improved the load-carrying capacity by up to 80%, and by 161% in the floor with pinned-pinned and fixed-fixed boundary conditions.

iii. Topping concrete over the half-length of dry board also contributed to the development of the compressive membrane action in the floor with restricted boundaries against horizontal translation and/or rotation by up to 166.84%.

iv. In the floor with continuous configuration, preventing the lateral translation did not facilitate the formation of the arching action and thus, no remarkable enhancement in the flexural capacity was achieved. The structural performance of the continuous floor with fixed-fixed boundary conditions was enhanced by up to 87%.

8.3 SUGGESTIONS FOR FUTURE WORK

The results achieved in the conducted research reported in this thesis brought the author into view that the PSSDB floor system has potential to get benefit from development of the membrane action and this research provided a valuable insight into overcoming the weaknesses of the system. In this regard, the author believes that further research have to be conducted to fulfil the following concerns:

i. The capability of Peva 45 and PRIMA*flex* was studied in this thesis. However, other types of the available steel sheeting and dry board in the market, applicable in the PSSDB floor, should also be examined experimentally and numerically. In addition, the effect of various grades of concrete infill should be considered as well.

ii. The development of membrane action in PSSDB system in case of roof application may also be of interest for further study in order to enhance the structural performance of PSSDB system.

iii. Dovetail and trapezoidal types of the profiled steel sheeting due to their geometry may have different effects on the formation of the arch from boundary to boundary in the PSSDB floor.

iv. Further experimental works are required in the PSSDB floor with fixed-fixed boundary condition. The upper flanges of the steel sheeting have to be properly welded to the supporting beams in order to avoid any possible rotations of the floor ends.

v. Some more experimental works on the PSSDB floor with topping are needed to explore the effect of topping on the development of the compressive membrane action.

vi. Further experimental study on the effect of topping over the full length and half-length of dry board could be of interest in formation of the arching action in the PSSDB floor.

vii. The effects of service openings in the PSSDB floor on the development of the membrane action must be also investigated.

viii. The development of the compressive membrane action in the floor with double profiled sheeting and double skin dry board should be considered for further research in this area.

REFERENCES

ABAQUS. 2008. *Documentation Version 6.8*, 2008 Edition, Karlson and Sorensen, Inc.

Abdullah, A.M. 2010. Analysis of Repaired/Strengthened R.C. Structures Using Composite Materials: Punching Shear. Ph.D Thesis. The University of Manchester.

Ahmed, E. 1996. Behaviour of profiled steel sheet dry board panel. M.Sc. Thesis. Universiti Kebangsaan Malaysia

Ahmed, E. 1999. Behaviour of profiled steel sheet dry board folded plate structures. Ph.D Thesis. Universiti Kebangsaan Malaysia.

Ahmed, E. & Wan Badaruzzaman, W.H. 2005. Finite element prediction on the structural performance of profiled steel sheet dry board structural composite system proposed as a disaster relief shelter. *Construction and Building Materials*. 19(4): 285-295.

Ahmed, E. & Wan Badaruzzaman, W.H. 2006. Bondok II/cemboard composite floor panel: Development, structural performances and applications. *Proceedings of the Earth East Asia-Pacific Conferences on Structural Engineering and Construction*, pp. 591-596.

Ahmed, E., Wan Badaruzzaman, W.H. & Khalim, A. R. 1996. A simplified elastic composite floor section analysis with incomplete interaction. *Jurnal Kejuruteraan*. 8: 67-78.

Ahmed, E., Wan Badaruzzaman, W.H. & Khalim Rashid, A. 1996. Composite Partial Interaction of Profiled Steel Sheeting Dry Board Floor Subject to Transverse Loading. *Proceeding of the CIB International Conference on Construction Modernization and Education*, pp. 1-6.

Ahmed, E., Wan Badaruzzaman, W.H. & Wright, H.D. 2000. Experimental and finite element study of profiled steel sheet dry board folded plate structures. *Thin-Walled Structures*. 38: 125–143.

Ahmed, E., Wan Badaruzzaman, W.H. & Wright, H.D. 2002. Two-way bending behavior of profiled steel sheet dry board composite panel system. *Thin-Walled Structures*. 40: 971–990.

Akhand, A.M. 2001. Nonlinear finite element modelling and partial plastic analysis of composite profiled steel sheeting dry board continuous floor. Ph.D Thesis. Universiti Kebangsaan Malaysia.

Akhand, A.M., Al-Sanjery, K. & Wan Badaruzzaman, W.H. 2004. An improved design method for a lightweight floor of profiled steel sheeting and dry board.

Second International Conference on Steel & Composite Structures. Seoul, Korea. pp. 550 – 556.

Akhand, A.M., Wan Badaruzzaman, W.H. & Wright, H.D. 2004. Combined flexure and web crippling strength of a low-ductility high strength steel decking: experiment and a finite element model. *Thin-Walled Structures.* 42(7): 1067-1082.

Alam, A.K. M.J. 1997. Punching shear behavior of reinforcement concrete slabs. M.Sc. Thesis. Bangladesh University of Engineering & Technology.

Ålenius, M. 2003. Finite element modelling of composite bridge stability. M.Sc. Thesis. Royal Institute of Technology, Stockholm.

American Iron and Steel Institute (AISI). 1996. *Specification for the Design of Cold-Formed Steel Structural Members*. Washington, DC.

Arya, C. 2009. *Design of Structural Elements*. Third Edition. London and Newyork: Spon Press.

ASCE Standard 1984. *Specifications for the Design and Construction of Composite Slabs*. New York: American Society of Civil Engineers.

Asia Roofing Industries Sdn. Bhd. 1996. Ajiya Building Materials. Ajiya Peva 45.

Awang, H., Wan Badaruzzaman, W.H. & Fauzi, M. 2006. Folded plate profiled steel sheet dry board (PSSDB) as alternative roofing system. *Seminar Penyelidikan Siswazah Fakulti Kejuruteraan (SPS2006)*, pp. 29-30.

Awang, H.B. 2008. Pembangunan Sistem Panel Bumbung Kepingan Keluli Berprofil Papan Kering (PSSDB). Ph.D Thesis. Universiti Kebangsaan Malaysia.

Bailey, C.G. 2001. Membrane action of unrestrained lightly reinforced concrete slabs at large displacements. *Engineering Structures.* 23(5): 470-483.

Bailey, C.G. 2004. Membrane action of slab/beam composite floor systems in fire. *Engineering Structures.* 26(12): 1691-1703.

Bailey, C.G. & Moore, D.B. 2000. The structural behaviour of steel frames with composite floorslabs subject to fire: Part 1: Theory. *Structural Engineer.* 78(11): 19-27.

Bailey, C.G., Toh, W.S. & Chan, B.M. 2008. Simplified and advanced analysis of membrane action of concrete slabs. *Aci Structural Journal.* 105(1): 30-40.

Bazan, M.L. 2008. Response of reinforced concrete elements and structures following loss of load bearing elements. Ph.D Thesis. Northeastern University, Boston, Massachusetts.

Benayoune, A.G. 1998. Behaviour of profiled steel sheeting dry board panel as wall units. M.Sc. Thesis. Universiti Kebangsaan Malaysia.

Benayoune, A.G. & Wan Badaruzzaman, W.H. 2000. Limit state behaviour of profiled steel sheeting/dry board wall panel. *Proceeding of APSEC.*

Bradford, M.A., Abas, F.M., Gilbert, R.I. & Foster, S.J. 2012. Strength of Continuous Composite Slabs Containing Fibre Reinforced Concrete. *10th International Conference on Advances in Steel Concrete Composite and Hybrid Structures*. Singapore. pp. 461-468.

Brochie, J.F., Holley, M.J. & Okubo, S. 1965. *Effect of Membrane Action on Slab Behavior*. Department of Civil Engineering, Massachusetts Institute of Technology.

Bryan, E.R. & Leach, P. 1984. *Design of profiled sheeting as permanent formwork* London: Construction Industry, Research Information, Association (CIRIA).

BS 8110 Part 1. 1997. *Code for practice for design and construction. Structural use of concrete*, British Standards Institution.

Chin, C.K., AI-Bermani, F.G.A. & Kitipornchai, S. 1993. A finite element method for buckling analysis of plate structures. *Journal Structural. Engineering, ASCE* 119 (4): 1048-68.

Cook, R.D., Malkus, D.S., Plesha, M.E. & Witt, R.J. 2002. *Concepts and applications of finite element analysis*. New York: John Wiley & Sons.

CP117 part 1. 1965. *Composite construction in structural steel and concrete. Simply supported beams in building*, British Standards Institution.

Crisfield, M.A. 1982. Local instabilities in the non-linear analysis of reinforced concrete beamsand slabs. *Proc. Instn. Civ. Engrs. Part 2, 73*. pp. 135-145.

Crisfield, M.A. 1996. *Non-Linear Finite Element Analysis of Solids and Structures-Essentials*. New York: John Wiley & Sons Inc.

Dall'Asta, A. & Zona, A. 2002. Non-linear analysis of composite beams by a displacement approach. *Computers and Structures.* 80(27–30): 2217-2228.

Datta, T.K. & Ramesh, C.K. 1975. Some Experimental Studies on a Reinforced Concrete Slab-Beam System. *Magazine of Concrete Research.* 27(91): 111-120.

DIN 18807 Part 3. 1987. *Trapezoidal sheeting in building: Trapezoidal steel sheeting determination of loadbearing capacity by testing*. Berlin: Beuth Verlag GmbH.

Egilmez, O.O., Helwig, T.A., Jetann, C.A. & Lowery, R. 2007. Stiffness and strength of metal bridge deck forms. *Journal of Bridge Engineering.* 12(4): 429-437.

Eurocode 4. 1994. *Design of composite steel and concrete structures-Composite slabs.* Stephen Hicks BEng Silwood Park.

Evans, H.R. 1967. The analysis of folded plate structures. Ph.D Thesis. University of Wales, Swansea, United Kingdom.

Eyre, J.R. 2007. Surround stiffness to membrane action in concrete slabs. *Magazine of Concrete Research.* 59(2): 107-119.

Eyre, J.R. & Kemp, K.O. 1983. A graphical solution for predicting the increase in strength of concrete slabs due to membrane action. *Magazine of Concrete Research*, pp. 151-156.

Gamble, W.L., Flug, H. & Sozen, M.A. 1970. *Strength of Slabs Subjected to Multiaxial Bending and Compression*, University of illinois, Urbana, Illinois. Civil Engineering Studies, Structural Research Series No. 369.

Gamble, W.L., Sozen, M.A. & Siess, C.P. 1961. *An Experimental Study of a Reinforced Concrete Two-Way Floor Slab*, University of illinois, Urbana, illinois. Civil Engineering Studies, Structural Research Series No. 211.

Gamble, W.L., Sozen, M.A. & Siess, C.P. 1969. Tests of a Two-Way Reinforced Concrete Floor Slab. *Journal of the Structural Division, Proceedings of the American Society of Civil Engineers*, 95(ST6).

Gandomkar, F.A. 2012. Determining comfort level of profiled steel sheeting dry board floor system. Ph.D Thesis. Universiti Kebangsaan Malaysia.

Goldberg, J.E. & Leve, H.L. 1957. Theory of prismatic folded plate structures. *Publ. Int. Assn. Bridge & Struct. Eng.* 17: 59-86.

Guice, L.K., Slawson, T.R. & Rhomberg, E.J. 1986. Membrane Analysis of Flat Plate Slabs. *ACI Structural Journal.* 86(10): 83-92.

Hayes, B. & Taylor, R. 1969. Load-Testing RC slabs. *The Consulting Engineer*, pp. 46–47.

Hiriyur, B. K.J. & Schafer, B.W. 2005. Yield-line analysis of cold-formed steel members. *International Journal of Steel Structures.* 5(1): p43-54.

Hognestad, E. 1951. *A Study of Combined Bending and Axial Load in Reinforced Concrete Members*. New York: University of Illinois Press.

Hon, A., Taplin, G. & Al-Mahaidi, R.S. 2005. Strength of reinforced concrete bridge decks under compressive membrane action. *ACI Structural Journal.* 102(3): 393-401.

Huang, Z., Burgess, I. & Plank, R. 2003. Modeling Membrane Action of Concrete Slabs in Composite Buildings in Fire. I: Theoretical Development. *Journal of structural engineering.* 129(8): 1093-1102.

Hume Cemboard Bhd. 2007. PRIMA*flex*: General purpose cladding sheet. Petaling Jaya.

Keenan, W.A. 1969. *Strength and Behavior of Restrained Reinforced Concrete Slabs Under Static and Dynamic Loadings*. United States: Defense Atomic Support Agency

Krauthammer, T. 2008. *Modern protective structures*. Hoboken: Taylor & Francis Ltd.

Li, G. & Zhang, N. 2010. Experimental study of membrane action of composite floor slabs under fire. *Tumu Gongcheng Xuebao/China Civil Engineering Journal*. 43(3): 24-31.

Lim, L., Buchanan, A., Moss, P. & Franssen, J. 2004. Computer Modeling of Restrained Reinforced Concrete Slabs in Fire Conditions. *Journal of structural engineering.* 130(12): 1964-1971.

Lim, L.C.S. 2003. Membrane Action in Fire Exposed Concrete Floor Systems. Ph.D Thesis. University of Canterbury, Christchurch, New Zealand.

Mangesha, W.J. 1992. Composite Profiled Steel Sheeting/Dry Board Panels. M.Sc. Thesis University of Strathclyde, United Kingdom.

Marciukaitis, G., Jonaitis, B. & Valivonis, J. 2006. Analysis of deflections of composite slabs with profiled sheeting up to the ultimate moment. *Journal of Constructional Steel Research.* 62(8): 820–30.

May, I.M., Naji, J.H. & Ganaba, T.H. 1988. Displacement control for the non-linear analysis of reinforced concrete structures. *Engineering Computations.* 5(4): 266 - 273.

Meamarian, N., Krauthammer, T. & O'Fallon, J. 1994. Analysis and Design of Laterally Restrained Structural Concrete One-Way Members. *Structural Journal.* 91(6): 719-725.

Miltenburg, R. J. 1998. Membrane behaviour in one-way prestressed concrete slab. M.Sc. Thesis. The University of Western Ontario, London, Ontario.

Mohd Shokory, S. & Wan Badaruzzaman, W.H. 2000. Kajian Teori Kelakuan Dinding Keluli Berprofil / Papan Kering (Theoretical Study on the Behaviour of Profiled Steel Sheet/Dry boards Wall). *Prosiding Kejuruteraan Awam UKM (UKM Civil Engineering Proceedings)*, pp. 107-116.

Muthu, K.U., Amarnath, K., Ibrahim, A. & Mattarneh, H. 2006. Load-deflection behaviour of restrained RC slab strips. *Structural concrete.* 7(1): 17–26.

Muthu, K.U., Amarnath, K., Ibrahim, A. & Mattarneh, H. 2007. Load deflection behaviour of partially restrained slab strips. *Engineering Structures.* 29(5): 663-674.

Nethercot, D.A. 2003. *Composite Construction*. New York: Spon Press.

Newmark, N.M., Siess, C.P. & I.M., V. 1951. Test and analysis of composite beams with incomplete interaction. *Proceeding Society for Experimental Stress Analysis*. pp. 75-95.

Ockleston, A.J. 1955. Load Tests on a Three Story Reinforced Concrete Building in Johannesburg. *Structural Engineer (London).* 33(10): 304-322.

Park, R. 1964a. Ultimate strength of rectangular concrete slabs under short-term uniform loading with edges restrained against lateral movement. *Proc. Inst. Civ. Eng.* pp. 125-150.

Park, R. 1964b. The ultimate strength and long term behaviour of uniformly loaded two-way concrete slabs with partial lateral restraint at all edges. *Magazine of Concrete Research.* 16(48): 139-152.

Park, R. 1964c. Tensile membrane behaviour of uniformly loaded rectangular reinforced concrete slabs with fully restrained edges. *Magazine of Concrete Research.* 16(46): 39-44.

Park, R. 1965. The lateral stiffness and strength required to ensure membrane action at the ultimate load of a reinforced concrete slab and beam floor. *Magazine of Concrete Research.* 17(50): 29–38.

Park, R. & Gamble, W.L. 1980. *Reinforced Concrete Slabs*. New York: John Wiley and Sons.

Park, R. & Gamble, W.L. 2000. *Reinforced Concrete Slabs*. New York: John Wiley and Sons.

Patrick, M. 1989. Design of Continuous Composite Slabs - The Issue of Ductility. *Steel Construction journal.* 23(3): 2-10.

Patrick, M. & Bridge, R.Q. 1994. partial shear connection design of composite slabs. *Engineering structures.* 16(5): 348-362.

Plank, R.J. & Wittrick, W.H. 1974. Buckling under combined loading of thin, flat-walled structures by a complex finite strip method. *International Journal for Numerical Methods in Engineering.* 8(2): 323–339.

Plum, D. & Horne, M. 1975. The analysis of continuous composite beams with partial interaction. *ICE Proceedings*. 59(4), pp. 625 –643.

Powell, D. 1956. Ultimate strength of concrete panels subjected to uniformly distibuted loads. Ph.D Thesis. Cambridge University, UK.

Qingxiang, W., Gang, W. & Zhongjun, L. 2010. Experiment Study on Compressive Membrane Action of Slab Strips Restrained by Shear Walls. *Key Engineering Materials.* 417-418: 805-808.

Queiroz, F.D., Vellasco, P.C.G.S. & Nethercot, D.A. 2007. Finite element modelling of composite beams with full and partial shear connection. *Journal of Constructional Steel Research.* 63(4): 505-521.

Ramesh, C.K. & Datta, T.K. 1973. Ultimate Strength of Reinforced Concrete Slab-Beam Systems: A New Approach. *Indian Concrete Journal.* 47: 301-308.

Ramm, E. & Stegmueller, H. 1982. The displacement finite element method in nonlinear buckling analysis of shells-Buckling of shells. *Proceedings of a state-of-the-art colloquium* Univ. Stuttgart. pp. 201-235.

Rankin, G.I.B., Skates, A.S., Niblock, R.A. & Long, A.E. 1991. Compressive membrane action strength enhancement in uniformly loaded, laterally restrained slabs. *Structural Engineer.* 69: 287-95.

Roberts, T.M. 1985. Finite difference analysis of composite beams with partial interaction. *Computers and Structures.* 21(3): 469-73.

Rockey, K.C. & Evans, H.R. 1969. The Behaviour of Corrugated Flooring System. *Thin Walled Steel Structures: Their design and use in buildings*. pp. 236-258.

Shodiq, H.B.M. 2004. Performance of new profiled steel sheeting dry board floor system with concrete infill. Ph.D Thesis. Universiti Kebangsaan Malaysia.

Shodiq, H.M., Wan Badaruzzaman, W.H. & Khalim, A. 2003. The Effect of Concrete Infill and Topping to the Structural Behaviour of Profiled Steel Sheeting Dry Board (PSSDB) Flooring System. *Proceeding of the World Engineering Congress & Exhibition WEC 2002, Kuching*, pp. 245-247.

Steel Deck Institute (SDI) 2000. *SDI Manual of Construction with Steel Deck*. Fox River Grove, IL 60021.

Surat, M., W. Badaruzzaman, W.H., Tahir, M.M. & Abdullah, N.A.G. 2008. Current Application of Pressed Steel Sheet Dry Board (PSSDB) Modulation Panels for Annex Classroom Blocks in Melaka Malaysia. *ICCBT 2008.*

Taylor, S.E., Rankin, G.I.B. & Cleland, D.J. 2001. Arching action in high-strength concrete slabs. *Proceedings of the Institution of Civil Engineers-Structures and Buildings.* 146(4): 353-362.

Uy, B. & Bradford, M.A. 1994. Inelastic local buckling behaviour of thin steel plates in profiled composite beams. *The Structural Engineer.* 72(16): 259-67.

Uy, B. & Bradford, M.A. 1995. Local buckling of thin steel plates in composite construction: Experiment and theory - Structures and Buildings. *Proceedings of the Institution of Civil Engineers.* 110 pp. 426-440.

Vecchio, F.J. & Tang, K. 1990. Membrane action in reinforced concrete slab. *Canadian Journal of Civil Engineering.* 17: 686-697.

Vulcu, C., Gernay, T., Zaharia, R. & Franssen, J.M. 2010. Numerical Modelling of Membrane Action of Composite Slabs in Fire Situation. *Proceedings of the Sixth International Conference Structures in Fire*. pp. 474-483.

Wan Badaruzzaman, W.H. 1994. The Behavior of Profiled Steel Sheet/Dryboard System. Ph.D Thesis. University of Wales.

Wan Badaruzzaman, W.H., Ahmed, E. & Khalim Rashid, A. 1996. Behaviour of profiled steel sheet dry board system. *CIB W89 Beijing International Conference*.

Wan Badaruzzaman, W.H., Ahmed, E., Osman, S.A. & Akhand, A.M. 1999a. Dry boards in loadbearing structural building panel system. *Proceeding of the World Engineering Congress & Exhibition WEC '99*, pp. 25-30.

Wan Badaruzzaman, W.H., Akhand, A.M., Yusof, K.M., Mohd Kasby, N.A., Ahmed, E., Osman, S.A., Ismail, A. & Zain, M.F.M. 1999. Fire resistance performance of Bondek II/ Cemboard Composite Flooring Panel (BCCFP) system. *Proceeding of the World Engineering Congress & Exhibition WEC '99*, pp. 73–80.

Wan Badaruzzaman, W.H., Aszuan, A. & Wan Mohtar, W.H.M. 2007. Behaviour of Profiled Steel Sheet Dry Board (PSSDB) composite floor system with foamed concrete infill material. *Third International Conference on Steel and Composite Structures*, pp. 977-981.

Wan Badaruzzaman, W.H., Awang Adeni, A.Z., Mutalib, A.A. & Wan Mohtar, W.H.M. 2008. The development of a new composite floor system experimentally. *Fifth International Conference on Thin-Walled Structures*.

Wan Badaruzzaman, W.H., Awang, H., Nordin, N. & Shaini, A.B. 2009. Development of a new composite flooring system based on improved profiled steel sheet dry board (PSSDB) system. *Fifth International Conference on Construction in the 21st Century (CITC-V) "Collaboration and Integration in Engineering, Management and Technology"*. pp. 1563-1570.

Wan Badaruzzaman, W.H., Azmi, A.E., Eng, J. & Wan Mohtar, W.H. M. 2006. Profiled steel sheet dry board system as an Alternative Construction System - Focussing on thermal comfort performance. *Proceedings of the Tenth East Asia-Pacific on Structural Engineering and Construction (EASEC-10)*. pp. 139-144.

Wan Badaruzzaman, W.H., Hamid, N.A., Harsoyo, M.S., Hamzah, N., Khalim, A.R. & Ibrahim, A. 2003. Indicative bending behaviour of 'double profiled sheeting and double skin dry board' PSSDB floor system. *Proceedings of the 3rd International Conference on Advances in Strategic Technologies (ICAST 2003),* pp. 1103-1108.

Wan Badaruzzaman, W.H., Harsoyo, M.S. & Eng, J. 2006. Performance improvement of profiled steel sheet dry board floor system by concrete infill. *Proceedings of* *the Tenth East Asia-Pacific on Structural Engineering and Construction (EASEC-10)*. pp. 381-386.

Wan Badaruzzaman, W.H., Harsoyo, M.S., Noor, S.M.K., Hamzah, N., Khalim, A. R., Taib, K.A. & Ibrahim, A. 2003. Flexural behaviour of double profiled sheeting and single skin dry board floor system. *2nd International Conference on Construction Technology (CONTEC)*. pp. 200-208.

Wan Badaruzzaman, W.H., Shodiq, H.M. & Akhand, A.M.E., J. 2006. Prediction of fire resistance performance of profiled steel sheet dry board floor system. *Proceeding of the 6th Asia-Pacific Structural Engineering & Construction Conference APSEC*. Kuala Lumpur, Malaysia.

Wan Badaruzzaman, W.H., Shodiq, H.M. & Khalim, A.R. 2002. The effect of concrete infill and topping to the structural behaviour of Profiled Steel Sheeting Dry Board (PSSDB) flooring system. *In Proceeding of the World Engineering Congress & Exhibition WEC*. pp. 245–247.

Wan Badaruzzaman, W.H., Zain, M.F.M., Akhand, A.M. & Ahmed, E. 2003. Dry boards as load bearing element in the profiled steel sheet dry board floor panel system-structural performance and applications. *Construction and Building Materials*. 17(4): 289–297.

Wan Badaruzzaman, W.H., Zain, M.F.M., Shodiq, H.M., Akhand, A.M. & Sahari, J. 2003. Fire resistance performance of profiled steel sheet dry board (PSSDB) flooring panel system. *Building and Environment*. 38(2003): 907 – 912.

Wang, G., Wang, Q.-x. & Li, Z.-j. 2010. Lateral restraint force of RC slabs under membrane action. *Mechanic Automation and Control Engineering (MACE), 2010 International Conference*. pp. 742-745.

Welch, R.W., Hall, W.J. & Gamble, W.L. 1999. Compressive Membrane Capacity Estimates in Laterally Edge Restrained Reinforced Concrete One-Way Slabs. University of Illinois at Urbana-Champaign.

Welch, R.W., Hall, W.J. & Gamble, W.L. 2008. Specializing Park's Compressive Membrane Theory. *Journal of Structural Engineering*. 134(5): 854-858.

Weman & Klas. 2003. *Welding Processes Handbook*. New York: NY: CRC Press LLC.

Wood, R.H. 1961. *Plastic and Elastic Design of Slabs and Plates*. London, England: Thames and Hudson.

Woodson, S. & Krauthammer, T. 1999. Design for severe dynamic loads. *The design of two-way slabs*. 183(Special Publication): 17-36.

Woodson, S.C. 1985. *Effects of Shear Stirrup Details on Ultimate Capacity and Tensile Membrane Behavior of Reinforced Concrete Slabs*. U.S. Army Engineer Waterways Experiment Station.

Woodson, S.C. 1994. *Effects of Shear Reinforcement on the Large-Deflection Behavior of Reinforced Concrete Slabs*. Army Engineer Waterways Experiment Station.

Wright, H.D. 1993. Buckling of Plates in Contact with a Rigid Medium. *The Structural Engineer*. 71(12): 209-15.

Wright, H.D. & Evans, H.R. 1986. Profiled Steel Sheeting for the Replacement of Timber Flooring in Building Renovation, SERC Grant GR/D/76875. United Kingdom.

Wright, H.D. & Evans, H.R. 1987. A Folded Plate Method of Analysis for Profiled Steel Sheeting in Composite Floor Construction. *Thin-Walled Structures.* 5(1): 21-37.

Wright, H.D., Evans, H.R. & Burt, C.A. 1989. Profiled steel sheet/dry boarding composite floors. *The Structural Engineer* 67(7): 114–129.

Wright, H.D., Evans, H.R. & Harding, P.W. 1987. The Use of Profiled Steel Sheeting in Floor Construction. *Construct. Steel Research.* 7: 279-295.

Wright, H.D. & Hossain, K.M.A. 1997. In-plane shear behaviour of profiled steel sheeting. *Thin-Walled Structures.* 29(1-4): 79-100.

Xu, Y.L. & Teng, J.G. 1994. Local plastic failure of light gauge steel roofing sheets: Finite element analysis versus experiment. *Journal of Constructional Steel Research.* 30(2): 125-150.

Zhang, F.Z. & Yi, W.J. 2009. Experimental Research on Collapse Mechanism of a RC Flat Plate. *Isiss '2009: Innovation & Sustainability of Structures*, pp. 417-423.

Zheng, Taylor, S., Robinson, D. & Cleland, D. 2010. Investigation of Ultimate Strength of Deck Slabs in Steel-Concrete Bridges. *ACI Structural Journal.* 107(01): 82-91.

Zheng, Y., Robinson, D., Taylor, S. & Cleland, D. 2009. Finite element investigation of the structural behaviour of deck slabs in composite bridges. *Engineering structures.* 31(8): 1762-1776.

Zheng, Y., Robinson, D., Taylor, S., Cleland, D. & Shaat, A. 2008. Analysis of compressive membrane action in concrete slabs. *Proceedings of the Institution of Civil Engineers: Bridge Engineering.* 161(1): 21-31.

Zheng, Y., Robinson, D., Taylor, S.E. & Cleland, D. 2007. Investigation of the Compressive Membrane Action in composite steel-concrete bridge decks. *Proceedings of the 3rd International Conference on Steel and Composite Structures, ICSCS07 - Steel and Composite Structures*. pp. 521-532.

Zheng, Y., Taylor, S.E. & Robinson, D. 2010. Prediction methods of loading carrying capacities in concrete bridge deck slabs with consideration of compressive membrane action. *Harbin Gongye Daxue Xuebao/Journal of Harbin Institute of Technology*. 42(4): 644-651.

APPENDIX A

MIX DESIGN OF CONCRETE GRADE 30 USED IN THIS THESIS

A.1 MIX DESIGN

The strength of the concrete is highly associated with the composition and types of its ingredients. The mix design of concrete was considered according to recommendation and guidelines of Dobrowolski (1998) in concrete construction handbook. More description about the assumptions and method of design is provided as follow:

A.1.1 Assumptions

i. Density of coarse aggregate was 1600 kg/m^3.

ii. Specific gravity of Portland cement was assumed 3.15

iii. Specific gravity of both fine and coarse aggregate was 2.65

iv. The slump of the concrete was assumed to be 75-100 mm.

v. The maximum size of aggregate was 12.5 mm

vi. Total air content of 5.5% was assumed which was according to the maximum aggregate size.

vii. Absorption of fine and coarse aggregate was assumed 1.0% and 0.5%.

A.1.2 Calculation

The mix design of the concrete grade 30 according to the abovementioned assumptions and Dobrowolski (1998) could be summarised as follow:

Table 11.5 in Dobrowolski (1998) provides the water-cement ratio of 0.46 for this grade of concrete. In addition the amount of water for 1 m^3 based on Table 11.7 is 193 litres. Accordingly, the required cement would be:

$\frac{193}{0.46} = 419.56$ kg

Table 11.9 provides the volume of the coarse aggregate for 1m^3 of concrete as 0.57 in which:

$0.57 \times 1600 \times (1 + 0.005) = 916.6$ kg : Weight of coarse aggregate

$\frac{916.6}{2.65 \times 1000} = 0.346\ m^3$: Volume of coarse aggregate

$\frac{419.56}{3.15 \times 1000} = 0.133\ m^3$: Volume of cement

$\frac{193}{1000} = 0.193\ m^3$: Volume of water

5.5% of volume of concrete = 0.055 m^3 : Volume of air

Total volume of the mentioned materials:

$$0.346 + 0.133 + 0.193 + 0.055 = 0.727\ m^3$$

Therefore the volume of fine aggregate is:

$$1 - 0.727 = 0.273\ m^3$$

And hence the weight of fine aggregate is:

$$0.273 \times 2.65 \times 1000 = 723.45 \text{ kg}$$

Accordingly, the weight of cement, water, coarse aggregate, and fine aggregate for 1 m^3 are 419.56 kg, 193.45 kg, 916.6 kg, and 723.45 kg. The total weight of concrete also was calculated as 2253 kg/m^3.

APPENDIX B

COMPRESSIVE STRENGTH OF CONCRETE CUBE SAMPLES

The compressive strength of the used concrete in this study was measured by crushing of the concrete cube samples in the Unit Test Machine. Dimension, weight, and the compressive strength of the samples are tabulated in the Table B.1. Nine samples were considered for the studied specimens with three different boundary conditions as explained in chapter 5.

Table B.1 Details of the compressive strength test

Sample No	Dimension of Cube (mm)			Average area of bed face (mm^2)	Weight of the cube (N)	Weight per unit volume (kg/m^3)	Max load at failure (kN)	Compressive strength (N/mm^2)
	Length	Width	Depth					
1	150	150	150	22500	77.8	2305.19	796	35.38
2	151	150	150	22650	78	2295.81	755	33.33
3	150	149	150	22350	78.1	2329.60	747	33.42
4	150	148	150	22200	78	2342.34	712	32.07
5	150	150	150	22500	78.6	2328.89	726	32.27
6	150	149	150	22350	79.4	2368.38	783	35.03
7	150	150	150	22500	79	2340.74	764	33.96
8	150	150	150	22500	77.8	2305.19	756	33.60
9	150	153	150	22950	79.8	2318.08	705	30.72

APPENDIX C

CALCULATION OF RIGIDITIES IN TABLE OF RESULTS

The calculation of (elastic) rigidities provided in table of results is described here. Figure C.1 is used as an example to show the procedure.

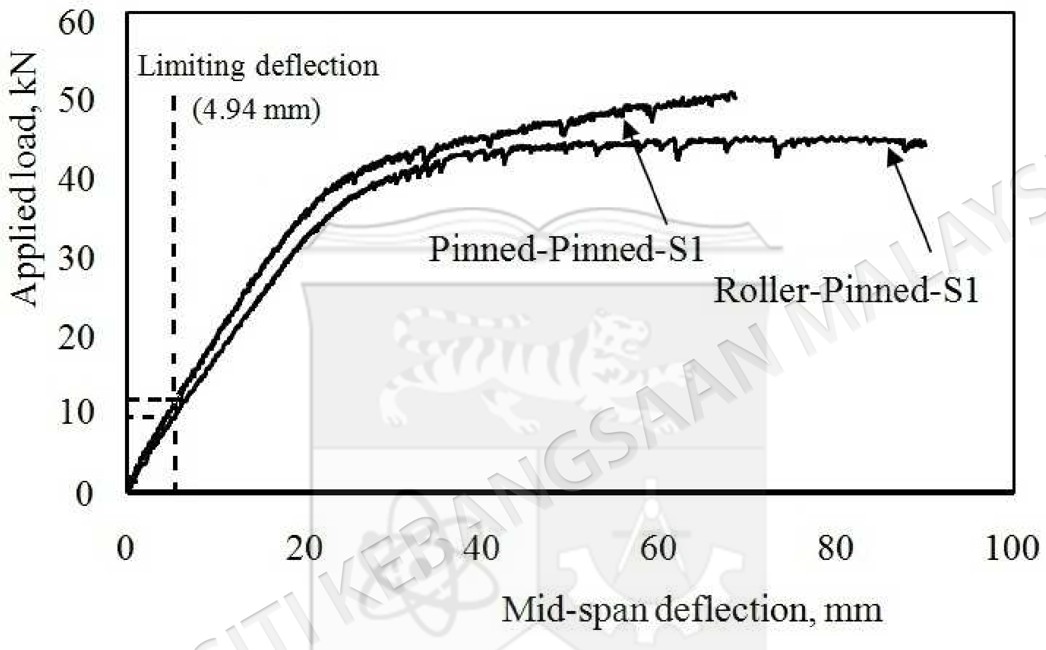

Figure C.1 : Load-deflection curve

The elastic rigidity of the model is the slope of load-deflection curve. For instance for model Pinned-Pinned-S1, the rigidity is:

$$Rigidity = \frac{10.70}{4.94} = 2.16$$

The same calculation can be done for the rigidity of model Roller-Pinned-S1 and the rigidity is achieved as 1.7.

APPENDIX D

SERVICEABILITY LIMIT STATE DEFLECTION BASED ON BS 8110

3.2 Serviceability limit states

3.2.1 Excessive deflections due to vertical loads

3.2.1.1 *Appearance.* For structural members that are visible, the sag in a member will usually become noticeable if the deflection exceeds $l/250$, where l is either the span or, in the case of a cantilever, its length.

This shortcoming can in many cases be at least partially overcome by providing an initial camber. If this is done, due attention should be paid to the effects on construction tolerances, particularly with regard to thicknesses of finishes.

This shortcoming is naturally not critical if the element is not visible.

3.2.1.2 *Damage to non-structural elements.* Unless partitions, cladding and finishes, have been specifically detailed to allow for the anticipated deflections, some damage can be expected if the deflection after the installation of such finishes and partitions exceeds the following values:

a) $L/500$ or 20 mm, whichever is the lesser, for brittle materials;

b) $L/350$ or 20 mm, whichever is the lesser, for non-brittle partitions or finishes; where L is the span or, in the case of a cantilever, its length.

NOTE: These values are indicative only.

These values also apply, in the case of pre-stressed construction, to upward deflections.

APPENDIX E

LIST OF PUBLICATIONS

The papers presented in the conferences and also the papers published in and submitted to the journals are as follow:

D.1 Conferences

- Seraji, M., Wan Badaruzzaman, W. H. & Osman, S. A. 2011. Study the effect of membrane action in profiled steel sheet dry board (PSSDB) floor. *EPC 2011 Regional Engineering Postgraduate Conference 2011, UKM.* Bangi,

- Seraji, M., Wan Badaruzzaman, W. H. & Osman, S. A. 2012. Experimental Study on the Compressive Membrane Action in Profiled Steel Sheet Dry Board (PSSDB) Floor System. *International Journal on Advanced Science, Engineering and Information Technology* **2**(2012 No. 2): 46-48.

- Seraji, M., Wan Badaruzzaman, W. H., Osman, S. A. & Seraji, J. 2012. Nonlinear finite element prediction on the membrane action effect in profiled steel sheet dry board (PSSDB) floor. *10th International Conference on Advances in Steel Concrete Composite and Hybrid Structures* Singapore. pp. 469-476.

D.2 Journals

- Seraji, M., Wan Badaruzzaman, W. H. & Osman, S. A. 2013. Membrane action in PSSDB floor slab system. *Journal of Engineering Science and Technology* **8**(2).

- Seraji, M., Wan Badaruzzaman, W. H. & Osman, S. A. 2012. Nonlinear Analysis on Membrane Action Effect in Profiled Steel Sheeting Dry Board Flooring System for Practical Applications. Sent to *Construction & Building Materials*.